Journal
of
The Franklin Institute
Devoted to Science and the Mechanic Arts

Vol. 266 SEPTEMBER, 1958 No. 3

ON THE OPTIMUM TRAJECTORY OF A ROCKET *

BY

ROBERT R. NEWTON [1]

ABSTRACT

In this paper, the problem of optimizing some functional of a rocket trajectory is examined. It is shown that an optimum trajectory may be found if no more than four (in a two-dimensional theory) auxiliary conditions are specified. The trajectories to give maximum range and to put a satellite into an orbit most efficiently are calculated, in a vacuum and including effects of the atmosphere. The effects of air for the satellite problem are discussed only qualitatively, since the method of allowing for them is quite similar to that used for the maximum range problem.

1. INTRODUCTION

Let the thrust of a rocket be some arbitrary function of time, $T(t)$; and let $\phi_1(t)$, $\phi_2(t)$, be two coordinates which give the orientation of the line of action of the thrust. Then, in an external force field of known properties, the three functions (T, ϕ_1, ϕ_2) determine the trajectory $r(t)$. We want to choose (T, ϕ_1, ϕ_2) so as to make $r(t)$ an optimum, in some sense.

The collection of optimum trajectory problems can be categorized in various ways:

(a) By the function of the rocket. The maximum range problem and the orbit problem (that is, putting the rocket at the end of burning into a specified orbit, which may or may not intersect the Earth's surface) are two examples. Each of these problems may be phrased in either of two ways: We may seek to maximize the range, maximum

* Most of this work was performed under a contract between Tulane University and Redstone Arsenal, as a part of Project TU2-9F. Some revision, mostly editorial in nature, was carried out at The Applied Physics Laboratory, under Contract NORD-7386, Navy Bureau of Ordnance.

[1] Formerly, Department of Physics, Tulane University, New Orleans, La.; presently, Applied Physics Laboratory, The Johns Hopkins University, Silver Spring, Md.

(Note—The Franklin Institute is not responsible for the statements and opinions advanced by contributors in the JOURNAL.)

altitude, or other such property, for a given fuel consumption, or we may specify such a property and seek to minimize the fuel consumed.

(*b*) By the degrees of freedom allowed. If $T(t)$ is fixed, and only the orientation is varied, we shall call this the restricted problem. If both T and the orientation angles may be varied, we have what we shall call the general problem. Between these two problems lies what we shall call the burning-time problem. In this problem, the shape of the thrust curve is specified, but not the scale; that is, $T(t) = f(at)$, where f is known, but the scale factor a is free.

(*c*) By other attendant circumstances. We may assume a flat or curved Earth; if curved, it may be rotating or non-rotating. We may neglect or include aerodynamic forces.

Fried and Richardson (1)[2] have discussed the restricted maximum range problem, with both a flat and curved Earth. Fried and Lawden (2) have discussed the restricted orbit problem in a vacuum. Several writers (3, 4, 5, 6) have discussed the general problem of reaching maximum altitude in vertical firing. Bryson and Ross (5) also considered non-vertical firing, but with the special assumption that the angle of attack of the rocket is always zero. Lawden (6) also considered non-vertical firing, but neglected the dependence of aerodynamic forces upon the attitude, a dependence which we shall show to be important. Hibbs (7) has discussed the best thrust function for horizontal flight, while Miele (8) has considered the minimization of aerodynamic heating effects.

We shall discuss the maximum range problem for all categories under (*b*) above, with and without aerodynamic effects. The discussion will include vertical firing for maximum altitude as a special case; our results differ slightly from those of earlier writers for reasons which will be discussed later. We shall neglect the Earth's curvature during burning; it will become apparent that the distance travelled during burning with optimum conditions is so short that this is quite accurate.

We shall discuss the orbit problem in detail only in a vacuum. The techniques for including aerodynamic effects are so similar to those for the maximum range problem that their separate detailed discussion for the orbit problem does not seem warranted. Our treatment will differ from that of Fried (2) in that we shall allow a period of no thrust to occur within the over-all burning period, thus effecting a considerable saving. The advantages of a "coasting" period have been pointed out by Lawden (2) and others.

We tacitly assume throughout this paper that the rocket is in near-vacuum conditions for most of its unpowered flight.

It is possible to "over-determine" an optimum trajectory problem by specifying too many boundary conditions. The nature of the allowable

[2] The boldface numbers in parentheses refer to the references appended to this paper.

boundary conditions is not obvious, and we shall discuss this topic in the next section. A problem may also fail to have a solution for other reasons. We have not found any general existence theorem, but in some problems with no solution, or at least with no analytic solution, we can demonstrate the non-existence by qualitative arguments.

2. ALLOWABLE BOUNDARY CONDITIONS

Over a flat Earth, it is obvious that the optimum trajectory during burning should lie in the vertical plane containing the position and the velocity vector at burn-out. Accordingly, we use two coordinate axes in this plane, ξ taken horizontal and η vertical. Let ϕ be the angle from ξ to the direction of thrust. Further useful coordinates are

$$\Theta = \tan^{-1}(\dot{\eta}/\dot{\xi}), \tag{2.1}$$

$$\alpha = \phi - \Theta. \tag{2.2}$$

The forces assumed acting on the rocket are: (*a*) the jet thrust T, (*b*) gravity, (*c*) aerodynamic drag, and (*d*) aerodynamic lift. If M is the instantaneous mass, so that $-\dot{M}$ is the rate of burning fuel, and if ρ, v, A are air density, rocket speed, and a reference area of the rocket, we assume:

$$T = -\dot{M}v_e, \tag{2.3}$$

$$\text{drag} = C_D\rho v^2 A/2, \tag{2.4}$$

$$\text{lift} = C_L\rho v^2 A/2, \tag{2.5}$$

with v_e constant. C_D and C_L are functions of Mach number; C_D is an even function, and C_L an odd function, of α.

The equations of motion are:

$$\left.\begin{aligned} M\ddot{\xi} &= T\cos\phi - \tfrac{1}{2}C_D A\rho v\dot{\xi} - \tfrac{1}{2}C_L A\rho v\dot{\eta}, \\ M\ddot{\eta} &= T\sin\phi - \tfrac{1}{2}C_D A\rho v\dot{\eta} + \tfrac{1}{2}C_L A\rho v\dot{\xi} - Mg. \end{aligned}\right\} \tag{2.6}$$

These are to be solved subject to initial conditions:

$$\xi(0) = \eta(0) = 0, \quad \dot{\xi}(0) = \dot{\eta}(0) = 0. \tag{2.6a}$$

Since we assume that the orientation is controlled, we do not need any rotational equations of motion.

In the general problem, the functions $\dot{M}$, T, and ϕ are not known *a priori*. We can solve Eqs. 2.2, 2.3, and 2.6 for these functions; the solution for $\dot{M}$ is of the form:

$$\dot{M} = f(M, \xi, \dot{\xi}, \ddot{\xi}, \eta, \dot{\eta}, \ddot{\eta}). \tag{2.7}$$

In this section, we are interested only in the arguments of f, and not its form; let the arguments be denoted, respectively, by $M, x_1, x_2, \cdots, x_6$.

The optimum trajectory is that set of functions $x_i(t)$, $i = 1, \cdots, 6$, which makes

$$M(t_b) = M(0) + \int_0^{t_b} \dot{M}(t)dt$$

a maximum, for a given $M(0)$, and subject to conditions not yet stated. Let t_b be the burning time on the correct trajectory, and let t_1 be the burning time on a varied trajectory, with $\delta t_b = t_1 - t_b$. Taking variations in Eq. 2.7:

$$\delta\dot{M} = f_M \delta M + \sum_{i=1}^{6} f_{x_i} \delta x_i, \tag{2.8}$$

using a subscript to denote a formal partial derivative. Since δM is independent of M, Eq. 2.8 can be integrated; since we want $\delta M(t_1)$ to be zero:

$$0 = \delta M(t_1) = \delta M(t_b) + \dot{M}(t_b)\delta t_b$$
$$= \exp\left(\int_0^{t_b} f_M(t)dt\right)\int_0^{t_b} \exp\left(-\int_0^{t} f_M(\tau)d\tau\right)$$
$$\times \left(\sum_i f_{x_i}(t)\delta x_i(t)\right)dt + \dot{M}(t_b)\delta t_b.$$

Now we replace each x, by its original symbol, and proceed, in the usual fashion, to eliminate each variation of a derivative, such as $\delta\dot{\xi}$, using integration by parts. This process gives:

$$0 = \dot{M}(t_b)\delta t_b + [f_{\dot{\xi}}\delta\xi + (f_M f_{\dot{\xi}} - (f_{\dot{\xi}})^{\cdot} + f_\xi)\delta\xi]_{t=t_b}$$
$$+ \exp\left(\int_0^{t_b} f_M(t)dt\right)\int_0^{t_b} \exp\left(-\int_0^{t} f_M(\tau)d\tau\right)\{f - (f_{\dot{\xi}})^{\cdot} +$$
$$f_M f_{\dot{\xi}} + (f_{\dot{\xi}})^{\cdot\cdot} - 2f_M(f_{\dot{\xi}})^{\cdot} + (f_M)^2 f_{\dot{\xi}} - (f_M)^{\cdot} f_{\dot{\xi}}\}\delta\xi(t)dt$$
$$+ \text{similar terms in } \eta.$$

The integrated terms contain no part from $t = 0$, because of Eqs. 2.6a.

$\delta\xi(t)$ and $\delta\eta(t)$ are independent, arbitrary, functions of t, except at the end points. Hence, the coefficients of $\delta\xi(t)$ and $\delta\eta(t)$ must be identically zero:

$$\left.\begin{aligned} f_\xi - (f_{\dot{\xi}})^{\cdot} + f_M f_{\dot{\xi}} + (f_{\dot{\xi}})^{\cdot\cdot} - 2f_M(f_{\dot{\xi}})^{\cdot} + (f_M)^2 f_{\dot{\xi}} - (f_M)^{\cdot} f_{\dot{\xi}} = 0, \\ f_\eta - (f_{\dot{\eta}})^{\cdot} + f_M f_{\dot{\eta}} + (f_{\dot{\eta}})^{\cdot\cdot} - 2f_M(f_{\dot{\eta}})^{\cdot} + (f_M)^2 f_{\dot{\eta}} - (f_M)^{\cdot} f_{\dot{\eta}} = 0. \end{aligned}\right\} \tag{2.9}$$

Also, the entire integrated part must be zero, but not the individual coefficients of $\delta\xi(t_b)$, etc., because the end-point variations need not be independent. If we let $\delta\xi_b = \delta\xi(t_b)$, etc.:

$$f_{\dot{\xi}}(t_b)\delta\xi_b + [f_\xi - (f_{\dot{\xi}})^\cdot + f_M f_{\ddot{\xi}}]_b\delta\xi_b + f_{\dot{\eta}}(t_b)\delta\dot{\eta}_b + [f_\eta - (f_{\dot{\eta}})^\cdot + f_M f_{\ddot{\eta}}]_b\delta\eta_b + \dot{M}(t_b)\,\delta t_b = 0. \quad (2.10)$$

So far, we have not said whether we are treating a maximum range problem or an orbit problem. Therefore, Eqs. 2.9 and 2.10, as well as 2.6*a*, hold in all cases. Each of Eqs. 2.9 is fourth order, and the pair is a system of eighth order, and, in addition, the first order equation (2.7) must be satisfied. The optimum trajectory thus satisfies a differential equation system of the ninth order, in three variables M, ξ, η, whose general solution contains nine arbitrary constants, in addition to the unknown time interval t_b. Thus, altogether ten, and only ten, boundary conditions may be specified.

The initial value of M gives one of these conditions; Eqs. 2.6*a* give four more. Thus there are exactly five boundary conditions yet unspecified. We shall find that these five are specified by the conditions imposed at the end of burning.

The range is a function of the conditions at the end of burning, that is, at $t = t_1$; in a rectangular geometry, for example, in a vacuum:

$$R = \xi_1 + (\dot{\xi}_1/g)[\dot{\eta}_1 + \sqrt{\dot{\eta}_1^2 + 2g\eta_1}]. \quad (2.11)$$

In the maximum range problem, we can fix R, and optimize M. In other problems, we fix different functions of ξ_1, $\dot{\xi}_1$, η_1, $\dot{\eta}_1$. Thus, for either type of problem, we require s functions of the coordinates and velocities at the end of burning to vanish:

$$g_r(\xi_1, \dot{\xi}_1, \eta_1, \dot{\eta}_1) = 0, \quad r = 1, 2, \cdots, s, \quad (2.12)$$

where the value of s depends upon the problem.

When we vary the trajectory, $\xi_1 = \xi_b + \delta\xi_1$, etc., where ξ_b is the value for the correct trajectory, and $\delta\xi_1 = \delta\xi_b + \dot{\xi}_b\delta t_b$, etc. The change in g_r is thus

$$\delta g_r = (\partial g_r/\partial\xi_1)(\delta\xi_b + \dot{\xi}_b\delta t_b) + \cdots + (\partial g_r/\partial\dot{\eta}_1)(\delta\dot{\eta}_b + \ddot{\eta}_b\delta t_b) = 0, \quad r = 1, \cdots, s.$$

This set of s equations can be solved for s of the variations $\delta\xi_b, \cdots, \delta\dot{\eta}_b, \delta t_b$, in terms of the remaining $(5 - s)$ variations,[3] and the results substituted into Eq. 2.10. The $(5 - s)$ variations remaining in Eq. 2.10 are now arbitrary and independent, so the coefficient of each must vanish. Thus, Eq. 2.10 gives us $(5 - s)$ boundary conditions, and Eqs.

[3] Hence, s cannot exceed 4, since the equations are homogeneous.

2.12 give us s more, making 5 in all. This exhausts the allowable number of boundary conditions.

To summarize the general problem, then, we minimize the fuel consumed, subject to specifying the following conditions: the initial mass, position, and velocity, and no more than four[4] conditions on the position and velocity at the end of burning.

In the restricted problem, we must proceed somewhat differently We must first recognize that it does not make good sense to specify that the functions g_r of Eqs. 2.12 shall vanish. For example, a rocket with a given $M(t)$ function might be capable of a range of 6×10^6 ft. We could certainly find an orientation function $\phi(t)$ such that the function $g = R - 3 \times 10^6$ vanishes, that is, such that the range is half of the potential range, but this does not tell us anything about how to use the given rocket most efficiently. Hence, we shall always phrase the restricted problem in terms of maximizing some function of the conditions at burn-out.

We can also phrase the general problem in similar terms, by fixing the mass M at the end of burning, maximizing one of the g's, say g_1, while still fixing $g_2, \cdots, g_s$. The discussion of the general problem is altered in only one trivial respect. Equations 2.9 still hold, we get $(5 - s)$ conditions from Eq. 2.10, $(s - 1)$ from fixing $g_2, \cdots, g_s$, and one from fixing M_b.

Since the restricted problem is a special case of the general problem, it cannot allow any more freedom in choosing boundary conditions. Also, by inspection of the allowed conditions for the general problem, we see that the restricted problem allows all of them. Hence, the same boundary conditions are allowed for both problems.

This conclusion obviously holds for the burning-time problem as well.

We have assumed a rectangular coordinate system; however, the arguments used make use only of the number of coordinates, and the orders of their derivatives which occur, and hence do not depend upon the coordinate system. If we generalize to three dimensions, we add another fourth-order differential equation to Eqs. 2.9; we add two terms, and hence get two more boundary conditions, in Eq. 2.10; and have one more coordinate and velocity to specify initially.

However, we can now allow s, the number of conditions at burn-out in Eqs. 2.12, to be increased to six. This is the only change needed in the earlier statement of conditions which may be specified, for any coordinate system in three dimensions.

3. MAXIMUM RANGE PROBLEMS

The problems of maximum range, whether general, restricted, or burning time, are capable of an almost endless amount of variation, and we shall not pretend to be exhaustive. Also, except in a few simple

[4] For three-dimensional motion, this is increased to six conditions. See the last paragraph of this section.

cases, we cannot expect to get an answer in closed form. What we do hope to accomplish is to obtain methods of approximation which can be applied in a wide variety of cases.

a. The Restricted Problem in a Vacuum

This problem has been solved by Fried and Richardson (1); we shall apply the results, in our notation, to the special case of constant thrust and constant gravitation. The central result for this problem is that $\phi(t)$ is constant, given by

$$\tan \phi = \xi_b / \sqrt{\dot{\eta}_b^2 + 2g\eta_b}. \tag{3.1}$$

This result holds for any form of the function $T(t)$. The values of ξ_b, $\dot{\eta}_b$, and η_b of course depend upon $T(t)$, as well as upon the value of ϕ, so that Eq. 3.1 is a transcendental equation to be solved for ϕ.

For constant thrust, $\dot{M}$ is constant, and:

$$T = -\dot{M}v_e, \quad M = M_0 + \dot{M}t, \quad \dot{M} < 0. \tag{3.2}$$

Letting

$$\beta = -\dot{M}/M_0, \quad \mu_b = 1 - \beta t_b, \tag{3.3}$$

the position and velocity at the end of burning are readily found to be:

$$\left.\begin{aligned} \dot{\xi}_b &= -v_e \cos\phi \ln \mu_b, \\ \xi_b &= v_e \cos\phi(\mu_b \ln \mu_b + 1 - \mu_b)/\beta, \\ \dot{\eta}_b &= -v_e \sin\phi \ln \mu_b - g(1 - \mu_b)/\beta, \\ \eta_b &= [v_e \sin\phi(\mu_b \ln \mu_b + 1 - \mu_b)/\beta] - g(1 - \mu_b)^2/2\beta^2. \end{aligned}\right\} \tag{3.4}$$

If we substitute these into Eq. 3.1, we find[5]

$$(\cos 2\phi / \sin^2 \phi) = [2(\ln \mu_b + 1 - \mu_b)/\ln^2 \mu_b](g/\beta v_e). \tag{3.5}$$

Since $\cos 2\phi = 1 - 2\sin^2\phi$, this is a cubic to be solved for $\sin\phi$. Substituting for β from Eq. 3.5 into Eqs. 3.4 and then into 2.11, we obtain

$$gR = (v_e^2 \ln^2 \mu_b)(\cos\phi / 2\sin^3\phi). \tag{3.6}$$

Since $\ln \mu_b + 1 - \mu_b$ in Eq. 3.5 is negative, $\cos 2\phi$ must be negative, and $\phi > 45°$, as we expect.

As a numerical example, suppose

$$\left.\begin{aligned} \mu_b &= 0.19, \quad t_b = 50 \text{ sec.}, \quad v_e = 7000 \text{ ft./sec.}, \\ \beta &= 0.0162 \text{ sec.}^{-1}, \quad \ln \mu_b = -1.66\,073. \end{aligned}\right\} \tag{3.7}$$

[5] $\ln^2 \mu_b$ means $(\ln \mu_b)^2$.

Substituting into Eq. 3.5 and solving for ϕ, we find

$$\left.\begin{aligned} \phi &= 0.819\,622 \text{ rad.} = 46.96°, \\ \sin\phi &= 0.730\,888, \cos\phi = 0.682\,497, \end{aligned}\right\} \tag{3.8}$$

using $g = 32.2$ ft./sec.^{2} exactly. For the range, we get

$$R = 366.8 \times 10^4 \text{ ft.}$$

A few other quantities are of interest. βv_e is the initial acceleration due to the jet, about $3.5g$. The initial horizontal acceleration is $2.40g$, the vertical is $1.58g$. Just before the end of burning, the jet acceleration is 598 ft./sec.^{2}, or $18.6g$. The burnt velocities are $\xi_b = 7954$ ft./sec., $\dot{\eta}_b = 6887$ ft./sec. The trajectory at burn-out makes an angle of 40.9° with the horizontal. This is less than the angle which maximizes the range after burning, so in maximizing the range, it is not correct to impose as conditions at the end of burning those conditions which maximize the range of the corresponding inert projectile.

It is usually adequate to neglect ξ_1 and η_1 in Eq. 2.11, yielding:

$$gR = 2\xi_1\dot{\eta}_1.$$

Using this,

$$(\cos 2\phi/\sin\phi) = (g/\beta v_e)(1 - \mu_b)/\ln\mu_b, \tag{3.9}$$

$$gR = 2v_e^2 \ln^2\mu_b(\cos^2\phi/\sin\phi), \tag{3.10}$$

in place of Eqs. 3.5 and 3.6. Using the numerical values of Eq. 3.7, we get $\phi = 47.95°$ instead of 46.96°. If we used the incorrect ϕ, we should get an actual range of 366.6×10^4 ft., a loss of less than one part in a thousand.

b. The General Problem in a Vacuum

As is well known, the equations for the general problem in a vacuum, that is Eqs. 2.9 and 2.10, have no analytic solution. We can easily see this by looking first at the burning-time problem, with the aid of Eqs. 3.5 and 3.6. In Eq. 3.6, for a constant value of $v_e \ln\mu$, the greatest range is attained when $\phi = 45°$. This does not happen because there is a relative maximum of R at 45°; instead, 45° is the smallest value of ϕ with physical significance, and R decreases as ϕ increases. From Eq. 3.5, when ϕ is 45°, β is infinite, and t_b is zero. Thus there is no analytic solution; the closer we can come to instantaneous burning, the better.

If t_b is zero, ξ_b and η_b are zero, while $\dot{\xi}_b$ and $\dot{\eta}_b$ are not. The range is then

$$R = 2\dot{\xi}_b\dot{\eta}_b/g. \tag{3.11}$$

If we reach the condition of instantaneous burning as the limit of any other burning curve than a constant, it does not affect the results, because the velocity depends only upon v_e and the ratio of initial to final mass. Therefore, all modes of instantaneous burning give the same range.

If we take a more inclusive approach, we shall find that there is an optimum burning curve, even in a vacuum. Suppose we have a rocket with constant burning rate, having a long burning time. We can improve the range by shortening t_b, but not as rapidly as Eqs. 3.5 and 3.6 indicate: As we shorten t_b, we must increase the burning rate, the motor pressure, and the motor weight. Eventually, the loss from increased motor weight out-weighs the gain from a shorter t_b, so there is an optimum t_b. Further, the optimum shape of the burning rate curve is probably nearly constant; if it were not, the motor weight would be determined by the maximum burning rate, and most of the time we should therefore be carrying excess weight, and losing range as a result.

The loss of range from having a non-zero burning time is readily estimated from Eqs. 3.5 and 3.6, provided the parameter $\beta v_e/g$, the initial ratio of thrust to weight, is not too small. Assuming that $\beta v_e/g$ is large, we can expand Eqs. 3.5 and 3.6 in powers of $\phi - (\pi/4)$, keep only terms through the first power, and eliminate ϕ, obtaining:

$$gR = v_e^2 \ln^2 \mu_b \{1 - (g/\beta v_e)[\sqrt{2}(\mu_b - 1 - \ln \mu_b)/\ln^2 \mu_b]\}. \quad (3.12)$$

This is quite accurate even for $\beta v_e/g$ as small as 3. We see that the loss in range varies inversely as $\beta v_e/g$; for our example, this loss is 12.6 per cent.

c. The Restricted Problem in Air

The first question which one would probably ask about the problem in air is the accuracy to which the vacuum problem approximates it. One can estimate this accuracy by estimating the aerodynamic forces, using velocities calculated from the vacuum theory; the most important aerodynamic force for present purposes is the drag at zero angle of attack.

As the rocket climbs through the air, its velocity increases, while the air density decreases exponentially. We shall write the air density ρ as

$$\rho = \rho_{SL} f(\eta), \quad (3.13)$$

where ρ_{SL} is the density at sea level. For convenience, we shall assume:

$$f(\eta) = \exp(-a\eta), \quad (3.13a)$$

where $a = 3.34 \times 10^{-5}$ ft.$^{-1}$; this is accurate up to 35,000 ft. Since the air density decreases so rapidly, the drag force should reach a maximum, which we wish to estimate roughly.

Assuming a straight trajectory at an angle Φ with the horizontal, traversed at constant acceleration G, and a drag proportional to some power, α say, of velocity, we want the maximum of $t^\alpha \exp(-aGt^2 \sin \Phi/2)$. This maximum is found to occur always at the same altitude, $\alpha/2a$, independent of G. The velocity at this altitude, which is about 20,000 ft., is almost surely well into the supersonic region; in this region, $\alpha = 1$ with reasonable accuracy over a considerable velocity range. Writing the drag as $g_D v f(\eta)$, $f(\eta)$ is about 0.6 when drag is a maximum, and the maximum is about $0.6 g_D (G/a \sin \Phi)^{1/2}$. We now need some estimates for g_D.

For a rocket of cross-sectional area A, and a drag coefficient of 0.2 at Mach number 4, we get $g_D = 30A$ in f.p.s. units. This must be compared with the mass in order to be significant; for an over-all density of 100 lb./ft.^{3} for the rocket, and a length-to-weight ratio of about 10, the mass M is about $10^3 A^{3/2}$. Thus:

$$g_D \approx 0.3 M^{2/3}.$$

For the ratio, maximum drag divided by weight, we correspondingly obtain:

$$G^{1/3} M^{-1/3},$$

using f.p.s. units for G and M. For rockets capable of reaching high altitudes, this ratio is not likely to exceed unity, hence the ratio of drag to thrust for such rockets is expected to be much less than unity.

From the preceding discussion, we can reach two conclusions: First, the vacuum theory gives a reasonable approximation for a wide variety of cases. Second, aerodynamic forces are probably most important at supersonic velocities. In accordance with the latter conclusion, we shall find it convenient to write:

$$\left.\begin{aligned} \text{drag} &= g_D f(\eta) v (1 + k_D \alpha^2), \\ \text{lift} &= g_L f(\eta) v \alpha, \end{aligned}\right\} \tag{3.14}$$

with $f(\eta)$ defined by (3.13), and with g_D and g_L being slowly varying functions of velocity. The constant k_D is a measure of induced drag; k_D is approximately equal to $1 + (g_L/g_D)$. For numerical examples, we shall use

$$g_D = 0.0162 M_0 \text{ lb./sec.}, \quad g_L = 5 g_D, \quad k_D = 6. \tag{3.15}$$

These values were chosen for convenience, and seem to us to make aerodynamic forces about as large as they are likely to be for the class

of problems we are considering. In any actual case in which aerodynamic data are available, one should either use actual values, or use the best fit to the form of Eqs. 3.14 at the velocities where drag is expected to be largest.

We shall continue, in this section, to neglect drag after the end of burning, and to use Eq. 2.11 for the range. Unless the drag after burning is quite high, the conditions which maximize the range in vacuum should be close to those which maximize the actual range.

If the vacuum theory furnishes a reasonable approximation, what we must do is to calculate differences from the vacuum theory. This suggests that we transform to the coordinate system of Fig. 1, with an

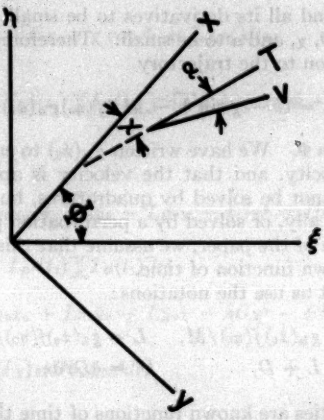

FIG. 1. Coordinates used for the maximum range problem in air.

x-axis rotated from the ξ-axis by an angle Φ. For Φ, we use the constant value of ϕ furnished by the vacuum theory. We have chosen the y-axis in the direction shown so as to make y positive for the vacuum solution. Let χ be the angle between the rocket axis, which is the direction of the jet thrust T, and the x-axis, and let α be the angle of attack. All angles are positive if they have the senses of rotation shown in the figure. If θ is the angle between x and the velocity v, so that

$$\theta = \tan^{-1}(\dot{y}/\dot{x}) \approx \dot{y}/v, \tag{3.16}$$

the angles θ, χ, and α are related by

$$\theta = \chi + \alpha. \tag{3.17}$$

If the (x, y) coordinate system, the equations of motion (2.6) become, upon using Eqs. 3.14 for drag and lift, and after dividing by the mass M, and letting $G = T/M$

$$\left.\begin{aligned}\ddot{x} &= G\cos\chi - g\sin\Phi - M^{-1}f(\eta)g_D(1 + k_D\alpha^2)\dot{x} + M^{-1}f(\eta)g_L\alpha\dot{y},\\ \ddot{y} &= G\sin\chi + g\cos\Phi - M^{-1}f(\eta)g_D(1 + k_D\alpha^2)\dot{y} - M^{-1}f(\eta)g_L\alpha\dot{x},\end{aligned}\right\} \tag{3.18}$$

the transformation from x, y to ξ, η, being:

$$\left.\begin{aligned}\xi &= x\cos\Phi + y\sin\Phi,\\ \eta &= x\sin\Phi - y\cos\Phi.\end{aligned}\right\} \tag{3.19}$$

We expect y and all its derivatives to be small, and therefore also expect the angles θ, χ, and α to be small. Therefore, we take as a zero-order approximation to the trajectory

$$\ddot{x}_0 = G - g\sin\Phi - M^{-1}f(\eta_0)g_D(\dot{x}_0)\dot{x}_0, \tag{3.20}$$

in which η_0 is $x_0\sin\Phi$. We have written $g_D(\dot{x}_0)$ to emphasize that g_D is a function of velocity, and that the velocity is approximated by $\dot{x}_0$. Equation 3.20 cannot be solved by quadratures, but it can readily be integrated numerically, or solved by a perturbation procedure. In the rest of this portion of the paper, we assume that this has been done, so that $x_0(t)$ is a known function of time.

For brevity, let us use the notations:

$$\left.\begin{aligned}D &= g_D(\dot{x}_0)f(\eta_0)/M, \quad & L &= g_L(\dot{x}_0)f(\eta_0)/M,\\ N &= L + D, & D' &= \partial D/\partial\eta_0;\end{aligned}\right\} \tag{3.21}$$

all of these quantities are known functions of time through our knowledge of x_0. Let us further define three quantities y_0, x_1, and y_1 by means of the differential equations

$$\left.\begin{aligned}&\ddot{y}_0 + N\dot{y}_0 = G\chi + g\cos\Phi + L\dot{x}_0\chi,\\ &\ddot{x}_1 + D\dot{x}_1 = -(G\chi^2/2) + y_0\cos\Phi D'\dot{x}_0 + L\theta_0\dot{y}_0 - L\dot{y}_0\chi - Dk_D\dot{x}_0\alpha^2,\\ &\ddot{y}_1 + N\dot{y}_1 = -Dk_D\dot{y}_0\alpha^2,\end{aligned}\right\} \tag{3.22}$$

with $\theta_0 = \dot{y}_0/\dot{x}_0$. These equations can be solved successively by quadratures. By direct substitution, remembering Eq. 3.17, we can verify that

$$x = x_0(t) + x_1(t), \quad y = y_0(t) + y_1(t), \tag{3.23}$$

are the solutions of the equations of motion (3.18), through the first order of small quantities. We assume that $g_D(v)$ can always be re-

placed by $g_D(\dot{x}_0)$; this should be highly accurate, since g_D varies slowly with v, and the y component of velocity hardly alters the speed.

By repeated integrations in the first of Eqs. 3.22, we can obtain successively $\dot{y}_0(t)$ and $y_0(t)$. Then, by substitution into the other equations, further integrations yield $x_1(t)$ and $y_1(t)$. By systematic reversal of the order of integration in all multiple integrations, we can write all results in terms of single integrals, if we make use of the functions

$$I_N(t) = \exp\left[-\int_0^t N(t_1)dt_1\right], \quad I_{N^1}(t) = \int_0^t I_N(t_1)dt_1, \tag{3.24}$$

and similarly defined functions $I_D(t)$ and $I_{D^1}(t)$. The results are:

$$\dot{y}_0 = I_N(t)\int_0^t (I_N)^{-1}[G\chi + g\cos\Phi + L\dot{x}_0\chi]dt_1, \tag{3.25}$$

$$y_0 = \int_0^t [I_{N^1}(t) - I_{N^1}(t_1)][I_N(t_1)]^{-1}[G\chi + g\cos\Phi + L\dot{x}_0\chi]dt_1, \tag{3.26}$$

$$\dot{x}_1 = I_D(t)\int_0^t (I_D)^{-1} \times [D'\cos\Phi y_0\dot{x}_0 + L\theta_0\dot{y}_0 - L\dot{y}_0\chi - \tfrac{1}{2}G\chi^2 - Dk_D\dot{x}_0\alpha^2]dt_1, \tag{3.27}$$

$$x_1 = \int_0^t [I_{D^1}(t) - I_{D^1}(t_1)][I_D(t_1)]^{-1} \times [D'\cos\Phi y_0\dot{x}_0 + L\theta_0\dot{y}_0 - L\dot{y}_0\chi - \tfrac{1}{2}G\chi^2 - Dk_D\dot{x}_0\alpha^2]dt_1, \tag{3.28}$$

$$\dot{y}_1 = -I_N(t)\int_0^t (I_N)^{-1}Dk_D\dot{y}_0\alpha^2dt_1, \tag{3.29}$$

$$y_1 = -\int_0^t [I_{N^1}(t) - I_{N^1}(t_1)][I_N(t_1)]^{-1}Dk_D\dot{y}_0\alpha^2dt_1. \tag{3.30}$$

Dummy variables of integration have been omitted where there seems little danger of ambiguity.

By taking variations in Eq. 2.11

$$\delta R = \delta\xi_b + t_f\delta\dot{\xi}_b + \dot{\xi}_b(\dot{\eta}_b^2 + 2g\eta_b)^{-1/2}(\delta\eta_b + t_f\delta\dot{\eta}_b),$$

where

$$gt_f = \dot{\eta}_b + (\dot{\eta}_b^2 + 2g\eta_b)^{1/2}, \tag{3.31}$$

t_f being the time of flight after burning. It is clear that

$$\left.\begin{aligned}\delta\xi_b &= \delta x_{1b}\cos\Phi + (\delta y_{0b} + \delta y_{1b})\sin\Phi,\\ \delta\eta_b &= \delta x_{1b}\sin\Phi - (\delta y_{0b} + \delta y_{1b})\cos\Phi,\end{aligned}\right\} \tag{3.32}$$

since x_0 does not involve χ, and hence δx_0 is zero. Then:

$$\delta R = 0 = \{\cos\Phi + \xi_b(\dot\eta_b^2 + 2g\eta_b)^{-1/2}\sin\Phi\}\{\delta x_{1b} + t_f\delta\dot x_{1b}\} + \{\sin\Phi - \xi_b(\dot\eta_b^2 + 2g\eta_b)^{-1/2}\cos\Phi\}\{\delta y_{0b} + \delta y_{1b} + t_f(\delta\dot y_{0b} + \delta\dot y_{1b})\}.$$

We adopt further abbreviations:

$$\left.\begin{aligned} A &= (\dot\eta_b^2 + 2g\eta_b)^{1/2}\cos\Phi + \xi_b\sin\Phi, \\ S &= (\dot\eta_b^2 + 2g\eta_b)^{1/2}\sin\Phi - \xi_b\cos\Phi, \end{aligned}\right\} \tag{3.33}$$

in terms of which

$$A(\delta x_{1b} + t_f\delta\dot x_{1b}) + S[\delta y_{0b} + \delta y_{1b} + t_f(\delta\dot y_{0b} + \delta\dot y_{1b})] = 0.$$

A and S are not known, because the terminal position and velocity depend upon χ.

We get the variations δy_{0b}, etc., from Eqs. 3.25 to 3.30 by a succession of simple steps: Replace t by t_b, allowing us to replace t_1 by t without ambiguity, then take the variations of the integrals. Since the limits are fixed, we can take variations under the integral sign; quantities in the integrands which are to be varied are χ, y_0, $\dot y_0$, θ_0, and α. The only independent variation is $\delta\chi$; for the others, we take

$$\delta\dot y_0 = I_N(t)\int_0^t (I_N)^{-1}(G + L\dot x_0)\delta\chi\,dt,$$

$$\delta y_0 = \int_0^t [I_N{}^1(t) - I_N{}^1(t_1)][I_N(t_1)]^{-1}(G + L\dot x_0)\delta\chi\,dt,$$

$$\delta\theta_0 = \delta\dot y_0/\dot x_0, \quad \delta\alpha = \delta\theta_0 - \delta\chi,$$

it being understood that the last two are to be expressed in terms of $\delta\chi$, using the integral for $\delta\dot y_0$.

When we carry out all of these steps, we finally arrive at a single integral which is equal to zero, and whose integrand is the product of $\delta\chi$ with a complicated function involving x_0, y_0, χ, etc. Since $\delta\chi$ is arbitrary, the function which multiplies $\delta\chi$ must equal zero. Using still another abbreviation:

$$g_N(t_b, t) = [I_N{}^1(t_b) - I_N{}^1(t) + t_f I_N(t_b)]/I_N(t), \tag{3.34}$$

and a similar abbreviation $g_D(t_b, t)$, this function is

$$\begin{aligned} &- Ag_D(t_b, t)(G\chi + L\dot y_0) + Sg_N(t_b, t)(G + L\dot x_0) + 2Ag_D(t_b, t) \\ &\quad \times Dk_D\dot x_0(\theta_0 - \chi) + 2Sg_N(t_b, t)Dk_D\dot y_0(\theta_0 - \chi) + (I_N)^{-1}(G + L\dot x_0) \\ &\quad \times \int_t^{t_b} \{I_N Ag_D(t_b, t_1)[L(2\theta_0 - \chi) - 2Dk_D(\theta_0 - \chi)] \\ &\qquad + [I_N{}^1(t_1) - I_N{}^1(t)]Ag_D(t_b, t_1)D'\cos\Phi\dot x_0\}dt_1 = 0. \end{aligned}$$

S is small compared with A, and $\dot{y}_0$ is small compared with $\dot{x}_0$. Hence, the fourth term can be neglected in comparison with the third. The function $\chi(t)$ must now be chosen so as to satisfy this equation.

This equation is a complicated integral equation for χ. Not only does χ occur explicitly, but also implicitly, since the functions y_0, θ_0, g_N, and g_D, as well as the constants A and S, depend upon the choice of χ. The equation is best solved by successive approximations; a convenient form of the equation for this purpose is[6]

$$I_N g_D (G + 2Dk_D\dot{x}_0)(G + L\dot{x}_0)^{-1}\chi$$

$$= (Sg_N I_N/A) + \int_t^{t_b} [I_N^1(t_1) - I_N^1(t)] g_D(t_b, t_1) D' \cos\Phi \dot{x}_0 dt_1$$

$$+ g_D I_N (2Dk_D - L)(G + L\dot{x}_0)^{-1}\dot{y}_0 + \int_t^{t_b} I_N g_D(t_b, t_1)$$

$$\times [L(\chi + 2\alpha) - 2Dk_D\alpha] dt_1. \quad (3.35)$$

None of the terms on the right is really independent of χ, however, the first two depend upon χ but slightly.

Hence, we have the following steps in calculating an approximate solution $\chi(t)$ for the best orientation of the axis:

1. Find the best value of ϕ in a vacuum from Eq. 3.5, or an equivalent equation if T is not constant. Call this value Φ.
2. Solve Eq. 3.20. Using the solution x_0, tabulate the functions D, L, D', I_N, I_N^1, I_D, I_D^1, defined in Eqs. 3.21 and 3.24.
3. Assuming that y is identically zero, and that x equals x_0, calculate A, S, $g_N(t_b, t)$, and $g_D(t_b, t)$ from Eqs. 3.33 and 3.34.
4. Neglecting the last two terms in the right member of Eq. 3.35, solve that equation to get a first approximation to χ, say χ_0.
5. Use χ_0 for χ in Eqs. 3.25 and 3.26 to calculate y_0 and $\dot{y}_0$, and then calculate α from $\alpha = (\dot{y}_0/\dot{x}_0) - \chi_0$.
6. Using the values from Step 5, calculate the last two terms on the right of Eq. 3.35, and combine with the estimate already made of the first two terms to get a new approximation for χ, say χ_1.

We have carried this process out, with the numerical values used in our previous numerical examples. The results for $\chi_0(t)$ and $\chi_1(t)$ are shown in Fig. 2. We see that χ_1 differs considerably from χ_0 for small t. Such behavior would normally lead us to think that the method of successive approximations used in calculating χ_1 does not converge rapidly, and hence that χ_1 itself is a poor approximation. However, the early values of χ are determined to a considerable extent by the values of χ late in burning, when χ_0 and χ_1 agree rather well, and χ_1 seems to be actually a good approximation to the solution of Eq. 3.35.

[6] As we shall see in a minute, χ can be replaced by $\tan\chi$ in the left member of Eq. 3.35, but not in the right member.

However, there is still a possible difficulty. The early values of χ_1 may be large enough that the use of χ for $\sin \chi$ may not be justified. This difficulty disappears if we note that, when t and hence $\dot{x}_0$ are small, the left member of Eq. 3.35 is approximately

$$I_{N\vartheta_D}(G\chi/G).$$

If we trace through the derivation, we note that $G\chi$, in the numerator, came from differentiating $G \cos \chi$, yielding $-G \sin \chi$, then approximating this by $-G\chi$, and finally changing the sign. The G in the denominator came from differentiating $G \sin \chi$, yielding $G \cos \chi$, then replacing $\cos \chi$ by unity. Hence, χ in the left member of Eq. 3.35, but not elsewhere, can be replaced by $\tan \chi$. Thus, as a final step 7 to follow the steps previously enumerated:

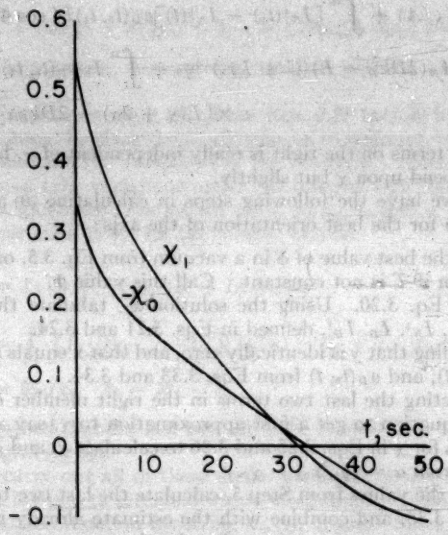

FIG. 2. An optimum orientation function for the maximum range problem. χ_0 is the zero-order approximation, χ_1 is the tangent of the angle given by the first-order approximation.

7. For the optimum $\chi(t)$, use $\tan^{-1} \chi_1$.

Equation 3.35 equates the change in a loss, the left member, to the sum of the changes in several gains, as we try to improve the range by pointing the axis up more steeply than the constant angle Φ. The gains are:

1. Lift, which is upward and tends to increase the range.
2. Increased altitude, which decreases the drag.
3. Smaller α, which decreases the induced drag.

For our example, the effects of increased altitude and of induced drag are about equal (χ_0 primarily depends upon the altitude effect, and $\chi_0 - \chi_1$ upon the induced drag effect). If the lift is large, so is the induced drag, and induced drag gives the dominant effect of these three. The loss is a very severe one; as we point the axis away from the desired direction of travel, we acquire momentum in an undesired direction. This momentum must be killed by adding yet more momentum in the equally undesired opposite direction. Hence, we cannot tolerate pointing the rocket off the desired heading very long.

In summary, the optimum trajectory in air is determined mostly by allowing a small loss in the form of undesired momentum to be balanced by the advantages of a small angle of attack, and a steep climb of short duration, in order to decrease air density. The optimum trajectory, then, tends to be characterized by small angles of attack.

We took the function $\chi(t)$, calculated as above, and used it in a numerical integration of the equations of motion. We also integrated the equations of motion using the constant tilt angle furnished by the vacuum solution, that is, with $\chi(t) \equiv 0$. Using $\chi \equiv 0$, the resultant range was 76.25 per cent of the range in vacuum; the other $\chi(t)$ function gave 77.56 per cent of the range in vacuum, a gain of 1.31 per cent of the vacuum range, or 1.69 per cent of the actual range.

Such a small gain is to be expected. By using the optimum $\chi(t)$, we do not affect the gravity loss, only the drag loss, which is 23.75 per cent of the vacuum range if we use the vacuum theory. Even if we could fire vertically, we would only expect to reduce the drag loss by a factor of about $\sqrt{2}$ (by decreasing the distance travelled in air), saving about 7 per cent of the vacuum range. Since we cannot hold the axis vertical for very long, the best gain we can expect is a small fraction of 7 per cent.

Because the gain which can be expected over the results given by vacuum theory is typically so small, we feel that it is not important to have an accurate theory in allowing for aerodynamic effects. This constitutes the ultimate justification for some of the assumptions we have made, which would be considered quite crude for some purposes.

Figure 3 shows the shapes of the trajectories using the optimum $\chi(t)$ and using $\chi = 0$, the vacuum theory result. The optimum trajectory has only a slight curvature, a result which we expect to hold unless the initial thrust-to-weight ratio is very nearly unity. The x-axis is also shown in Fig. 3 for comparison.

In this portion of Sec. 3, we have considered the thrust to be a known function of time, and varied only the orientation. In the remaining parts of this section, we consider both the thrust and the orientation to

be variable. However, the results of this section allow us to separate, to satisfactory accuracy, the variations in thrust and orientation: Since the optimum trajectory is nearly straight, we can study the thrust variations by assuming the rocket to be constrained to a straight line, and optimize the range under this constraint. Using the thrust function so determined, we find the best orientation function for this thrust program. If we wish, we can repeat the process, using the newly determined curve as the curve of constraint, and so on, but it seems

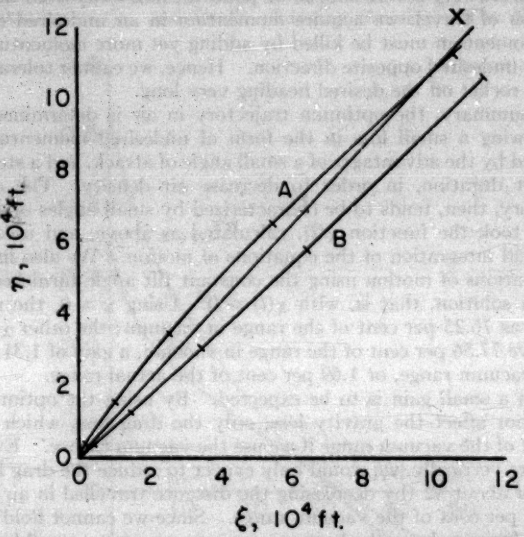

FIG. 3. Shape of an optimum trajectory for the maximum range problem. Curve *A* is the optimum trajectory; Curve *B* is the trajectory which would be followed in air by a rocket using the orientation function which is optimum in a vacuum. The cross-marks on the curves are at time intervals of 10 sec. The *x*-axis is shown for comparison.

unlikely that this repetition will be warranted in most cases, particularly since we shall find that the optimum initial thrust is many times the initial weight.

Through the first step of this process, the problem of studying the thrust function to give maximum range is identical with the problem of attaining maximum summit altitude in vertical firing, provided that we use the appropriate component of gravity and the appropriate dependence of air density upon position. If we use (3.13*a*) for the variation of density, the latter means simply changing the constant a in the exponent. Hence, in the remaining maximum range problems, we shall speak as though we were studying vertical firing.

d. The Burning-Time Problem in Air

In this problem, we start with a given shape of the thrust-time curve, and vary the burning time while keeping the total fuel consumption constant.

If the total distance travelled by the rocket is large compared with the burning distance and with the effective thickness of the atmosphere, the losses can be considered as applied impulsively, and maximization of distance is equivalent to minimizing the non-conservative losses in velocity. These losses are two: (1) gravity loss during burning, which is simply gt_b, and (2) the total velocity loss to drag.

To study the latter loss, let $\mathfrak{D}$ denote the drag force, and let:

$$\left.\begin{aligned} \mu &= M/M_0, \\ \mathfrak{D} &= Cv^\alpha \exp(-as), \end{aligned}\right\} \tag{3.36}$$

where s is distance travelled. The velocity loss is the time integral of $\mathfrak{D}/M$ over the time interval for which drag is significant; because the density decreases so rapidly, we can make the upper limit infinity without appreciable error.

We therefore need to choose the burning time so as to minimize

$$gt_b + (C/M_0)\int_0^\infty (v^{\alpha-1}/\mu)\exp(-as)ds. \tag{3.37}$$

For a given shape of the thrust-time curve, the entire curve can be identified by a single parameter β. t_b is then a function of β; v and μ can be considered as formal functions of s and β. We want the derivative of expression (3.37) with respect to β to vanish[7]:

$$g(dt_b/d\beta) + (C/M_0)\int_0^\infty \exp(-as)\{[(\alpha-1)v^{\alpha-2}(\partial v/\partial\beta)/\mu] - [v^{\alpha-1}(\partial\mu/\partial\beta)/\mu^2]\}ds = 0. \tag{3.38}$$

$(\partial v/\partial\beta)$ and $(\partial\mu/\partial\beta)$ are to be evaluated at constant s; after the end of burning, $\partial\mu/\partial\beta = 0$. It will usually be accurate enough to use values of v and μ from vacuum theory; if this is done, Eq. 3.38 is readily solved numerically.

In order to proceed further, we need to assume an explicit thrust function. We shall again assume constant thrust, and shall let the parameter β be the β of Sec. 3.*a*. We shall also use $\alpha = 1$, replacing C by the g_D of Sec. 3.*c*. v and s are the same as $\dot{\eta}_b$ and η_b in Eqs. 3.4, if we let $\sin\phi = 1$, use the component of g along s, and replace μ_b by μ. Substituting into Eq. 3.38, and transforming the variable of integration to μ,

[7] As we shall show in Sect. 3.e, C is discontinuous at the end of burning. This introduces another term into the left member of Eq. 3.38, which we shall ignore here.

$$1 - \mu_b = (g_D v_e / M_0 g) \int_{\mu_b}^{1} \mu^{-2} \exp(-as) \times [\mu \ln \mu + 1 - \mu - (g/\beta v_e)(1-\mu)^2] d\mu. \quad (3.39)$$

We can write as in the form

$$as = (av_e^2/g)(g/\beta v_e)[\mu \ln \mu + 1 - \mu - (g/2\beta v_e)(1-\mu)^2].$$

If the trajectory is a straight line in an arbitrary direction, a and g depend individually upon the direction, but their ratio does not. For given μ_b, then, we can evaluate the integral in (3.39) as a function of the parameter $\beta v_e/g$, and use the results either for vertical firing or in

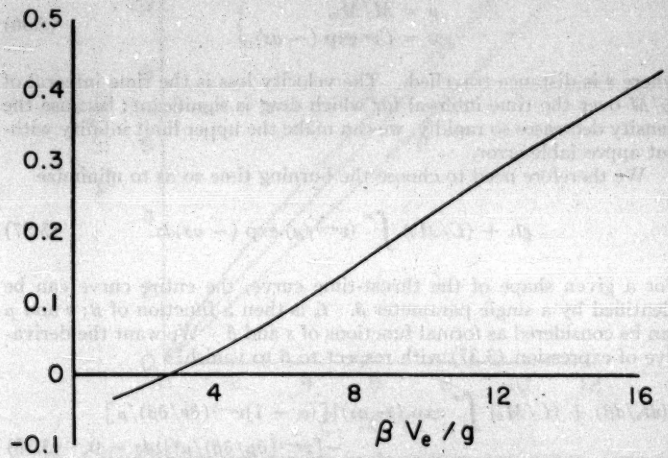

FIG. 4. The integral used in calculating the optimum constant thrust, as a function of the initial thrust-to-weight ratio ($\beta v_e/g$).

firing for maximum range. Figure 4 shows how the integral varies with this parameter for values from unity to 16. Values less than unity are not physically significant; for values greater than about four, for which our theory is principally intended to apply, the integral is almost a linear function of ($\beta v_e/g$), the initial thrust-to-weight ratio. We have continued to use $\mu_b = 0.19$ and $v_e = 7000$ ft./sec.

For firing at 45° with the horizontal, which gives very nearly maximum range, and $g_D = 0.0162\, M_0$, as before, the integral must equal 0.163. From Fig. 4, $\beta v_e/g = 8.35$, requiring that βv_e equal $(8.35)(32.2/\sqrt{2}) = 190$ ft./sec.^{2}, whence $\beta = (190/7000) = 0.0271$ sec.$^{-1}$,

and $t_b = 29.9$ sec. For vertical firing, the integral must equal 0.230, making $\beta v_e = 333$ ft./sec.^{2}, $\beta = 0.0475$ sec.$^{-1}$, and $t_b = 17.0$ sec.

It seems plausible that these results give the distance travelled during burning more accurately than the time itself, because the variation of the integral with $\beta v_e/g$ is dominated by the appearance of that parameter in exp $(-\alpha s)$. In the last example, the altitude at burn-out is 68,000 ft. If we wish to correct the time to reach this altitude because of velocity lost to drag, making a very rough calculation of the correction, we change t_b to 18.4 sec. and $\beta = 0.0441$ sec^{-1}.

As a check, we integrated the equations of motion numerically for $\beta = 0.0441$ sec^{-1}. To facilitate comparison with the results of the next part, where we calculate the optimum thrust function, we calculated the velocity at an altitude of 108,650 ft., and found it to be 9765.1 ft./sec. Since the maximum obtainable with variable thrust, but with other parameters unchanged, is shown to be 9970.6 ft./sec. at this altitude, we must be quite close to the maximum obtainable with constant thrust.

The method of this section can readily be extended to include any variation in structural weight with acceleration or burning time; all that is needed is to differentiate M_0 in expression (3.37), as well as the other quantities which depend upon the acceleration. Investigating the dependence of M_0 upon β is beyond the scope of this paper.

e. The General Problem in Air

As we pointed out earlier, the problem of determining the thrust function to give maximum range is almost identical with the optimum thrust problem in vertical firing, provided that we use appropriate values for g and for the constant in the air density variation. The vertical firing problem has been discussed by earlier writers (3, 4, 5, 6); we shall first summarize briefly their results.

The problem is now one-dimensional, so we now have to deal with only one of Eqs. 2.9, we have two conditions at the beginning of burning, namely $\eta = \dot{\eta} = 0$, and will have three boundary conditions imposed at the end of burning. However, the differential equation degenerates to second-order, so that there are two boundary conditions too many. Thus, there is no analytic solution to the problem.

That the differential equation is only second-order can be discovered by substituting into the general form of Eqs. 2.9, or perhaps more simply by deriving the Euler-Lagrange equation for the problem directly. Writing $\mathfrak{D}(\eta, \dot{\eta})$ for the drag force, the equation of motion is simply

$$-\dot{M}v_e = M(\ddot{\eta} + g) + \mathfrak{D}(\eta, \dot{\eta}).$$

This integrates immediately to:

$$M = \exp[-(\dot{\eta}+gt)/v_e]\left\{M_0 - v_e^{-1}\int_0^t \mathfrak{D}(\eta, \dot{\eta}) \exp[(\dot{\eta}+gt)/v_e]dt\right\}. \quad (3.40)$$

Since the integral involves only η and $\dot{\eta}$, the Euler-Lagrange equation is second-order; it is in fact

$$v_s(\partial \mathfrak{D}/\partial \eta) - v_s(\partial \mathfrak{D}/\partial \dot{\eta})^{\cdot} - \dot{\mathfrak{D}} - (\ddot{\eta} + g)[(\partial \mathfrak{D}/\partial \dot{\eta}) + (\mathfrak{D}/v_s)] = 0. \quad (3.41)$$

This depends only upon the form of the drag function, and not upon the size of the drag coefficient.

Since there are too many boundary conditions, there must be discontinuities in $\dot{\eta}$, unless the surplus boundary conditions are automatically satisfied by the solution of the problem formed by omitting them. It has been shown that $\dot{\eta}$ changes discontinuously from 0 to some positive value, $\dot{\eta}_0$ say, at $t = 0$. This naturally suggests the use of a booster, and Leitmann (4) has investigated the modified problem posed by having the booster drop off. It has been shown that there is no discontinuity in $\dot{\eta}$ at the end of burning, but the proof depends upon assuming no change in the drag coefficient at the end of burning. However, there are at least three reasons why the drag coefficient should decrease after burning:

1. The payload may be detached from the motor. This may produce a large change.
2. Cessation of the jet may alter the air flow around the rocket. This is probably a small effect.
3. Cessation of the jet decreases the drag coefficient by the ratio of the base pressure to the free stream dynamic pressure.

The last effect can be appreciable. Using M for Mach number momentarily, the ratio of static to dynamic pressure is $(\frac{1}{2}\gamma M^2)^{-1}$; for a diatomic gas, this is $(0.7\,M^2)^{-1}$. The fractional change in C_D is $1/(0.7\,M^2 C_D) \approx 1/0.56\,M$, using our earlier assumption about the behavior of C_D. At Mach 5, the change is one part in 2.8, at Mach 10, one part in 5.6.

We must now formulate the problem in a way which allows a discontinuity in $\dot{\eta}$ at the end of burning. Equation 3.40 still correctly describes the mass variation, and correctly charges to total fuel consumption the fuel required to produce the initial discontinuity $\dot{\eta}_0$ in $\dot{\eta}$. Equation 3.41 will still be obeyed by η until time t_b; at this time, let $\eta = \eta_2$, $\dot{\eta} = \dot{\eta}_2$, and $M = M_2$. Then we shall allow $\dot{\eta}$ to change discontinuously to the value $\dot{\eta}_b$, and M to the value M_b, without changing η. There is the obvious requirement that $\dot{\eta}_b \geq \dot{\eta}_2$. Let the drag function during burning be denoted by $\mathfrak{D}^-(\eta, \dot{\eta})$, and after burning by $\mathfrak{D}^+(\eta, \dot{\eta})$.

We shall speak in terms of fixing the summit altitude, and minimizing the fuel consumption. To impose the condition of fixing the summit altitude, we follow Leitmann (4), and imagine the equation of motion after burning to be integrated, and the result expressed as

$\dot{\eta} = g(\eta)$. When $\dot{\eta}$ is zero, η has a fixed value which is the summit altitude. Evaluating at the beginning of unpowered flight:

$$\dot{\eta}_b = g(\eta_2) \tag{3.42}$$

is the condition to be imposed.

When we take the variation of M_b, the quantities to be varied are t_b, η_2 and $\dot{\eta}_b$, as well as $\eta(t)$ and $\dot{\eta}(t)$ for all $t \leq t_b$. Since we already know the differential equation of the trajectory, we need consider only variations in the end conditions. Proceeding in the usual fashion, we get

$$M_2\delta\dot{\eta}_b + [gM_2 + \mathfrak{D}^-(\eta_2, \dot{\eta}_2)]\delta t_b + [(\partial\mathfrak{D}^-/\partial\dot{\eta}_2) + v_e^{-1}\mathfrak{D}^-(\eta_2, \dot{\eta}_2)]\delta\eta_2 = 0, \tag{3.43}$$

from $\delta M_b = 0$. From taking variations in Eq. 3.42,

$$\delta\dot{\eta}_b - g'(\eta_2)[\delta\eta_2 + \dot{\eta}_2\delta t_b] = 0. \tag{3.44}$$

Upon eliminating δt_b between Eqs. 3.43 and 3.44, $\delta\dot{\eta}_b$ and $\delta\eta_2$ become independent, so their coefficients vanish, yielding

$$g'(\eta_2)\dot{\eta}_2M_2 + gM_2 + \mathfrak{D}^-(\eta_2, \dot{\eta}_2) = 0, \tag{3.45}$$

$$\dot{\eta}_2[(\partial\mathfrak{D}^-/\partial\dot{\eta}_2) + v_e^{-1}\mathfrak{D}^-(\eta_2, \dot{\eta}_2)] - gM_2 - \mathfrak{D}^-(\eta_2, \dot{\eta}_2) = 0. \tag{3.46}$$

These, along with $\eta(0) = 0$, are conditions to be imposed upon the solution of Eq. 3.41; this is the correct number of conditions, since the end time t_b is unknown.

The solution of the system is straightforward in principle. Leitmann (4) has shown that the solution of

$$\dot{\eta}[(\partial\mathfrak{D}^-/\partial\dot{\eta}) + v_e^{-1}\mathfrak{D}^-] - gM - \mathfrak{D}^- = 0 \tag{3.47}$$

satisfies Eq. 3.41, as well as (3.46). We therefore have only to integrate (3.47), with $\eta(0) = 0$, until (3.45) is satisfied. Since $\dot{\eta}_b$ can be calculated from (3.42) once η_2 is known, we have the solution to the problem.

It is useful to rewrite the boundary conditions in a way which involves the discontinuity. The acceleration immediately after burning can be written as $\dot{\eta}_b g'(\eta_2)$, hence the equation of motion immediately after burning is

$$g'(\eta_2)\dot{\eta}_bM_b + gM_b + \mathfrak{D}^+(\eta_2, \dot{\eta}_b) = 0.$$

Eliminating $g'(\eta_2)$ between this and Eq. 3.45, we get

$$\dot{\eta}_2^{-1}[g + M_2^{-1}\mathfrak{D}^-(\eta_2, \dot{\eta}_2)] = \dot{\eta}_b^{-1}[g + M_b^{-1}\mathfrak{D}^+(\eta_2, \dot{\eta}_b)]. \tag{3.48}$$

If $\mathfrak{D}^-$ and $\mathfrak{D}^+$ are positive and increase monotonically to infinity as $\dot{\eta} \to \infty$, it is not difficult to show the following, regarding $\dot{\eta}_b$ as the unknown in Eq. 3.48:

1. If $\mathfrak{D}^+ \equiv \mathfrak{D}^-$, $\dot{\eta}_b = \dot{\eta}_2$ is the only root, and is double.
2. If $\mathfrak{D}^+ > \mathfrak{D}^-$ for the same values of the arguments, the only possible roots are with $\dot{\eta}_b < \dot{\eta}_2$, which violates the constraints. Hence, there is no terminal discontinuity in $\dot{\eta}$ for this case, which is unlikely to occur.
3. If $\mathfrak{D}^+ < \mathfrak{D}^-$ for the same values of the arguments, which is the most probable case, there are two roots; one and only one has $\dot{\eta}_b > \dot{\eta}_2$, and is the desired root.

Continuing with the numerical values we have used before, we solved the system of equations numerically for vertical firing, first under the assumption that $\mathfrak{D}^+ \equiv \mathfrak{D}^-$. The initial velocity $\dot{\eta}_0$ was 3,008.7 ft./sec. The acceleration was 105.4 ft./sec.^{2} immediately after the initial impulse; at burn-out, which occurred at 20.63 sec., $\bar{\eta} = 946.4$ ft./sec.^{2}, $\dot{\eta} = 9970.6$ ft./sec. and $\eta = 108{,}650$ ft. This is the case to be compared with the optimum constant thrust, which gave $\dot{\eta} = 9765.1$ ft./sec. at the same altitude, a loss of 2 per cent in velocity. Considering the higher structural weights which would be required with the variable thrust program, the difference would be even less.

To investigate the effect of changing the drag function, we assumed that the drag coefficient changed by 14 per cent, which happened to be convenient for numerical reasons. The trajectory was the same until the discontinuity occurred, which was at 17.1 sec., with $\eta_2 = 78{,}450$ ft., $\dot{\eta}_2 = 7363.4$ ft./sec., $\dot{\eta}_b = 10{,}177.8$ ft./sec. At 108,650 ft., $\dot{\eta}$ was 9979.5 ft./sec., a gain of about one part in a thousand. We expect the change in drag coefficient to be greater than 14 per cent at 7360 ft./sec., even with no detachment of the payload, but even so, the gain from using an impulse at the end of burning will not be large unless there is detachment.

One further interesting property of the optimum solution should be pointed out. In Eq. 3.47, if $\mathfrak{D}^-$ is proportional to $\dot{\eta}^\alpha$, $\partial \mathfrak{D}^- / \partial \dot{\eta} = \alpha \mathfrak{D}^- / \dot{\eta}$, and the equation becomes

$$(gM/\mathfrak{D}^-) = \alpha - 1 + (\dot{\eta}/v_e).$$

Since $\dot{\eta}$ is initially rather large, this says that drag and weight are always roughly equal for the optimum. This result seems plausible for the constant thrust case, also, since gravity loss and drag loss change in opposite directions as we change the thrust, but it is difficult to establish it rigorously.

The fact that the optimum variable thrust function gives only a slight improvement over the optimum constant thrust shows that, in

this problem as well as in the restricted maximum range problem, the optimum is very flat; a wide departure from optimum conditions causes a loss of only one or two per cent. This is perhaps our most important conclusion, and it has two important corollaries. First, it is not necessary to use a highly accurate theory in calculating an optimum trajectory. Second, it is not necessary that a rocket follow the optimum trajectory closely.

4. ORBIT PROBLEMS

In this section, we turn from the maximum range problem to the more difficult orbit problem. There is, of course, a wide variety of possible orbits, and we cannot try to treat them all in detail. We choose for treatment the typical one of requiring that the rocket attain a horizontal velocity of specified magnitude at a specified altitude.

The orbit problem is more difficult than the maximum range problem because it poses a variational problem with auxiliary conditions, requiring the use of Lagrange multipliers. We shall not try to solve the problem in air, but shall make a few comments about the effect of air, after discussing vacuum problems. We shall also discuss some of the effects of a round Earth.

a. The General Problem in a Vaccum

We require that the rocket, at the end of burning, have zero vertical velocity, and specified values of altitude, say η_s, and of horizontal velocity, say ξ_s. Thus, we have three functions of the type used in Eq. 2.12,

$$\left.\begin{aligned} g_1 &= \dot{\eta}_b = 0, \\ g_2 &= \xi_b - \xi_s = 0, \\ g_3 &= \eta_b - \eta_s = 0. \end{aligned}\right\} \tag{4.1}$$

We wish to minimize the fuel consumption, subject to these conditions.

It is not difficult to set up the differential Eqs. 2.9 for the optimum trajectory, along with the requisite boundary conditions, and it is not difficult to show that the system of equations has no analytic solution. Instantaneous burning is obviously not the solution, either, because with it, η_b equals zero, rather than η_s.

The trouble lies with conditions (4.1), which do not properly reflect our desires. We want the rocket to satisfy these conditions at some point, but not necessarily at the end of burning. In the case of a flat Earth, we can always find a ballistic trajectory, starting from some point on the surface, which satisfies the required conditions at its summit. This trajectory has initial horizontal velocity ξ_s, and initial vertical velocity $\sqrt{2g\eta_s}$. If we use instantaneous burning with these

values of burnt velocity, we have a more efficient rocket than any which burns all the way to the altitude η_b.

Over a round Earth, we cannot use this procedure, because the desired orbit may not be one which intersects the Earth's surface. Instead, we use the well-known idea of transfer orbits. The rocket, at the Earth's surface, is initially in a circular orbit, because of the Earth's rotation. In order to establish it in a different orbit, we launch it, using instantaneous burning, along an intermediate or transfer orbit, which is tangent to both the initial and the desired final orbit. When it arrives at the point of tangency with the desired final orbit, we give it the necessary increment of velocity, again using instantaneous burning, to put it into the final, rather than the intermediate, orbit.

Even if we neglect the Earth's rotation, so that the rocket is not, properly speaking, in any orbit to start with, it is still not difficult to show that the intermediate orbit should be tangent to the Earth's surface and to the final orbit. The losses which result from using an orbit which is not tangent to the Earth's surface have been discussed by Ehricke (9).

b. The Restricted Problem in a Vacuum

We shall work only in rectangular coordinates, even if we are discussing a rocket which is destined to become a satellite. We shall discuss the validity of this in part *c* of this section.

As we said in Sec. 2, the restricted problem mustal ways be phrased in terms of maximizing some function of $\xi_b, \cdots, \dot{\eta}_b$, hence we cannot use Eqs. 4.1 as they stand, or as modified by the conclusions of part *a*. However, forgetting the conclusions of part *a* for the moment, we can use the first two of conditions (4.1), and require that η_b be a maximum. For any other orbit problem, we can still find one function to maximize, while holding two others fixed.

For arbitrary jet acceleration $G(t)$ and arbitrary orientation $\phi(t)$, the coordinates and velocities at the end of burning are:

$$\left.\begin{aligned} \xi_b &= \int_0^{t_b} G\cos\phi\,dt, \quad \xi_b = \int_0^{t_b} (t_b - t)G\cos\phi\,dt, \\ \dot{\eta}_b &= \int_0^{t_b} G\sin\phi\,dt - gt_b, \quad \eta_b = \int_0^{t_b} (t_b - t)G\sin\phi\,dt - \tfrac{1}{2}gt_b^2. \end{aligned}\right\} \tag{4.2}$$

When we vary ϕ, $\delta\eta_b$ is to be zero because η_b is to be a maximum; $\delta\xi_b$ and $\delta\dot{\eta}_b$ are to be zero because ξ_b and $\dot{\eta}_b$ are fixed. Using the standard procedure in the calculus of variations, we multiply $\delta\dot{\eta}_b$ by λ_1 and $\delta\xi_b$ by λ_2. Then

$$\delta\eta_b + \lambda_1\delta\dot{\eta}_b + \lambda_2\delta\xi_b = 0 = \int_0^{t_b} \{(t_b - t)\cos\phi + \lambda_1\cos\phi - \lambda_2\sin\phi\} G\delta\phi\,dt.$$

The quantity in brackets must vanish identically if $G \neq 0$, hence

$$\tan \phi = (\lambda_1 + t_b - t)/\lambda_2. \tag{4.3}$$

This holds for any form of the function $G(t)$, and has been obtained by Fried (2).

We can solve Eq. 4.3 for $\sin \phi$ and $\cos \phi$, and substitute into the integrals for ξ_b and $\dot{\eta}_b$. The result is two transcendental equations to be solved for λ_1 and λ_2. If we assume constant thrust, and let

$$\left.\begin{aligned} X_0^2 &= (\beta\lambda_1 + 1 - \mu_b)^2 + \beta^2\lambda_2^2, \quad X_b^2 = \beta^2\lambda_1^2 + \beta^2\lambda_2^2, \\ a^2 &= (\beta\lambda_1 - \mu_b)^2 + \beta^2\lambda_2^2, \end{aligned}\right\} \tag{4.4}$$

we get

$$\left.\begin{aligned} (\xi_b/v_e) &= -(\beta\lambda_2/a) \ln [(\mu_b a X_0 + \mu_b a^2 + \mu_b\beta\lambda_1 \\ &\quad - \mu_b^2)/(aX_b + a^2 + \mu_b\beta\lambda_1 - \mu_b^2)], \\ [(\dot{\eta}_b + gt_b)/v_e] &= \ln [(X_0 + 1 + \beta\lambda_1 - \mu_b)/(X_b + \beta\lambda_1)] \\ &\quad - [(\beta\lambda_1 - \mu_b)/a] \ln [(\mu_b a X_0 + \mu_b a^2 \\ &\quad + \mu_b\beta\lambda_1 - \mu_b^2)/(aX_b + a^2 + \mu_b\beta\lambda_1 - \mu_b^2)]. \end{aligned}\right\} \tag{4.5}$$

With $\xi_b = \xi_s$ and $\dot{\eta}_b = 0$, these are the equations to be solved simultaneously for λ_1 and λ_2. The resulting value of η_b is then given by

$$(\beta/v_e)(\eta_b + \tfrac{1}{2}gt_b^2) = X_0 - X_b - \mu_b[(\dot{\eta}_b + gt_b)/v_e]. \tag{4.6}$$

For a numerical example, we used a hypothetical rocket burning 94 per cent of its original weight, with

$$v_e = 10^4 \text{ ft./sec.}, \quad \beta = 0.0064 \text{ sec.}^{-1}, \quad t_b = 146.875 \text{ sec.}$$
$$g = 32.0 \text{ ft./sec.}^2, \quad \mu_b = 0.06, \quad \xi_s = 25{,}856 \text{ ft./sec.}$$

We found $\beta\lambda_1 = -0.1420$, $\beta\lambda_2 = 0.5615$. The maximum value of η_b came out to be 43.64 miles.

Remembering now the conclusions of part *a*, we ask what would happen if we do not require $\dot{\eta}_b$ to be zero, but instead allow it to be free, and maximize $\eta_b + (\dot{\eta}_b^2/2g) = H$, while holding ξ_b fixed. Forming $\delta H + \lambda\delta\xi_b = 0$, and proceeding as before, we get

$$\tan \phi = (\dot{\eta}_b + gt_b - gt)/\lambda. \tag{4.7}$$

This is the same as Eq. 4.3, if we let

$$\lambda_1 = (\dot{\eta}_b/g), \quad \lambda_2 = (\lambda/g).$$

Equations 4.5 still hold for constant thrust except that we do not require $\dot{\eta}_b = 0$, but instead require that $\dot{\eta}_b = \lambda_1 g$.

We gain considerably from not requiring $\dot{\eta}_b = 0$. Using the same numerical values as before, we find

$$\beta\lambda = 3.586, \qquad \dot{\eta}_b = 6265 \text{ ft./sec.},$$
$$\eta_b = 34.94 \text{ miles}, \quad H = 151.1 \text{ miles}.$$

The gain in maximum altitude is 107.5 miles, a distance in which a freely falling body would gain slightly over 6000 ft./sec. in vertical velocity.

The values of $\tan\phi$ and $\dot{\phi}$ are

$$\tan\phi = (342.7 - t)/560.3, \quad \dot{\phi} = -1/560.3(1 + \tan^2\phi).$$

Initially, $\phi = 31.50°$, $\dot{\phi} = -0.0744°$/sec.; at the end of burning, $\phi = 19.30°$, $\dot{\phi} = -0.0910°$/sec.

c. Modifications of the Restricted Problem Produced by a Round Earth with an Atmosphere

If we are dealing with a round Earth with no atmosphere, we begin by modifying the equations of motion during burning. For purposes of determining the optimum, rather than any specific, trajectory, we can surely assume that the motion lies in a plane, and modify the equations of motion to

$$r^{-1}d(r^2\dot{\theta})/dt = G\cos\phi, \quad \ddot{r} - r\dot{\theta}^2 = G\sin\phi - (g\rho^2/r^2). \qquad (4.8)$$

In these, we are using circular coordinates in the plane, with r initially equal to ρ, and are using g as the acceleration due to gravity at the initial value of r. ϕ is the angle made by the rocket axis with the local horizontal.

We assume that the rocket has a first burning period, at the end of which it is established in an intermediate orbit. When the intermediate orbit is tangent to the final orbit, a second burning period, which we shall assume is instantaneous, occurs, at the end of which the rocket is in its final orbit. We assume that the total fuel consumption in the two burning periods is fixed, but that the partition between the two stages is unknown. We wish to determine this partition, and the function $\phi(t)$, required to put the rocket into a circular orbit of radius R, with a maximum value of R.

First, we wish an expression for the fuel consumed during the second burning period, as a function of the final orbit and of conditions at the end of the first burning period. If a subscript b denotes a value at the end of first burning, we have[8]

[8] See any discussion of central force orbits, such as Page, "Introduction to Theoretical Physics," New York, D. Van Nostrand, 1935, Chap. I.

$$\left.\begin{aligned} h &= r^2\dot{\theta} = r_b^2\dot{\theta}_b, \\ -U &= \tfrac{1}{2}\dot{r}_b^2 + \tfrac{1}{2}r_b^2\dot{\theta}_b^2 - (g\rho^2/r_b) = \tfrac{1}{2}\dot{r}^2 + \tfrac{1}{2}r^2\dot{\theta}^2 - (g\rho^2/r), \end{aligned}\right\} \tag{4.9}$$

along the intermediate orbit. If the final orbit is to be a circle of radius R, the value of $\dot{r}$ in the intermediate orbit must be zero when $r = R$. One readily verifies that

$$R = [g\rho^2 + (g\rho^2 - 2h^2U)^{1/2}]/2U, \tag{4.10}$$

which connects the desired R with conditions at the end of first burning; one also finds that the velocity in the intermediate orbit when $r = R$ is h/R. The required velocity in the final orbit is $(g\rho^2/R)^{1/2}$, so that an increment of velocity ΔV is required:

$$\Delta V = (g\rho^2/R)^{1/2} - (h/R).$$

Let μ_b be the ratio of the mass at the end of first burning to the initial mass, and let μ_f be the ratio of the mass at the end of second burning to the initial mass. Then

$$\Delta V = (g\rho^2/R)^{1/2} - (h/R) = v_e \ln (\mu_b/\mu_f). \tag{4.11}$$

Equation 4.11 is the desired relation involving fuel consumption during second burning.

The most important difference between Eqs. 4.8 and the equations in rectangular coordinates is probably the term $r\dot{\theta}^2$, which becomes slightly larger than g. However, it does so only near the end of burning, when G is probably large. The next most important difference is probably that between g and $(g\rho^2/r^2)$. Hence, a good zero-order approximation (r_0, θ_0) to (r, θ) should be the solution to the system

$$\rho\dot{\theta}_0 = G\cos\phi, \quad \ddot{r}_0 = G\sin\phi - g. \tag{4.12}$$

Hence, we can use Eqs. 4.2, if we replace ξ by $\rho\dot{\theta}_0 - \rho\omega$, and η by $r_0 - \rho$, using ω as the initial angular velocity produced by the Earth's rotation. We assume that $G(t)$ is known, and that G is reduced to zero at $t = t_b$, the end of first burning. We vary $\phi(t)$ and t_b, but as t_b is varied, we do not vary G, as we did in the burning-time problem. Hence,

$$\left.\begin{aligned} \delta r_{0b} &= \int_0^{t_b} (t_b - t)G\cos\phi\delta\phi dt + \dot{r}_{0b}\delta t_b, \\ \delta\dot{r}_{0b} &= \int_0^{t_b} G\cos\phi\delta\phi dt + \ddot{r}_{0b}\delta t_b, \\ \rho\delta\dot{\theta}_{0b} &= -\int_0^{t_b} G\sin\phi\delta\phi dt + \rho\dot{\theta}_{0b}\delta t_b. \end{aligned}\right\} \tag{4.13}$$

Writing Eq. 4.10 as

$$R = R(r_b, \dot{r}_b, \theta_b), \tag{4.14}$$

and

$$\delta R = R_{r_b}\delta r_b + R_{\dot{r}_b}\delta \dot{r}_b + R_{\dot{\theta}_b}\delta \dot{\theta}_b,$$

we have, upon setting $\delta R = 0$

$$\int_0^{t_b} \{R_{r_b}(t_b - t)\cos\phi + R_{\dot{r}_b}\cos\phi - \rho^{-1}R_{\dot{\theta}_b}\sin\phi\}G(t)\delta\phi dt + [R_{r_b}\dot{r}_{0b} + R_{\dot{r}_b}\ddot{r}_{0b} + R_{\dot{\theta}_b}\ddot{\theta}_{0b}]\delta t_b = 0. \tag{4.15}$$

Since $\delta R = 0$, we have, upon taking the variation of Eq. 4.11,

$$\int_0^{t_b} \{2r_b\dot{\theta}_b(t_b - t)\cos\phi - (r_b^2/\rho)\sin\phi\}G(t)\delta\phi dt + [2r_b\dot{\theta}_b\dot{r}_{0b} + r_b^2\ddot{\theta}_{0b} - Rv_e(\dot{\mu}_b/\mu_b)]\delta t_b = 0, \tag{4.16}$$

in which $\dot{\mu}_b$ is the burning rate of fuel divided by the initial mass, evaluated at time t_b.

Multiplying Eq. 4.16 by λ, adding to Eq. 4.15, and equating the resulting coefficients of $\delta\phi$ and δt_b to zero, we have, for any form of $G(t)$:

$$\left.\begin{aligned} \tan\phi &= [R_{r_b} + \sigma_1(t_b - t)]/\sigma_2, \\ \sigma_1\dot{r}_{0b} + R_{\dot{r}_b}\ddot{r}_{0b} + \rho\sigma_2\ddot{\theta}_{0b} - \lambda v_e(\dot{\mu}_b/\mu_b) &= 0, \end{aligned}\right\} \tag{4.17}$$

with

$$\sigma_1 = R_{r_b} + (2\lambda r_b\dot{\theta}_b/R), \quad \sigma_2 = (R_{\dot{\theta}_b}/\rho) + (\lambda r_b^2/R\rho).$$

The form of $\tan\phi$ in Eq. 4.3 still holds, with proper choices for λ_1, λ_2.

Equations 4.5 and 4.6 still hold for values at the end of burning, assuming constant thrust. We now have five unknown constants, namely r_b, $\dot{r}_b$, $\dot{\theta}_b$, λ, t_b, which must be chosen to fit the five equations, namely Eqs. 4.5, 4.6, 4.11, and the second of Eqs. 4.17. The solution of these equations is undoubtedly simpler than determining an optimum trajectory purely by trial and error, but is still a difficult computing task. Hence, we do not give a numerical example.

The added complexity of the orbit problem in the presence of a round Earth does not come primarily from the equations of motion during burning, but rather from those considerations of the motion after burning which cause the first burning time to be unknown.

It is interesting to note that the form of $\phi(t)$ is unaltered, to good approximation, by the use of a round Earth instead of a flat Earth, provided that we interpret ϕ to be the angle with the local horizontal. This is similar to the conclusion reached by Fried and Richardson (1) for the maximum range problem.

If one wishes to include them, the effects of the atmosphere and of the terms neglected in Eqs. 4.12 (centrifugal acceleration, variation of gravity, etc.) can all be considered together in a perturbation process like that of Sec. 3.*c* but more complicated. However, the reasons which led to results which are quite insensitive to the trajectory when we are near the optimum are still valid, and we can use a simple process with quite adequate results. The exact process used mighr depend somewhat upon circumstances, but a typical one might beast follows:

We can start with the partition of fuel between the two burning times which is given by considering instantaneous burning, and assume that the consumption during the second burning period is fixed. We also compute the intermediate trajectory, and take as the conditions at the end of first burning that the rocket is to be established in the intermediate trajectory, with one of the variables, say r_b, being maximized. Allowing some extra fuel to compensate for losses to gravity and drag, and using the shortest burning time allowed by engineering considerations (which we assume is far above the optimum; if not, we might fix $r_b - \rho$ at about 10^3 ft. as a good approximation to the optimum r_b), we calculate a vacuum trajectory using Eqs. 4.5 and 4.6 for values at the end of burning, determining the parameters λ_1 and λ_2 to satisfy conditions at the end of burning. Thus, we have only two unknowns instead of five.

Finally, to allow for aerodynamic effects, we carry out a perturbation process similar to that of Sec. 3.*c*. Instead of using rectangular coordinates, we would use curvilinear coordinates, s and u, say, with s being arc length along the vacuum trajectory and u being the perpendicular distance from s. Use of this coordinate system introduces acceleration terms other than $\ddot{s}$, $\ddot{u}$, but we already have such terms anyway because of the Earth's curvature. All such acceleration terms are small compared with G, and can be put into the perturbation. Instead of maximizing the range, we would maximize $\dot{s}_b$ subject to $\dot{u}_b = 0$.

We expect the effects of the atmosphere to produce results like those obtained earlier, namely, causing a rotation of the axis, during the first few thousand feet of travel, at a rate required to keep the angle of attack small.

5. SUMMARY

In Sec. 2 of this paper, we examined the nature of the mathematical problem posed by optimizing a rocket trajectory, paying most attention to the possibility of auxiliary or "iso-perimetric" conditions. We concluded that no more than four auxiliary conditions in two-dimensional, or six in three-dimensional, motion can be specified, in addition to giving some function of the trajectory a stationary value.

In Sec. 3, we studied rather thoroughly the problem of maximizing the range, including aerodynamic effects. Contrary to a popular belief, the rocket should not have low acceleration in dense air and then increase its acceleration as it reaches high altitudes. Instead, it should have high acceleration in dense air, and should reach the end of burning at a comparatively low altitude, such that the loss of range produced by drag after burning is a few per cent. The altitude at burn-out should be, typically, in the range 50,000 to 100,000 ft. As a rule of thumb, we find that the drag should equal the weight under optimum conditions.

Also contrary to a popular belief, the rocket does not climb almost vertically until it reaches thin air, so as to reduce drag. According to the theory of this paper, it is true that it starts out rather steeply, and then rotates until it is pointed in the desired direction. However, the rotation to (almost) 45° is accomplished in a relatively short time. By starting out steeply, the rocket gains a little altitude, but rotates within a short time in order not to have too much vertical momentum, and at a rate which in its details is governed by the need of keeping the induced drag small.

Because the distance travelled during burning is so short for the optimum trajectory, effects of the Earth's curvature during burning are small. We may, however, have to consider effects of curvature after burning in determining the correct boundary conditions to apply at the end of burning.

In a vacuum, the tilt of the rocket axis should be constant in order to achieve maximum range. In air, as indicated above, there is a relatively short period during which the axis rotates from almost vertical to the desired direction.

In Sec. 4, we studied the problem of putting a rocket into an orbit most efficiently. Since the difference between the air and vacuum trajectories should be about the same for this problem as for the maximum range problem, we studied only the problem in vacuum. However, we outlined a procedure for determining the proper correction in air.

In a vacuum, the tangent of the tilt angle should be a linear function of time, so that the rocket should rotate very gradually toward the horizontal. This holds for any time variation of the thrust and mass, holds exactly for a flat Earth, and holds to good accuracy if we include the Earth's curvature. It is important that the rocket coast during most of the flight before it reaches its orbit.

From the standpoint of applications, an important conclusion is that the efficiency is very insensitive to the trajectory. In one example, we calculated the optimum trajectory in vacuum, then in air, and finally calculated the range which would actually result if the rocket followed the vacuum trajectory. The error caused by using the vacuum trajectory was about 2 per cent. In another example, we found that

the loss caused by using a constant rather than the optimum thrust function was only 2 per cent.

We conclude that there is little need for a more elaborate theory of the optimum trajectory than that which we have presented, although the details of any specific application may differ considerably.

Acknowledgment

We wish to acknowledge with thanks the assistance in some of the calculations given us by Dr. Richard E. Maerker of the Physics Dept., Tulane University, and also the helpful discussions with him, with Dr. William C. McCorkle and Mr. Charles Hussey of Ordnance Missile Laboratories, Redstone Arsenal, and with Dr. James W. Follin, Jr., of the Applied Physics Laboratory.

REFERENCES

(1) B. D. FRIED AND J. M. RICHARDSON, *J. Appl. Phys.*, Vol. 27, p. 955 (1956).
(2) B. D. FRIED, *Jet Propulsion*, Vol. 25, p. 641 (1957); D. F. LAWDEN, Proc. Fifth I. A. F. Congress, Innsbruck, 1954.
(3) H. S. TSIEN AND R. C. EVANS, *J. Am. Rocket Soc.*, Vol. 21, p. 99 (1951).
(4) G. LEITMANN, *Aero. Engr. Rev.*, Vol. 16, p. 63 (1957); *Astronautica Acta II*, p. 119 (1956).
(5) A. E. BRYSON, JR. AND STANLEY E. ROSS, "Optimum Rocket Trajectories with Aerodynamic Drag," *Jet Propulsion*, Vol. 28, p. 465 (1958).
1957.
(6) D. F. LAWDEN, *Quart. J. Mech. Appl. Math.*, Vol. 7, p. 488 (1954).
(7) A. R. HIBBS, *J. Am. Rocket Soc.*, Vol. 22, p. 204 (1952).
(8) A. MIELE, *Jet Propulsion*, Vol. 27, p. 1231 (1957).
(9) K. A. EHRICKE, *Astronautica Acta II*, p. 176 (1956).

New Compounds Protect Outdoor Storage of Bulk Materials.—A new compound that blankets and protects outdoor storage piles of bulk materials against loss from wind or rain erosion has been developed by Johnson-March Corp., Philadelphia, Pa. The spray-applied solution contains specially developed additives for maximum coverage and penetration.

The solution, called Compound SP, is a blend of synthetic, organic, long chain polymers in a water base that form a thin crust which is tough, durable and highly resistant to weathering. In a series of heavier concentrations adaptable to a wide range of material composition, particle size and climatic conditions, they are suitable for coating stock piles of Bauxite, carbon, chromite concentrations, coal, Fluorspar, ilmenite, silicon carbide, sulphur and many other types of materials in outdoor storage piles.

The formed crusts are said to reduce the serious economic losses suffered each year through the disappearance of large tonnages of valuable material. In addition, community or plant dust nuisances are abated. Protection lasts for periods in excess of a year.

Compound SP is described as being inert, unreactive and non-toxic and without adverse effect on the burning qualities of coal or the subsequent processing of sulphur, metal ores, carbon, etc.

Application of the compounds is said to be easily accomplished with any type of spraying equipment from the small portable type up to commercial orchard spraying equipment. The special additives are included to provide proper wetting, penetration and coverage of the surfaces of even the smallest particles on the storage pile.

The solution is supplied in a number of different grades ready for spraying at the rate of one gallon of spray per 100 feet of surface. When desired, a color indicator is included at no extra cost in Compound SP to show where treatment has been made.

New Ammonium Perchlorate Plant.—HEF, Inc., has launched construction of a multi-million pound per year plant for production of ammonium perchlorate, an oxidizer used in solid propellants for rockets and missiles. The new facility is adjacent to the Columbus, Mississippi, plant of the Hooker Chemical Corporation of Niagara Falls, N. Y.—one of the two parent firms. Foote Mineral Company of Philadelphia is the other owner of the jointly held subsidiary.

Formation of HEF, Inc., occurred earlier this year. After a preliminary study of the propellant market, Hooker and Foote formalized their intent to work together in the solid fuel propellants field by announcing on February 20th that the new subsidiary had been formed. The HEF, Inc. plant will utilize a process developed jointly by the research departments of Foote Mineral and Hooker Chemical.

Perchlorates have figured prominently in recent discussions involving rocket and missile propellants. Foote has researched certain areas of the propellant field, whereas Hooker is already a manufacturer of sodium perchlorate and potassium perchlorate. The joint venture is a bid for the larger market which is expected to develop as a result of the present interest in solid propellant systems.

Hooker Chemical Corporation is the largest manufacturer of sodium chlorate, the basic raw material for perchlorates. Presently Hooker is planning to spend one million dollars for its third major expansion of sodium chlorate production capacity at Columbus.

A NOTE ON THE OPERATIONAL SOLUTION OF LINEAR DIFFERENCE EQUATIONS *

BY

ELIAHU I. JURY [1] AND FRANCIS J. MULLIN [1]

SUMMARY

The z-transform is applied to the solution of linear difference equations with constant coefficients; boundary conditions are considered in the resulting solutions and certain theorems related to the z-transform are applied to obtain qualitative information about the solution. The z-transform is used to solve simultaneous difference equations with constant coefficients and the modified z-transform is used to solve difference equations whose coefficients are periodic functions. Finally, the z-transform is applied to the solution of difference equations with periodic coefficients.

The methods of solution are illustrated with various examples which indicate the straightforward procedure for applying the z-transform and the modified z-transform to the solution of difference equations.

INTRODUCTION

The z-transform (1,2)[2] and its modified form (3) have been successfully applied to the analysis and synthesis of sampled-data control systems. The sampled response of such systems can be described by a difference equation with constant coefficients (z-transform) while the continuous response can be described by a difference equation whose coefficients are periodic functions (modified z-transform). In view of this, it is evident that the z-transform and modified z-transform should be useful mathematical techniques for the solution of difference equations. It is the purpose of this paper to investigate this in detail.

Transform techniques for the solution of difference equations are not uncommon. Gardner and Barnes(4) have used the jump function and the Laplace transform, Fort (5) has used the Dirichlet Series transform, while Neufeld (6) has solved linear mixed difference-differential equations with a transform method. Stone (7) has used the Generalized Laplace transform to solve difference equations and Brown (8) has discussed the theoretical considerations of the method suggested by Tustin (9) for approximating differential equations by difference equations. Thus, the use of operators and transform methods for the solution of difference equations is not new and the z-transform can be considered as an extension to these methods.

* This research was supported by the United States Air Force through the Air Force Office of Scientific Research of the Air Research and Development Command, under Contract No. AF 18(600)-1521. Reproduction in whole or in part is permitted for any purpose of the United States Government.

[1] Electronics Research Laboratories, Department of Electrical Engineering, University of California, Berkeley, Calif.

[2] The boldface numbers in parentheses refer to the references appended to this paper.

SOLUTION OF LINEAR DIFFERENCE EQUATIONS WITH CONSTANT COEFFICIENTS

Consider the following difference equation:

$$\sum_{i=0}^{p} a_i X_{n+i} = \sum_{i=0}^{q} b_i Y_{n+i}. \tag{1}$$

a_i and b_i are constants, Y_n is the forcing function and is known for all values of n. It is desired to find X_n. X_n and Y_n are both functions of the parameter t but are defined only for $t = n$ where n is an integer equal to or greater than zero.[3] Let X_n and Y_n be represented by an impulse (delta function) occurring at $t = n$. With this representation for X_n and Y_n one may take the z-transform (1, 2) of Eq. 1 and solve for $X(z)$; X_n can then be found by performing the inverse z-transformation. For the purpose of completeness it should be noted that we are defining:

$$\mathfrak{z}[F(n)] \triangleq F(z) = \sum_{n=0}^{\infty} F(n)z^{-n} \tag{2}$$

$$\mathfrak{z}[F(n+k)] = \sum_{n=0}^{\infty} F_{n+k}z^{-n} = z^k\left[F(z) - \sum_{j=0}^{k-1} F(j)z^{-j}\right]. \tag{3}$$

With these definitions the z-transform of Eq. 1 is

$$\sum_{i=0}^{p} a_i z^i\left[X(z) - \sum_{j=0}^{i-1} X(j)z^{-j}\right] = \sum_{i=0}^{q} b_i z^i\left[Y(z) - \sum_{j=0}^{i-1} Y(j)z^{-j}\right]. \tag{4}$$

Solving for $X(z)$ one obtains

$$X(z) = \frac{Y(z)\sum_{i=0}^{q} b_i z^i + \sum_{i=0}^{p} a_i z^i\left(\sum_{j=0}^{i-1} X(j)z^{-j}\right) - \sum_{i=0}^{q} b_i z^i\left(\sum_{j=0}^{i-1} Y(j)z^{-j}\right)}{\sum_{i=0}^{p} a_i z^i}. \tag{5}$$

The inverse z-transformation can be accomplished using the Cauchy Contour Integral (see Eq. 16), the power series expansion method in which $X(z)$ is expanded in powers of z^{-1}, or with the aid of z-transform tables (2, 11). It is seen from Eq. 5 that the first p values of X_n can be arbitrarily chosen to meet given initial conditions; if one neglects the initial conditions on both X_n and Y_n, a particular solution is obtained.

Example 1

Find X_n, which is a solution of the difference equation

$$X_{n+2} - X_{n+1} + 0.632\,X_n = 0.368\,Y_{n+1} + 0.264\,Y_n. \tag{6}$$

[3] In this paper it is assumed that all quantities are 0 for $n < 0$.

The z-transform of this equation when solved for $X(z)$ gives

$$X(z) = \frac{(0.368\,z + 0.264)\,Y(z)}{z^2 - z + 0.632} + \frac{z^2 X_0 + z(X_1 - X_0 - 0.368\,Y_0)}{z^2 - z + 0.632}. \quad (7)$$

If Y_n = a constant = k for all $n \geqslant 0$, then $Y(z) = kz/(z-1)$. Using a contour integral for inversion we find:

$$X_n = k[1 - (0.632)^{n/2}\cos(0.89\,n) - 0.213\,(0.632)^{n/2}\sin(0.89\,n)] + (0.632)^{n/2}[1.282\,X_0\sin(0.89\,(n+1)) + 1.612\,(X_1 - X_0 - 0.368\,k)\sin(0.89\,n)]. \quad (8)$$

The power series expansion method gives

$$X(z) = X_0 + X_1 z^{-1} + (X_1 - 0.632\,X_0 + 0.632\,k)z^{-2} + (0.368\,X_1 - 0.632\,X_0 + 1.265\,k)z^{-3} + \cdots. \quad (9)$$

In this equation the coefficient of z^{-k} equals X_n for $n = k$. Needless to say, Eq. 9 is identical to Eq. 8 for the proper choice of n. If all initial conditions are neglected, then the two forms of the particular solution are

$$X_n = k[1 - (0.632)^{n/2}\cos(0.89\,n) - 0.213\,(0.632)^{n/2}\sin(0.89\,n)] \quad (10)$$

and

$$X_p(z) = k[0\,z^0 + 0.368\,z^{-1} + 1.0\,z^{-2} + 1.40\,z^{-3} + 1.40\,z^{-4} + \cdots. \quad (11)$$

The particular solution is shown in Fig. 1.

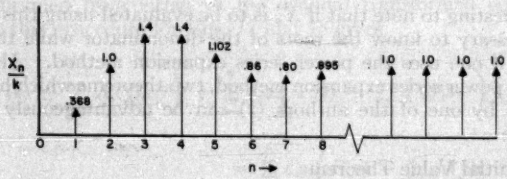

FIG. 1. Particular solution of Eq. 6 with Y_n = a constant k.

Example 2

Find X_n, which is a solution of the difference equation

$$10\,X_{n+3} - 5.0\,X_{n+2} + 2\,X_{n+1} + 3\,X_n = n. \quad (12)$$

Following the above procedure we obtain

$$X(z) = \frac{3}{(z-1)^2}\,\frac{1}{10z^3 - 5z^2 + 2z + 3} + \frac{10X_0z^3 + (10X_1 - 5X_0)z^2 + (10X_2 - 5X_1 + 2X_0)z}{10z^3 - 5z^2 + 2z + 3} \tag{13}$$

and inversion using the power series expansion method gives

$$X(z) = X_0 + X_1z^{-1} + X_2z^{-2} + 0.1(-3X_0 - 2X_1 + 5X_2)z^{-3} + 0.1(1 - \tfrac{3}{2}X_0 - 4X_1 + \tfrac{1}{2}X_2)z^{-4} + \cdots. \tag{14}$$

The particular solution for this equation is

$$X_p(z) = 0.1z^{-4} + 0.25z^{-5} + 0.405z^{-7} + 0.543z^{-1} + 0.665z^{-8} + \cdots. \tag{15}$$

This solution is shown in Fig. 2.

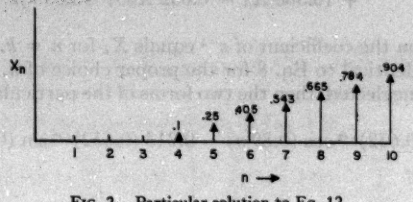

FIG. 2. Particular solution to Eq. 12.

The contour integral for X_n is

$$X_n = \frac{1}{2\pi j}\int_\Gamma X(z)z^{n-1}dz. \tag{16}$$

It is interesting to note that if X_n is to be evaluated using this integral, it is necessary to know the roots of the denominator while this is not required if one uses the power series expansion method. Also, when using the power series expansion method, two theorems which have been discussed by one of the authors (2) can be advantageously applied. These are

(*a*) Initial Value Theorem

$$X_0 = \lim_{z\to\infty}\frac{z-1}{z}X(z) \quad \text{if } X_n = 0 \text{ for all } n < 0.$$

(*b*) Final Value Theorem

$$\lim_{n\to\infty} X_n = \lim_{z\to 1}\frac{z-1}{z}X(z) \quad \text{if the final value exists.}$$

The stability requirements for a bounded solution are simply that the roots of the denominator lie within the unit circle in the z-plane. Single roots on the unit circle indicate conditional stability and double roots mean instability. It is to be understood that the final value theorem as given above applies only if a finite final value exists and does not constitute a stability test in itself. The test for the location of the zeros of the denominator can be performed using the Schur-Cohn criterion (12) or, if one uses the bilinear transformation $z = \dfrac{w+1}{w-1}$, then the Hurwitz criterion (12) can be applied to the numerator of the resulting polynomial in w.

SOLUTION OF SIMULTANEOUS LINEAR DIFFERENCE EQUATIONS WITH CONSTANT COEFFICIENTS

Consider the following set of simultaneous linear difference equations

$$\sum_{i=0}^{p} a_i X_{n+i} + \sum_{i=0}^{q} b_i Y_{n+i} = \sum_{i=0}^{r} c_i F_{n+i} \tag{17}$$

$$\sum_{i=0}^{u} d_i X_{n+i} + \sum_{i=0}^{v} e_i Y_{n+i} = \sum_{i=0}^{w} f_i G_{n+i}. \tag{18}$$

It is desired to find X_n and Y_n when F_n and G_n are known for all values of n. To find X_n and Y_n we take the z-transform of the two equations, solve one of the transformed equations for either $X(z)$ or $Y(z)$ in terms of the other, and substitute this into the remaining transformed equation. This equation can then be solved for one of the unknown transforms. With one of the unknown transforms determined the second can be obtained from either of the original transformed equations. Following this procedure for Eqs. 17 and 18 gives

$$\sum_{i=0}^{p} a_i z^i \left(X(z) - \sum_{j=0}^{i-1} X(j) z^{-j} \right) + \sum_{i=0}^{q} b_i z^i \left(Y(z) - \sum_{j=0}^{i-1} Y(j) z^{-j} \right)$$

$$= \sum_{i=0}^{r} c_i z^i \left(F(z) - \sum_{j=0}^{i-1} F(j) z^{-j} \right) \tag{19}$$

$$\sum_{i=0}^{u} d_i z^i \left(X(z) - \sum_{j=0}^{i-1} X(j) z^{-j} \right) + \sum_{i=0}^{v} e_i z^i \left(Y(z) - \sum_{j=0}^{i-1} Y(j) z^{-j} \right)$$

$$= \sum_{i=0}^{w} f_i z^i \left(G(z) - \sum_{j=0}^{i-1} G(j) z^{-j} \right). \tag{20}$$

From Eq. 19 we obtain

$$X(z) = \frac{\sum_{i=0}^{r} c_i z^i \left(F(z) - \sum_{j=0}^{i-1} F(j) z^{-j}\right) - \sum_{i=0}^{q} b_i z^i \left(Y(z) - \sum_{j=0}^{i-1} Y(j) z^{-j}\right) + \sum_{i=0}^{p} a_i z^i \sum_{j=0}^{i-1} X(j) z^{-j}}{\sum_{i=0}^{p} a_i z^i}$$

and substituting this into Eq. 20 gives an equation containing $Y(z)$ as its only unknown. From this equation we can find $Y(z)$ and knowing $Y(z)$ we can obtain $X(z)$ from Eq. 19 by substituting the correct expression for $Y(z)$. The inverse transformation will give X_n and Y_n.

Example 3

Determine the solution of the following set of difference equations

$$X_{n+2} + 5X_{n+1} - X_n + Y_{n+1} - 3Y_n = 2.0 \tag{21}$$

$$X_{n+1} + 3X_n + 4Y_{n+2} - Y_n = 5.0. \tag{22}$$

Taking the z-transform of Eq. 21 and solving for $X(z)$ gives

$$X(z) = \frac{1}{z^2+5z-1}\left(\frac{2z}{z-1} + z^2X_0 + z(X_1+5X_0+Y_0) - (z-3)Y(z)\right). \tag{23}$$

The z-transform of Eq. 22 is

$$(z+3)X(z) - zX_0 + (4z^2-1)Y(z) - 4z^2Y_0 - 4zY_1 = 5z/(z-1). \tag{24}$$

Substituting Eq. 23 into Eq. 24 and solving for $Y(z)$ gives

$$Y(z) = \frac{z}{z-1}\frac{5z^2+23z-11}{4z^4+20z^3-6z^2-5z+10} + \frac{4Y_0z^4+z^3(20Y_0+4Y_1)+z^2(-5Y_0+20Y_1-3X_0-X_1)+z(-3Y_0-4Y_1-16X_0-3X_1)}{4z^4+20z^3-6z^2-5z+10}. \tag{25}$$

With the aid of Eq. 25 we can rewrite Eq. 23 as

$$X(z) = \frac{z}{z-1}\frac{8z^2-5z+13}{4z^4+20z^3-6z^2-5z+10} + \frac{4X_0z^4+z^3(20X_0+4X_1)+z^2(-2X_0-12Y_0+4Y_1)+z(-2X_0-X_1-Y_0+12Y_1)}{4z^4+20z^3-6z^2-5z+10}. \tag{26}$$

Equations 25 and 26 represent the transformed solutions of the given difference equations and inversion will give the desired values of X_n and Y_n. On carrying out the inversion for the particular solutions we obtain

$$X_p(z) = 0z^0 + 0z^{-1} + 2z^{-2} - 9.25z^{-3} + 53.25z^{-4} + 273.625z^{-5} + \cdots \tag{27}$$

$$Y_p(z) = 0z^0 + 0z^{-1} + 1.25z^{-2} + 0.75z^{-3} + 2.375z^{-4} - 5.0625z^{-5} + \cdots. \tag{28}$$

Needless to say, this method is not restricted to two simultaneous equations; it can be applied to any number of equations by the obvious extension of the above procedure.

SOLUTION OF DIFFERENCE EQUATIONS WHOSE COEFFICIENTS ARE PERIODIC FUNCTIONS

Consider the following type of difference equation

$$\underset{(n+p)\leqslant t\leqslant(n+p+1)}{X(t)} = \sum_{i=0}^{p} f_i(t)X_{n+i} + \sum_{i=0}^{q} g_i(t)Y_{n+i}. \tag{29}$$

$f_i(t)$ and $g_i(t)$ are arbitrary periodic functions of the independent variable t with periods equal to 1; $X_n = X(t)|_{t=n}$ and Y_n is a known function of t which is defined only for $t = n$ where n is an integer equal to or greater than 0. Again, let X_n and Y_n be represented by impulses occurring at $t = n$. Because of the periodicity of $f_i(t)$ and $g_i(t)$, we may replace $f_i(t)$ and $g_i(t)$ by $f_i(m)$ and $g_i(m)$ where m is a parameter which varies from 0 to 1. With this change of variable the actual time scale becomes $t = (n - 1 + m)$ and Eq. 29 becomes

$$X(n + p + m) = \sum_{i=0}^{p} f_i(m)X_{n+i} + \sum_{i=0}^{q} g_i(m)Y_{n+i}. \tag{30}$$

Let us define the modified z-transform of $X(n - 1 + m)$ as

$$\mathfrak{z}_m[X(n - 1 + m)] \triangleq X(z, m)$$

and

$$\mathfrak{z}_m[X(n + k + m)] \triangleq z^{k+1}X(z, m).$$

With these definitions one can take the modified z-transform of Eq. 30 and obtain

$$z^{p+1}X(z, m) = \sum_{i=0}^{p} f_i(m)z^iX(z) + \sum_{i=0}^{q} g_i(m)z^iY(z). \tag{31}$$

Both $X(z)$ and $X(z, m)$ are unknown in this equation. However, $X(z)$ can be determined by noting that $X_n = X(n - 1 + m)|_{m=1}$. Thus, substituting $m = 1$ into Eq. 30 gives a difference equation with constant coefficients and $X(z)$ can be determined using this equation. The resulting expression for $X(z)$ can be substituted into Eq. 31 which can then be solved for $X(z, m)$. This would finally give

$$X(z, m) = \frac{Y(z)}{z^{p+1}}\left[\frac{\sum_{i=0}^{q} g_i(1)z^i \sum_{i=0}^{p} f_i(m)z^i}{z^{p+1} - \sum_{i=0}^{p} f_i(1)z^i} + \sum_{i=0}^{q} g_i(m)z^i\right]$$
$$+ \frac{1}{z^{p+1}}\left[\frac{z^{p+1}\sum_{i=0}^{p} X_iz^{-i} - \left(\sum_{i=0}^{p} f_i(1)z^i\right)\left(\sum_{j=0}^{i=1} X_jz^{-i}\right) - \left(\sum_{i=0}^{q} g_i(1)z^i\right)\left(\sum_{j=0}^{i=1} Y_jz^{-i}\right)}{z^{p+1} - \sum_{i=0}^{p} f_i(1)z^i}\right]\sum_{i=0}^{p} f_i(m)z^i. \tag{32}$$

$X(n-1+m)$ can then be found using the contour integral since m is a constant during the integration process, or with the aid of modified z-transform tables (3, 11) or by using the power series expansion method. If the power series expansion method were used (11), one would obtain

$$zX(z,m) = p_0(m)z^0 + p_1(m)z^{-1} + p_2(m)z^{-2} + p_3(m)z^{-3} + \cdots. \quad (33)$$

The coefficient of z^{-k} represents $X(t)$ for $k \leqslant t \leqslant (k+1)$ when m is varied from 0 to 1. Again, it is apparent that no knowledge of the roots of the characteristic equation is required to obtain a solution if one uses this method for inversion. The stability requirement for this type of equation is the same as that for a difference equation with constant coefficients. However, the initial value and final value theorems become:

(*a*) Initial Value:

$$X_0 = \lim_{\substack{m\to 0 \\ z\to\infty}} \frac{z-1}{z} zX(z,m)$$

(*b*) Final Value:

$$\lim_{\substack{n\to\infty \\ 0\leqslant m\leqslant 1}} X(n-1+m) = \lim_{z\to 1} \frac{z-1}{z} X(z,m) \quad \text{if the final value exists.}$$

If the final value is independent of m, then there is no steady state "ripple"; if it is not independent of m, then the steady state "ripple" can be determined by allowing m to vary from 0 to 1.

Example 4

Find $X(t)$ which is a solution of the following equation

$$\underset{(n+1)\leqslant t\leqslant(n+2)}{X(t)} = X_{n+1}(2.582 - 1.582\,e^{-t} - t) - X_n(1-e^{-t}) + Y_{n+1}(e^{-t}+t-1) + 0.418\,Y_n(1-e^{-t}) \quad (34)$$

assuming that the coefficients of X_k and Y_k are periodic. Replacing the t in these periodic functions by m gives the following equation

$$X(n+1+m) = X_{n+1}(2.582 - 1.582\,e^{-m} - m) + X_n(1-e^{-m}) + Y_{n+1}(e^{-m}+m-1) + 0.418\,Y_n(1-e^{-m}). \quad (35)$$

The modified z-transform of Eq. 35 is

$$z^2X(z,m) = (2.582 - 1.582\,e^{-m} - m)zX(z) - (1-e^{-m})X(z) + (e^{-m}+m-1)zY(z) + 0.418(1-e^{-m})Y(z). \quad (36)$$

To find $X(z)$, let $m = 1$ in Eq. 35 and take the z-transform of the resulting equation. Thus,

$$X_{n+2} = X_{n+1} - 0.632\,X_n + 0.368\,Y_{n+1} + 0.264\,Y_n \tag{37}$$

or

$$X(z) = \frac{(0.368\,z + 0.264)\,Y(z)}{z^2 - z + 0.632} + \frac{z^2X_0 + z(X_1 - X_0 - 0.368\,Y_0)}{z^2 - z + 0.632}. \tag{38}$$

Substituting this expression for $X(z)$ into Eq. 36 gives

$$X(z, m) = \frac{z^2(e^{-m}+m-1)+z(-2.0\,e^{-m}-1.368\,m+2.368)+(e^{-m}+0.368\,m-0.737)}{z(z^2-z+0.632)}\,Y(z)$$
$$+\frac{z^2X_0(2.582-1.582e^{-m}-m)+zX_0(-3.582+2.582e^{-m}-m)+(2.582-1.582e^{-m}-m)(X_1-0.368X_0)}{z(z^2-z+0.632)}$$
$$+\frac{(e^{-m}-1)(X_1-X_0-0.368\,Y_0)}{z(z^2-z+0.632)}. \tag{39}$$

The particular solution for $X(t)$ is found using the power series expansion method with $Y(z) = \dfrac{z}{z-1}$. This is written as

$$zX_p(z, m) = (e^{-m} + m - 1)z^0 + (0.368 + 0.632\,m)z^{-1}$$
$$+ (1.632 - 0.632\,e^{-m})z^{-2} + \cdots \tag{40}$$

where the coefficient of z^{-k} represents $X_p(t)$ for $k \leqslant t \leqslant k+1$. The final value of $X_p(t)$ is obtained by applying the final value theorem. This shows

$$X(n - 1 + m) = \lim_{z\to 1} \frac{z-1}{z}\,X(z, m) = 1.$$

The particular solution is shown in Fig. 3.

LINEAR DIFFERENCE EQUATIONS WITH PERIODIC COEFFICIENTS

We now wish to apply the z-transform to solve difference equations with periodic coefficients (10); that is, to the following equation

$$X_{n+1} = a_nX_n + Y_n. \tag{41}$$

a_n is a periodic coefficient whose period is equal to N; that is, $a_i = a_{N+i}$ for $i = 0, 1, 2, \cdots, (N-1)$. Y_n is a forcing function known for all values of n and Y_n and X_n are to be represented by impulses. To solve this equation we shall first form a constant coefficient difference equation which describes the solution for $n = KN$, $K = 0, 1, 2, \cdots$, and then use this result to find the solution for other values of n. This

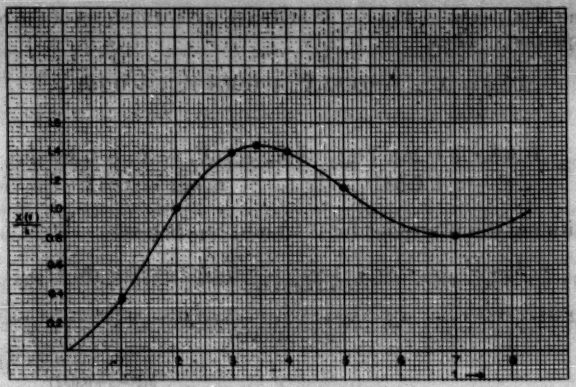

FIG. 3. Particular solution of Eq. 34 for Y_n = a constant k.

procedure, in essence, removes the periodicity of the coefficients from the analysis. From Eq. 3 we note that

$$\mathfrak{z}[Y_{KN}] = Y_0 + Y_N z^{-N} + Y_{2N} z^{-2N} + Y_{3N} z^{-3N} + \cdots$$
$$\mathfrak{z}[Y_{KN+1}] = Y_1 + Y_{N+1} z^{-N} + Y_{2N+1} z^{-2N} + Y_{3N+1} z^{-3N} + \cdots$$
$$\cdots\cdots\cdots\cdots\cdots\cdots\cdots\cdots\cdots\cdots\cdots\cdots\cdots\cdots$$
$$\mathfrak{z}[Y_{(K+1)N-1}] = Y_{N-1} + Y_{2N-1} z^{-N} + Y_{3N-1} z^{-2N} + Y_{4N-1} z^{-3N} + \cdots$$

With this pattern for X_n we proceed to solve Eq. 41. Let $n = KN$ so that $a_n = a_0$. We can then write

$$X_{KN+1} = a_0 X_{KN} + Y_{KN}$$
$$X_{KN+2} = a_1 X_{KN+1} + Y_{KN+1} = a_1 a_0 X_{KN} + a_1 Y_{KN} + Y_{KN+1}$$
$$X_{KN+3} = a_2 X_{KN+2} + Y_{KN+2} = a_2 a_1 a_0 X_{KN} + a_2 a_1 Y_{KN} + a_2 Y_{KN+1} + Y_{KN+2}$$
$$\cdots\cdots\cdots\cdots\cdots\cdots\cdots\cdots\cdots\cdots\cdots\cdots\cdots\cdots$$
$$X_{(K+1)N} = a_{N-1} X_{(K+1)N-1} + Y_{(K+1)N-1}$$
$$= (a_{N-1} a_{N-2} \cdots a_0) X_{KN} + (a_{N-1} \cdots a_1) Y_{KN}$$
$$+ (a_{N-1} \cdots a_2) Y_{KN+1} + (a_{N-1} \cdots a_3) Y_{KN+2}$$
$$+ \cdots a_{N-1} Y_{(K+1)N-2} + Y_{(K+1)N-1}.$$

Notice that the last of these equations given above is actually a constant coefficient difference equation involving only X_{KN} and the various forcing terms. The z-transform of this equation can be written as

$$z^N(X_{KN}(z) - X_0)$$
$$= (a_{N-1} \cdots a_0)X_{KN}(z) + (a_{N-1} \cdots a_1)Y_{KN}(z)$$
$$+ (a_{N-1} \cdots a_2)Y_{KN+1}(z) + \cdots a_{N-1}Y_{(K+1)N-2}(z)$$
$$+ Y_{(K+1)N-1}(z) \quad (42a)$$

or

$$X_{KN}(z) = \frac{1}{z^N - (a_{N-1} \cdots a_0)}[z^N X_0 + (a_{N-1} \cdots a_1)Y_{KN}(z) + \cdots$$
$$+ a_{N-1}Y_{(K+1)N-2}(z) + Y_{(K+1)N-1}(z)]. \quad (42b)$$

Knowing $X_{KN}(z)$ we can find $X_{KN+1}(z)$ from the first of the above equations, $X_{KN+2}(z)$ from the second of these equations, and so forth. The stability condition is simply that $|a_0a_1a_2 \cdots a_{N-1}| < 1$. If $Y_n = 0$ for all $n \geq 0$, then

$$X_{KN} = (a_0a_1 \cdots a_{N-1})^K X_0.$$

Example 5

Find X_n which is a solution of Eq. 41 with $a_i = 0.5$ for $i = 0, 1, 4, 5, 8, 9, \cdots$ and $a_i = -0.5$ for $i = 2, 3, 6, 7, 10, 11, \cdots$ and $Y_n = (-1)^n$.

As indicated by Eq. 42*b*, we first write

$$\mathfrak{z}[Y_{KN}] = 1 + z^{-4} + z^{-8} + \cdots = \frac{z^4}{z^4 - 1}$$
$$\mathfrak{z}[Y_{KN+1}] = -1 - z^{-4} - z^{-8} - \cdots = \frac{-z^4}{z^4 - 1}$$
$$Y_{KN+2} = Y_{KN}; \quad Y_{KN+3} = Y_{KN+1}.$$

Then using Eq. 42*b* we write

$$X_{KN}(z) = \frac{1}{z^4 - 0.0625}\left[z^4X_0 + \frac{0.125\,z^4}{z^4-1} + \frac{(0.25)(-z^4)}{z^4-1} - \frac{0.5\,z^4}{z^4-1} - \frac{z^4}{z^4-1}\right]$$

or with $X_0 = 0$

$$X_{KN}(z) = \frac{-1.625\,z^4}{(z^4 - 0.0625)(z^4 - 1)}.$$

Inversion using the contour integral gives

$$X_{4K} = -\frac{26}{15}\left[1 - \left(\frac{1}{2}\right)^{4K}\right].$$

Since we know

$$X_{4K+1} = 0.5\,X_{4K} + Y_{4K}$$

it readily follows that

$$X_{4K+1} = -\frac{13}{15}\left[1 - \left(\frac{1}{2}\right)^{4K}\right] + 1.$$

Similarly we find

$$X_{4K+2} = -\frac{13}{30}\left[1 - \left(\frac{1}{2}\right)^{4K}\right] - \frac{1}{2}$$

$$X_{4K+3} = \frac{13}{60}\left[1 - \left(\frac{1}{2}\right)^{4K}\right] + \frac{5}{4}.$$

The solution to this equation is shown in Fig. 4. It should be noted

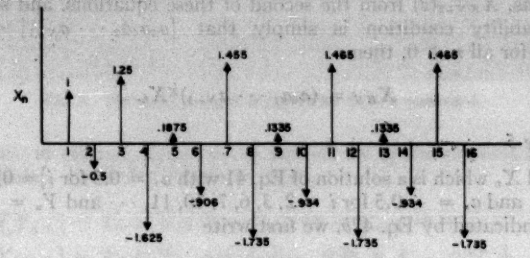

FIG. 4. Solution to Example 5.

that the inverse transformation can be carried out in a straightforward manner for this type of difference equation, since the roots of the denominator are readily calculated.

SOLUTION OF SIMULTANEOUS DIFFERENCE EQUATIONS WITH PERIODIC COEFFICIENTS

Consider the two following difference equations where a_n, b_n, c_n and d_n are periodic coefficients of period N, and P_n and Q_n are known for all n. $(n \geq 0)$

$$X_{n+1} = a_n X_n + b_n Y_n + P_n \tag{43}$$

$$Y_{n+1} = c_n X_n + d_n Y_n + Q_n. \tag{44}$$

A solution for these two equations can be obtained following a procedure similar to that used for a single equation with a periodic coefficient; that is, the $2N$ equations which correspond to a complete period of the coefficients are written and each equation is substituted into the following equation. This results in two constant coefficient difference equations which involve X_{KN}, Y_{KN} and various forcing function terms. These two equations can be simultaneously solved for the two unknowns using the procedure introduced earlier in this paper. With X_{KN} and

Y_{KN} known, one can then find X_{KN+1} and Y_{KN+1} using

$$X_{KN+1} = a_0X_{KN} + b_0Y_{KN} + P_{KN}$$
$$Y_{KN+1} = c_0X_{KN} + d_0Y_{KN} + Q_{KN}.$$

With X_{KN+1} and Y_{KN+1} determined, one can find X_{KN+2} and Y_{KN+2}, etc. The method is straightforward but unfortunately the notation involved in solving two equations of period N is too cumbersome to be useful. Rather than solve the general problem of period N, a solution will be obtained for $N = 2$ and $N = 3$, and this should illustrate clearly the procedure to be followed for larger N.

From Eqs. 43 and 44 with $n = NK$ we can write

$$X_{NK+1}=a_0X_{NK}+b_0Y_{NK}+P_{NK} \tag{45}$$

$$Y_{NK+1}=c_0X_{NK}+d_0Y_{NK}+Q_{NK} \tag{46}$$

$$X_{NK+2}=a_1(a_0X_{NK}+b_0Y_{NK}+P_{NK})+b_1(c_0X_{NK}+d_0Y_{NK}+Q_{NK})+P_{NK+1} \tag{47}$$

$$Y_{NK+2}=c_1(a_0X_{NK}+b_0Y_{NK}+P_{NK})+d_1(c_0X_{NK}+d_0Y_{NK}+Q_{NK})+Q_{NK+1} \tag{48}$$

$$\begin{aligned}X_{NK+3}=&a_2(a_1a_0X_{NK}+a_1b_0Y_{NK}+a_1P_{NK}+b_1c_0X_{NK}+b_1d_0Y_{NK}+b_1Q_{NK}+P_{NK+1})\\&+b_2(c_1a_0X_{NK}+c_1b_0Y_{NK}+c_1P_{NK}+d_1c_0X_{NK}+d_1d_0Y_{NK}+d_1Q_{NK}+Q_{NK+1})+P_{NK+2}\end{aligned} \tag{49}$$

$$\begin{aligned}Y_{NK+3}=&c_2(a_1a_0X_{NK}+a_1b_0Y_{NK}+a_1P_{NK}+b_1c_0X_{NK}+b_1d_0Y_{NK}+b_1Q_{NK}+P_{NK+1})\\&+d_2(c_1a_0X_{NK}+c_1b_0Y_{NK}+c_1P_{NK}+d_1c_0X_{NK}+d_1d_0Y_{NK}+d_1Q_{NK}+Q_{NK+1})+Q_{NK+2}.\end{aligned} \tag{50}$$

If $N = 2$, Eqs. 47 and 48 become

$$\begin{aligned}X_{2(K+1)} = &(a_1a_0 + b_1c_0)X_{2K} + (a_1b_0 + b_1d_0)Y_{2K}\\&+ a_1P_{2K} + b_1Q_{2K} + P_{2K+1}\end{aligned} \tag{47'}$$

$$\begin{aligned}Y_{2(K+1)} = &(c_1a_0 + d_1c_0)X_{2K} + (c_1b_0 + d_1d_0)Y_{2K}\\&+ c_1P_{2K} + d_1Q_{2K} + Q_{2K+1}.\end{aligned} \tag{48'}$$

The z-transform of these two equations can be written

$$\begin{aligned}z^2[X_{2K}(z) - X_0] = &(a_1a_0 + b_1c_0)X_{2K}(z) + (a_1b_0 + b_1d_0)Y_{2K}(z)\\&+ a_1P_{2K}(z) + b_1Q_{2K}(z) + P_{2K+1}(z)\end{aligned} \tag{51}$$

$$\begin{aligned}z^2[Y_{2K}(z) - Y_0] = &(c_1a_0 + d_1c_0)X_{2K}(z) + (c_1b_0 + d_1d_0)Y_{2K}(z)\\&+ c_1P_{2K}(z) + d_1Q_{2K}(z) + Q_{2K+1}(z).\end{aligned} \tag{52}$$

On solving Eqs. 51 and 52 for $X_{2K}(z)$ and $Y_{2K}(z)$ we find

$$X_{2K}(z) = \frac{(z^2 - K_4)(z^2X_0 + H_2(z)) + K_2(Y_0z^2 + G_2(z))}{(z^2 - K_1)(z^2 - K_4) - K_2K_3} \tag{53}$$

$$Y_{2K}(z) = \frac{(z^2 - K_1)(z^2Y_0 + G_2(z)) + K_3(X_0z^2 + H_2(z))}{(z^2 - K_1)(z^2 - K_4) - K_2K_3} \tag{54}$$

where

$$K_1 = a_1a_0 + b_1c_0 \tag{55a}$$

$$K_2 = a_1b_0 + b_1d_0 \tag{55b}$$

$$K_3 = c_1a_0 + d_1c_0 \tag{55c}$$

$$K_4 = c_1b_0 + d_1d_0 \tag{55d}$$

$$H_3(z) = a_1P_{2K}(z) + b_1Q_{2K}(z) + P_{2K+1}(z) \tag{56a}$$

$$G_3(z) = c_1P_{2K}(z) + d_1Q_{2K}(z) + Q_{2K+1}(z). \tag{56b}$$

Inversion of Eqs. 53 and 54 will give X_{2K} and Y_{2K} and knowing X_{2K} and Y_{2K} one can find X_{2K+1} and Y_{2K+1} using Eqs. 45 and 46. If $N = 3$, Eqs. 49 and 50 become

$$X_{3(K+1)} = K_5X_{3K} + K_6Y_{3K} + H_3(z) \tag{49'}$$

$$Y_{3(K+1)} = K_7X_{3K} + K_8Y_{3K} + G_3(z). \tag{50'}$$

The z-transforms of these two equations, when simultaneously solved for $X_{3K}(z)$ and $Y_{3K}(z)$, can be written as

$$X_{3K}(z) = \frac{(z^3 - K_8)(z^3X_0 + H_3(z)) + K_6(Y_0z^3 + G_3(z))}{(z^3 - K_5)(z^3 - K_8) - K_6K_7} \tag{57}$$

$$Y_{3K}(z) = \frac{(z^3 - K_5)(z^3Y_0 + G_3(z)) + K_7(X_0z^3 + H_3(z))}{(z^3 - K_5)(z^3 - K_8) - K_6K_7} \tag{58}$$

where

$$K_5 = a_2a_1a_0 + a_2b_1c_0 + b_2c_1a_0 + b_2d_1c_0 \tag{59a}$$

$$K_6 = a_2a_1b_0 + a_2b_1d_0 + b_2c_1b_0 + b_2d_1d_0 \tag{59b}$$

$$K_7 = c_2a_1a_0 + c_2b_1c_0 + d_2c_1a_0 + d_2d_1c_0 \tag{59c}$$

$$K_8 = c_2a_1b_0 + c_2b_1d_0 + d_2c_1b_0 + d_2d_1d_0 \tag{59d}$$

$$H_3(z) = (a_2a_1 + b_2c_1)P_{2K}(z) + a_2P_{2K+1}(z) + P_{2K+2}(z) + (a_2b_1 + b_2d_1)Q_{2K}(z) + b_2Q_{2K+1}(z) \tag{60a}$$

$$G_3(z) = (c_2a_1 + d_2c_1)P_{2K}(z) + c_2P_{2K+1}(z) + Q_{2K+2}(z) + (c_2b_1 + d_2d_1)Q_{2K}(z) + d_2Q_{2K+1}(z). \tag{60b}$$

Knowing X_{2K} and Y_{2K} one can find X_{2K+1} and Y_{2K+1} from Eqs. 45 and 46 and X_{2K+2} and Y_{2K+2} from Eqs. 47 and 48.

Example 6

Find X_n and Y_n which are solutions of Eqs. 43 and 44 with

$$a_n = (-1)^n; \quad b_n = \begin{cases} 0.5\ n \text{ even} \\ -0.5\ n \text{ odd} \end{cases}; \quad c_n = \begin{cases} 0.0\ n \text{ even} \\ 1.5\ n \text{ odd} \end{cases}; \quad d_n = (-1)^{n+1}$$

$$P_n = -Q_n = (-\tfrac{1}{2})^{n+1}.$$

For this example $N = 2$, so we first compute

$$P_{2K}(z) = -\tfrac{1}{2} - \tfrac{1}{8}z^{-2} - \tfrac{1}{32}z^{-4} + \cdots = \frac{-0.5\,z^2}{z^2 - 0.25} = -Q_{2K}(z)$$

$$P_{2K+1}(z) = \tfrac{1}{4} + \tfrac{1}{16}z^{-2} + \tfrac{1}{64}z^{-4} + \cdots = \frac{0.25\,z^2}{z^2 - 0.25} = -Q_{2K+1}(z).$$

Then using Eqs. 55 and 56 we find

$$K_1 = -1; \quad K_2 = 0; \quad K_3 = 1.5; \quad K_4 = -0.25$$

$$H_2(z) = \frac{0.5\,z^2}{z^2 - 0.25}$$

$$G_2(z) = \frac{-0.5\,z^2}{z^2 - 0.25}.$$

Finally substituting these values into Eqs. 53 and 54 and simplifying the resulting expressions gives, with $X_0 = Y_0 = 1.0$,

$$X_{2K}(z) = \frac{z^2(z^2 + 0.25)}{(z^2 + 1)(z^2 - 0.25)}$$

$$Y_{2K}(z) = \frac{z^2(z^4 + 1.75\,z^2 - 0.375)}{(z^2 + 1)(z^2 + 0.25)(z^2 - 0.25)}.$$

The inverses of these expressions are then written as

$$X_{2K} = \tfrac{2}{3}(\tfrac{1}{2})^{2K} + \tfrac{1}{3}(-1)^K$$

$$Y_{2K} = \tfrac{1}{3}(\tfrac{1}{2})^{2K} + 2[(\tfrac{1}{2})^{2K} - \tfrac{1}{3}](-1)^K.$$

Knowing X_{2K} and Y_{2K} it readily follows that

$$X_{2K+1} = (-1)^K(\tfrac{1}{2})^{2K}$$

$$Y_{2K+1} = \tfrac{3}{10}(\tfrac{1}{2})^{2K} - 2[(\tfrac{1}{2})^{2K} - \tfrac{1}{3}](-1)^K.$$

The complete solution for X_n and Y_n is shown in Figs. 5*a* and 5*b*.

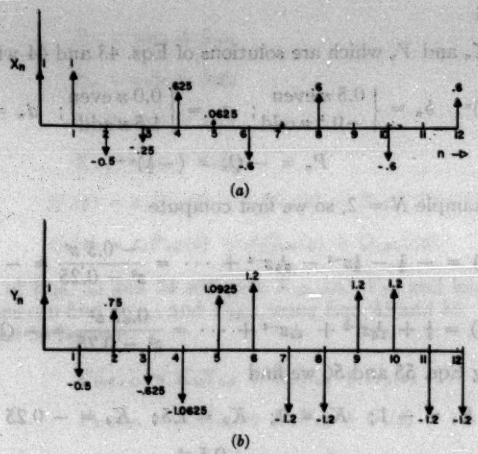

FIG. 5. Solutions of Example 6.

SUMMARY AND CONCLUSIONS

The theory of the z-transform and the modified z-transform has been applied to the solution of linear difference equations. These equations often arise in systems which employ magnetic amplifiers or digital computers as well as sampled-data control systems and the application of the transform method discussed in this paper tends to reduce the solution of these difference equations to a straight-forward, systematic process. The method solution presented is illustrated with a few examples to clarify the procedure involved. Further work on difference equations is certainly warranted, in particular, in the field of nonlinear difference equations about which little is known at the present time.

REFERENCES

(1) J. R. RAGAZZINI AND L. A. ZADEH, "The Analysis of Sampled-Data Systems," *A.I.E.E. Trans.*, Vol. 71, Part II, p. 225 (1952).

(2) E. I. JURY, "The Analysis and Synthesis of Sampled-Data Control Systems," *A.I.E.E. Trans.*, Vol. 73, Part II, p. 332 (1954).

(3) E. I. JURY, "Synthesis and Critical Study of Sampled-Data Control Systems," *A.I.E.E. Trans.*, Vol. 75, Part II, p. 141 (1956).

(4) M. F. GARDNER AND J. L. BARNES, "Transients in Linear Systems," New York, John Wiley & Sons, Inc., 1942.

(5) T. FORT, "Linear Difference Equations and the Dirichlet Series Transform," *Am. Mathematical Monthly*, Vol. 62, No. 9, p. 641 (1955).

(6) J. NEUFELD, "On the Operational Solution of Linear Mixed Difference Differential Equations," *Cambridge Phil. Soc.*, Vol. 30, p. 289 (1934).

(7) W. M. STONE, "A List of Generalized Laplace Transforms," Iowa State College, *Jour. Science*, Vol. 22, p. 215 (1948).
(8) B. M. BROWN, in "Automatic and Manual Control," edited by A. Tustin, London, Butterworth Scientific Publications, 1952.
(9) A. TUSTIN, "A Method of Analyzing the Behavior of Linear Systems in Terms of Time Series," *J. Inst. Electrical Engrs.*, Vol. 94, Part II-A, No. 1, p. 130 (1947).
(10) B. FRIEDLAND, "Theory of Time Varying Sampled-Data Systems," Technical Report T-19/B, Electronics Research Laboratories, Columbia University, p. 178.
(11) E. I. JURY, "Additions to the Modified z-Transform Method," Part 4, I.R.E. Wescon Convention Record of 1957, p. 136.
(12) M. MARDEN, "The Geometry of the Zeros of a Polynomial in a Complex Variable," New York, *Am. Mathematical Soc.*, Mathematical Survey III, 1949.

Test Room for Central Air Conditioning Systems.—A room simulating weather extremes and interior heat loads for demonstrating central air conditioning systems in virtually any new or existing multistory building to owners, architects, consultants or development engineers, has been announced by Carrier Corporation.

Industry representatives who have witnessed the versatile new environmental room report it is the "most completely flexible facility of its kind." It is one of a number of features built into a new Systems Engineering Laboratory at Carrier headquarters in Syracuse, N. Y.

"Occupants of a building still on the drawing boards can learn what working in their future office will be like," Charles V. Fenn, Carrier vice president, said. "They will actually see the air conditioning unit counteract freezing cold and feel it quickly remove scorching heat."

Temperature of air in the room, its velocity, sound level and distribution pattern at any point, as well as effects of radiation, can also be noted. Design theories for new air handling apparatus can be proven under typical conditions saving hundreds of man-hours. It can also be used to check architectural plans and interior motifs, eliminating expensive construction changes after the building has been completed, Mr. Fenn said.

For example, a prominent Chicago consulting firm tested various air conditioning systems with a novel ceiling it was planning for a new sky-scraper. Data collected in one day's experimentation provided essential information for designing the building around the year-round system.

The room can be made the exact size of standard spaces in a commercial structure, hotel or hospital. The ceiling is adjustable and the outside wall can be changed for glass ratios occupying 20 to 80 per cent of total area, which includes virtually all buildings. External conditions ranging between zero and 120° F. can be created to demonstrate downdraft, plus gains and losses due to radiation. The effect of venetian blinds or drapes can also be shown. Air velocity of better than 100 feet per minute has been recorded sweeping down the room's single thickness glass wall when outside temperature is zero and 75° F. is maintained inside. The degree with which different systems are able to neutralize this "waterfall effect" is easily one of the "most dramatic" demonstrations made in the room, Mr. Fenn stated.

For the finale, the air flow pattern provided by one of the air conditioning systems is vividly outlined by use of a fireworks smoke bomb.

The room permits comparison of the six most popular central systems: high velocity, induction; high or low pressure ceiling diffusion; high or low pressure side wall discharge and double duct. Radiant panel sections are also installed above the hung ceiling.

By means of an intercommunication system and large picture window, in one wall of the test module, larger groups can follow the scientific demonstrations.

THE CONJUGATE FRAME METHOD AND ITS APPLICATION IN THE ELASTIC AND PLASTIC THEORIES OF STRUCTURES

BY

S. L. LEE [1]

SYNOPSIS

This paper discusses the extension of the conjugate beam method to the study of the deformation of rigid-frame structures. The first part of the paper deals with the elastic analysis of such structures while the second part demonstrates the application of the proposed method to the deformation analysis of the structures under ultimate loads. The relationship between the conjugate frames and the actual structure is derived by means of the "generalized" theorems of area moment. Numerical examples are given to illustrate the procedure.

NOTATIONS

A, B, C,	Subscripts denoting points on the frame
EI	Flexural rigidity
H	Horizontal reaction component
h	Length
M	Bending moment
M_P	Plastic moment
m	Area of M/EI diagram
m_{DF}	Area of M/EI diagram between points D and F
P	Concentrated load
r	Number of redundant quantities remaining in the structure at ultimate load
s	Number of hinges, plastic hinges plus actual hinges
V	Vertical reaction component
w	Uniformly distributed load
x_{DF}, y_{DF}	Horizontal and vertical distances between points D and F
$\bar{x}$, $\bar{y}$	Centroidal distances of m to any point
$\bar{x}_D$, $\bar{y}_D$	Centroidal distances of m_{DF} to D, defined by $(2b, c)$
δ_x, δ_y	Horizontal and vertical deflections
θ	Rotation of a section or an actual hinge
ϕ	Rotation of a plastic hinge
$\sum M_{Fy}$	Summation of moment about point F in the conjugate frame for δ_y.

INTRODUCTION

The conjugate beam method (1, 2)[2] provides a powerful tool for the study of the deformation of beams. As such a tool, it is commonly

[1] Associate Professor of Civil Engineering, The Technological Institute, Northwestern University, Evanston, Ill.

[2] The boldface numbers in parentheses refer to the references appended to this paper.

employed in the elastic range not only to calculate the slope at any section and the deflection at any point of a beam under loads but also to determine the redundant quantities in statically indeterminate cases. The first part of this paper discusses the extension of this method to the elastic analysis of rigid-frame structures, the determination of the redundant quantities in statistically indeterminate frames and the displacement components of any point in such structures.

The plastic or yield hinge concept furnishes a simple and rational approach for calculating the plastic collapse loads (3, 4, 5, 6) or ultimate loads of rigid-frame structures and for estimating the deformation of the structures under such loads (7, 8, 9). This simple plastic theory is based upon an idealized moment-curvature relationship as shown in Fig. 1. The second part of this paper deals with the application of the

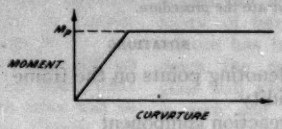

FIG. 1. Idealized moment-curvature relationship.

proposed method to estimate the hinge rotations and the displacement components of any point in a rigid-frame structure under ultimate loads.

THE CONJUGATE FRAME

Consider a continuous segment DEF (Fig. 2*d*) of the structure loaded as shown in Fig. 2*a*. The relationship between the displacement components θ_D, δ_{yD} and δ_{xD} of point D and those of point F may be expressed by means of the "generalized" theorems of area moment as follows

$$\begin{aligned} \theta_D &= \theta_F + m_{DF} \\ \delta_{yD} &= \delta_{yF} - \theta_F x_{DF} - m_{DF}\bar{x}_D \\ \delta_{xD} &= \delta_{xF} - \theta_F y_{DF} - m_{DF}\bar{y}_D, \end{aligned} \tag{1}$$

where

$$\begin{aligned} m_{DF} &= \int_D^F \frac{M ds}{EI} \\ m_{DF}\bar{x}_D &= \int_D^F \frac{M x ds}{EI} \\ m_{DF}\bar{y}_D &= \int_D^F \frac{M y ds}{EI} \end{aligned} \tag{2}$$

and EI denotes the flexural rigidity of the member. In Eq. 1, x_{DF} and y_{DF} denote the distances between points D and F along the coordinate axes. It is obvious from (2) that m_{DF} is the area of the M/EI diagram while $\bar{x}_D$ and $\bar{y}_D$ are the centroidal distances of m_{DF} with respect to point D. The directions of the bending moment M and the displacement components θ, δ_y and δ_x are positive as indicated in Fig. 2*d*. Thus clockwise θ and downward δ_y are positive while δ_x is positive if the point is displaced to the right of its original position.

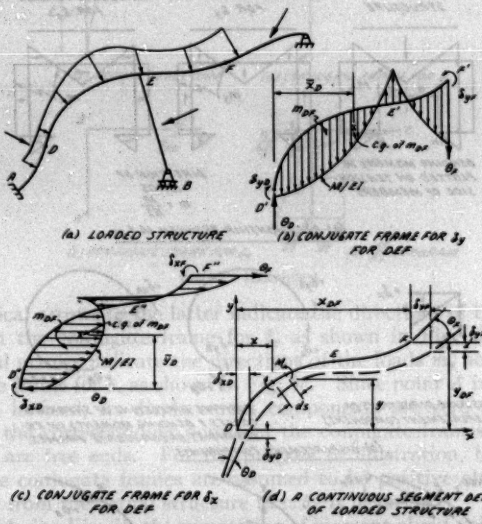
(a) LOADED STRUCTURE
(b) CONJUGATE FRAME FOR δ_y FOR DEF
(c) CONJUGATE FRAME FOR δ_x FOR DEF
(d) A CONTINUOUS SEGMENT DEF OF LOADED STRUCTURE

FIG. 2. Relationship between conjugate frames and loaded structure.

Next consider the conjugate frames shown in Fig. 2*b* and *c*. Similar to the conjugate beam, the conjugate frames are subjected to the loads m_{DF}, plotted on the tension side of the members, and supported at the extremities by the shearing forces θ's and the bending moments δ's. The only exception is that while the directions of m_{DF}, θ_D and θ_F in the conjugate frame for δ_y ($D'E'F'$ shown in Fig. 2*b*) are parallel to the y-axis, the directions of the same forces in the conjugate frame for δ_x ($D''E''F''$ shown in Fig. 2*c*) are parallel to the x-axis. With the positive directions of m_{DF}, θ's and δ's as indicated in the figures, it is obvious that the relationship expressed by (1) can be obtained directly from the conjugate frames by simply applying the laws of statics. Thus (1*b*) can be derived by equating to zero the summation of moment

about point D' in Fig. 2*b*, and (1*c*) can be obtained similarly by setting the summation of moment about point D'' in Fig. 2*c* equal to zero. Evidently (1*a*) may be derived from either of the two conjugate frames by equating the summation of forces to zero.

The relationship between the elements of the conjugate frames and those of the actual structure and the sign conventions mentioned above are summarized in Fig. 3*a* and *b* for reference.

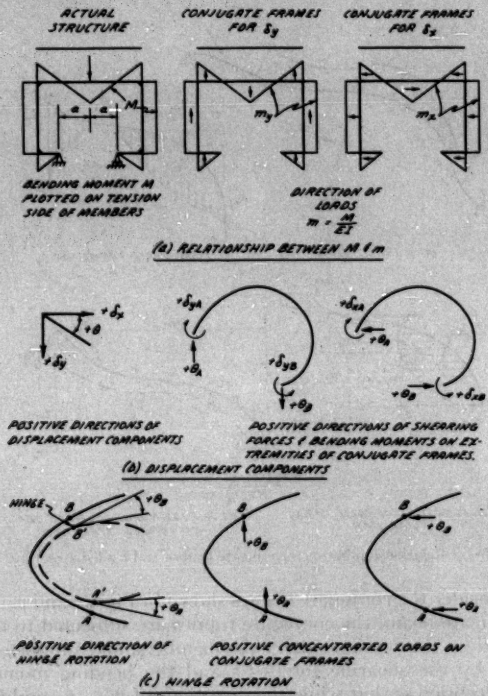
ACTUAL STRUCTURE
CONJUGATE FRAMES FOR δ_y
CONJUGATE FRAMES FOR δ_x
BENDING MOMENT M PLOTTED ON TENSION SIDE OF MEMBERS
DIRECTION OF LOADS $m = \frac{M}{EI}$
(a) RELATIONSHIP BETWEEN M & m
POSITIVE DIRECTIONS OF DISPLACEMENT COMPONENTS
POSITIVE DIRECTIONS OF SHEARING FORCES & BENDING MOMENTS ON EXTREMITIES OF CONJUGATE FRAMES.
(b) DISPLACEMENT COMPONENTS
HINGE
POSITIVE DIRECTION OF HINGE ROTATION
POSITIVE CONCENTRATED LOADS ON CONJUGATE FRAMES
(c) HINGE ROTATION

FIG. 3. Relationship between conjugate frames and actual structure and sign conventions.

ELASTIC ANALYSIS

The method of analysis is best illustrated by means of numerical examples. Its application in the elastic range is demonstrated in Examples 1 to 4.

Example 1

In order to determine the redundant reaction V_C and the displacement components of point C, θ_C and δ_{xC}, in the frame loaded as shown in Fig. 4*a*, the M/EI diagram is first constructed as shown in Fig. 4*d*.

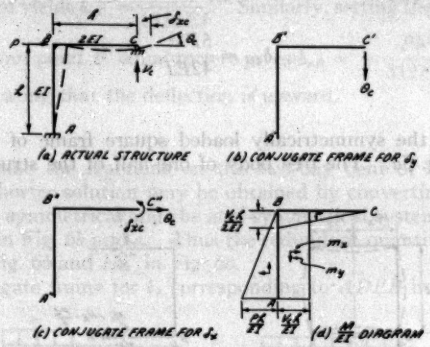

FIG. 4. Example 1.

The vertical arrows in the latter indicate the directions of the loads m_y acting on the conjugate frame for δ_y as shown in Fig. 4*b* while the horizontal arrows indicate the directions of the loads m_x acting on the conjugate frame for δ_x as shown in Fig. 4*c*. Since point A in the actual structure is fixed, its displacement components are zero and, consequently, the corresponding points in the conjugate frames, points A' and A'', are free ends. For the purpose of illustration, both θ_C and δ_{xC} in the conjugate frames are assumed to be positive although it is apparent from the actual structure that θ_C is negative.

Considering Fig. 3*b*, the summation of moment about point C' yields

$$\tfrac{1}{2}\left(\frac{Ph}{EI}\right)(h)(h) - \left(\frac{V_C h}{EI}\right)(h)(h) - \tfrac{1}{2}\left(\frac{V_C h}{2EI}\right)(h)(\tfrac{2}{3}h) = 0$$

or

$$V_C = \tfrac{3}{7}P.$$

Also, the summation of forces leads to

$$\tfrac{1}{2}\left(\frac{Ph}{EI}\right)(h) - \left(\frac{V_C h}{EI}\right)(h) - \tfrac{1}{2}\left(\frac{V_C h}{2EI}\right)(h) - \theta_C = 0$$

which, upon substitution of the value of V_C just obtained, yields

$$\theta_C = -\frac{Ph^2}{28EI}.$$

Next, considering Fig. 4*c*, the summation of moment about point C'' leads to

$$\tfrac{1}{2}\left(\frac{Ph}{EI}\right)(h)(\tfrac{2}{3}h) - \left(\frac{V_C h}{EI}\right)(h)\left(\frac{h}{2}\right) - \delta_{xC} = 0$$

or

$$\delta_{xC} = \frac{5Ph^3}{42EI}$$

Example 2

Consider the symmetrically loaded square frame of constant EI shown in Fig. 5*a*. The free body of one-half of the structure cut by

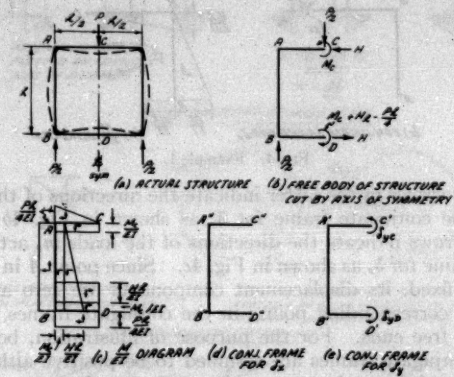

FIG. 5. Example 2.

passing a section through the axis of symmetry is shown in Fig. 5*b* and the corresponding M/EI diagram is shown in Fig. 5*c*. To determine the redundant quantities H and M_C, only the conjugate frame for δ_x shown in Fig. 5*d* needs be considered. It may be concluded from symmetry that $\theta_C = \theta_D = \delta_{xC} = \delta_{xD} = 0$ and, consequently, points C'' and D'' are both free ends. Equating to zero the summation of forces and the summation of moment about point C'' yield, respectively, upon simplification,

$$2M_C + Hh - \tfrac{1}{16}Ph = 0$$
$$M_C + \tfrac{1}{2}Hh - \tfrac{1}{4}Ph = 0$$

the solution of which yields $H = \frac{3}{32}P$ and $M_C = \frac{11}{64}Ph$.

To calculate the vertical deflections of points C and D, δ_{yC} and δ_{yD}

in the conjugate frame for δ_y shown in Fig. 5*e* are first assumed to be positive, or downward. Since member AB does not displace vertically, the bending moment at any point in member $A'B'$ should be zero. Considering member $A'C'$, equating the summation of moment about point A' to zero yields $\delta_{yC} = \frac{17Ph^3}{1536EI}$. Similarly, setting the summation of moment about point B' equal to zero gives $\delta_{yD} = -\frac{Ph^3}{512EI}$, the negative sign indicating that the deflection is upward.

Example 3

To determine the reactions on the two-bay bent of constant EI (Fig. 6*a*), a shorter solution may be obtained by converting the given loads into the symmetrical and the anti-symmetrical systems as shown, respectively, in Fig. 6*b* and *c*. Thus the redundant quantities are H_A'' and V_A'' in Fig. 6*b* and H_A' in Fig. 6*c*.

The conjugate frame for δ_x corresponding to $ADEB$ in Fig. 6*c* and

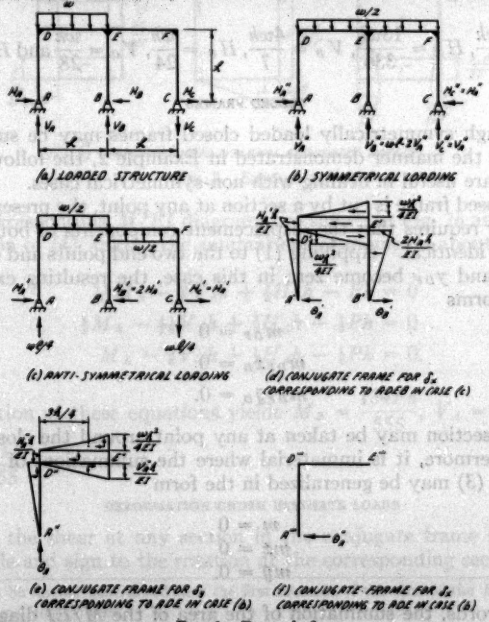
(a) LOADED STRUCTURE
(b) SYMMETRICAL LOADING
(c) ANTI-SYMMETRICAL LOADING
(d) CONJUGATE FRAME FOR δ_x CORRESPONDING TO ADEB IN CASE (c)
(e) CONJUGATE FRAME FOR δ_y CORRESPONDING TO ADE IN CASE (b)
(f) CONJUGATE FRAME FOR δ_x CORRESPONDING TO ADE IN CASE (b)

FIG. 6. Example 3.

the M/EI diagram are shown in Fig. 6*d*. Taking the summation of moment about A' eliminates both θ_A' and θ_B' and equating it to zero yields $H_A' = \frac{wh}{48}$. The conjugate frames for δ_y and δ_x corresponding to Fig. 6*b* and the M/EI diagram are shown respectively in Fig. 6*e* and *f*. The vertical arrows are associated with Fig. 6*e*, the horizontal ones with Fig. 6*f*. Observe in this case that the displacement components of point E are zero. Setting the summations of moment about point A'' in Fig. 6*e* and point A''' in Fig. 6*f* equal to zero leads to, after the elimination of the common factor $\frac{h^2}{EI}$,

$$\tfrac{1}{2}H_A'' - \tfrac{1}{3}V_A'' + \tfrac{1}{16}wh = 0$$
$$\tfrac{1}{3}H_A'' - \tfrac{1}{2}V_A'' + \tfrac{1}{12}wh = 0$$

solving which yields $H_A'' = \frac{wh}{56}$ and $V_A'' = \frac{3wh}{14}$.

Combining the results of Fig. 6*b* and *c* yields the required reactions

$$V_A = \frac{13wh}{28}, H_A = \frac{13wh}{336}, V_B = \frac{4wh}{7}, H_B = \frac{wh}{24}, V_C = \frac{wh}{28} \text{ and } H_C = \frac{wh}{336}.$$

CLOSED FRAMES

Although symmetrically loaded closed frames may be successfully treated in the manner demonstrated in Example 2, the following relationships are useful in dealing with non-symmetrical cases.

If a closed frame is cut by a section at any point, the preservation of continuity requires that the displacement components of both ends of the cut be identical. Applying (1) to the two end points and observing that x_{DF} and y_{DF} become zero in this case, the resulting expressions take the forms

$$\begin{aligned} m_{DF} &= 0 \\ m_{DF}\bar{x}_D &= 0 \\ m_{DF}\bar{y}_D &= 0. \end{aligned} \tag{3}$$

Since the section may be taken at any point around the closed frame and, furthermore, it is immaterial where the summations of moments are taken, (3) may be generalized in the form

$$\begin{aligned} m &= 0 \\ m\bar{x} &= 0 \\ m\bar{y} &= 0. \end{aligned} \tag{4}$$

In other words, the summation of the area of the M/EI diagram in a

closed frame and its first moments about any pair of coordinate axes must be zero.[3]

Example 4

To illustrate the application of (4), consider the non-symmetrical square frame loaded as shown in Fig. 7*a*. Cutting the section at corner

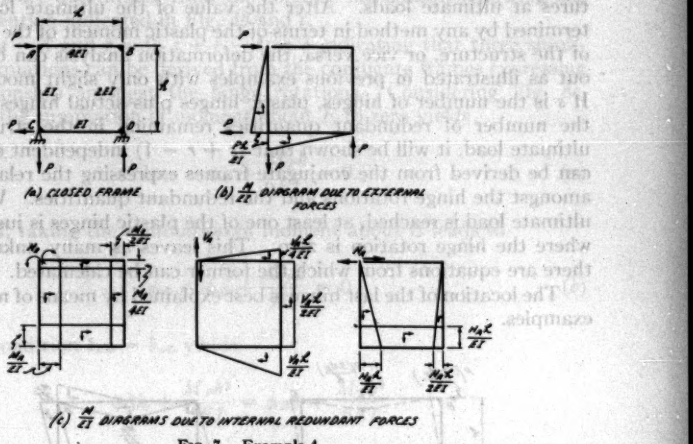

FIG. 7. Example 4.

A, the corresponding M/EI diagrams are shown in Fig. 7*b* and *c*. The application of (4), taking the summations of moments about corner C, leads to

$$\begin{aligned} \tfrac{11}{4}M_A - \tfrac{8}{3}V_A h + \tfrac{7}{4}H_A h - Ph &= 0 \\ \tfrac{8}{3}M_A - \tfrac{11}{3}V_A h + \tfrac{8}{3}H_A h - \tfrac{5}{6}Ph &= 0 \\ M_A - \tfrac{8}{3}V_A h + \tfrac{7}{4}H_A h - \tfrac{5}{6}Ph &= 0. \end{aligned}$$

The solution of these equations yields $M_A = \dfrac{134Ph}{555}$, $V_A = \dfrac{318P}{555}$ and $H_A = \dfrac{311P}{555}$.

DEFORMATION UNDER ULTIMATE LOADS

Since the shear at any section in the conjugate frame is equal in magnitude and sign to the rotation at the corresponding section in the

[3] It can be further generalized that the first moment of the area of the M/EI diagram about any axis must be zero.

deformed structure, the rotation of a hinge in the latter takes the form of a concentrated load in the former as illustrated in Fig. 3*c*. This is true for an actual hinge where the bending moment is zero as well as for a plastic hinge when the bending moment is equal to the plastic moment of the section commonly denoted by M_P.

The conjugate frame method can be employed with considerable advantage over existing methods to estimate the deformation of structures at ultimate loads. After the value of the ultimate load is determined by any method in terms of the plastic moment of the members of the structure, or vice versa, the deformation analysis can be carried out as illustrated in previous examples with only slight modification. If s is the number of hinges, plastic hinges plus actual hinges, and r is the number of redundant quantities remaining in the structure at ultimate load, it will be shown that $(s + r - 1)$ independent equations can be derived from the conjugate frames expressing the relationships amongst the hinge rotations and the redundant quantities. When the ultimate load is reached, at least one of the plastic hinges is just formed where the hinge rotation is zero. This leaves as many unknowns as there are equations from which the former can be calculated.

The location of the last hinge is best explained by means of numerical examples.

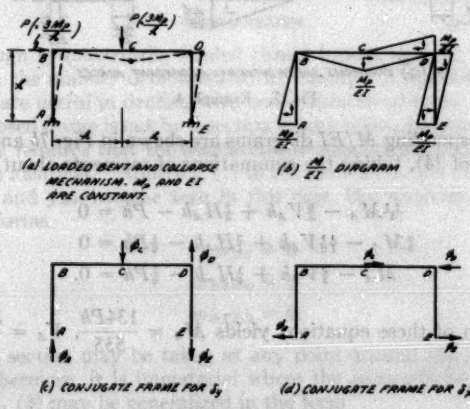
(a) LOADED BENT AND COLLAPSE MECHANISM. M_p AND EI ARE CONSTANT.
(b) $\frac{M}{EI}$ DIAGRAM
(c) CONJUGATE FRAME FOR δ_y
(d) CONJUGATE FRAME FOR δ_x

FIG. 8. Example 5.

Example 5

Consider the fixed-end bent shown in Fig. 8*a* subjected to a horizontal load P applied at joint B and a vertical load P applied at C.

It can be shown[4] that the value of the ultimate load is $P = 3\frac{M_P}{h}$. The collapse mechanism, with plastic hinges developed at A, C, D and E, is shown in dotted lines and the corresponding M/EI diagram is shown in Fig. 8*b*. The conjugate frames for δ_y and δ_x are shown, respectively, in Fig. 8*c* and *d* in which the directions of the hinge rotations ϕ_A, ϕ_C, ϕ_D and ϕ_E are determined from the collapse mechanism following the sign convention indicated in Fig. 3*b* and *c*.

Since $s = 4$ and $r = 0$, $s + r - 1 = 3$ indicating that three simultaneous equations can be derived from the conjugate frames expressing the relationship amongst the hinge rotations. Considering Fig. 8*c*, equating the summation of moment about E to zero yields

$$2\phi_A - \phi_C + \frac{M_P h}{6EI} = 0. \qquad (a)$$

In Fig. 5*d*, taking the summation of moment about E leads to

$$\phi_C - \phi_D + \frac{M_P h}{EI} = 0 \qquad (b)$$

and the condition $\delta_{xB} = \delta_{xD}$ yields

$$\phi_A h + \frac{M_P h^2}{3EI} = \phi_E h + \frac{M_P h^2}{6EI}$$

or

$$\phi_A - \phi_E + \frac{M_P h}{6EI} = 0. \qquad (c)$$

For the purpose of illustration, let us first assume that the last hinge is formed at C. In this case $\phi_C = 0$ which, upon substitution in (*a*) and (*b*), leads to $\phi_A = -\frac{M_P h}{12EI}$ and $\phi_D = \frac{M_P h}{6EI}$, respectively. Substituting the value of ϕ_A just obtained in (*c*) yields $\phi_E = \frac{M_P h}{12EI}$. The negative value of ϕ_A indicates that this assumption is incorrect since the collapse mechanism requires that ϕ_A be clockwise as shown in the conjugate frames. For the second trial, assuming that the last hinge is formed at A yields $\phi_A = 0$, $\phi_C = \frac{M_P h}{6EI}$, $\phi_D = \frac{M_P h}{3EI}$ and $\phi_E = \frac{M_P h}{6EI}$. Since the directions of all the rotations are consistent with the collapse mechanism, the second assumption leads to the correct solution.

[4] This example is taken from (10) in which the deformation analysis is carried out by means of slope-deflection equations.

To obtain the deflections of points B and C, the summation of moment about point C in Fig. 8c yields $\delta_{yC} = \frac{M_P h^2}{3EI}$ and taking the summation of moment about point B in Fig. 8d leads to $\delta_{xB} = \frac{M_P h^2}{3EI}$. The positive signs indicate that point C deflects downward and point B moves to the right.

Example 6

Consider the two-story bent loaded as shown in Fig. 9a. It can be demonstrated that the ultimate load[8] is $P = \frac{11M_P}{3h}$, the collapse mechanism being indicated in dotted lines with plastic hinges developed at

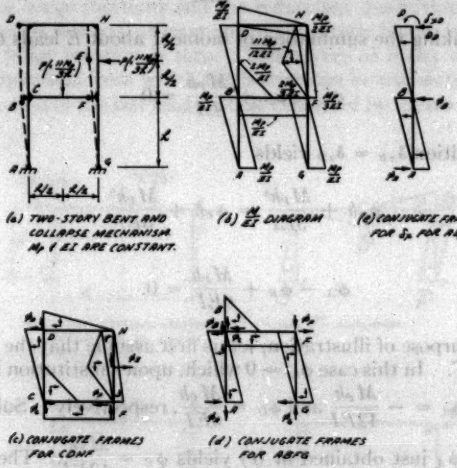
(a) TWO-STORY BENT AND COLLAPSE MECHANISM
(b) M/EI DIAGRAM
(c) CONJUGATE FRAMES FOR δy FOR ABD
(c) CONJUGATE FRAMES FOR CDHF
(d) CONJUGATE FRAMES FOR ABFG

FIG. 9. Example 6.

points A, B, C, D, E, F and G. The corresponding M/EI diagram is shown in Fig. 9b while the conjugate frames for $CDHF$ and $ABFG$ are shown, respectively, in Fig. 9c and d. To reduce the number of figures, the conjugate frame for δ_x and that for δ_y are combined in a single figure in each case. The vertical arrows are associated with the latter, the horizontal ones with the former. As in the last example, the directions of the hinge rotations are taken consistent with the collapse mechanism.

[8] See (6) for the determination of the ultimate load.

It should be observed that, in accordance with the sign convention shown in Fig. 3, the directions of ϕ_C, ϕ_F and the loads on member CF in Fig. 9*c* are opposite to those on member BF in Fig. 9*d*.

In this case $s = 7$ and $r = 0$, hence $s + r - 1 = 6$ indicating that six independent equations can be derived from the conjugate frames. In Fig. 9*c*, $\sum M_{F_v} = 0$,[6] $\sum M_{C_v} = 0$ and $\sum M_{F_z} = 0$ yield, respectively,

$$\begin{aligned} \phi_D - \phi_C + \frac{5M_Ph}{6EI} &= 0 \\ \phi_E - \phi_F + \frac{M_Ph}{8EI} &= 0 \\ \phi_E - 2\phi_D - \frac{35M_Ph}{72EI} &= 0. \end{aligned} \tag{d}$$

Considering Fig. 9*d*, $\sum M_{A_y} = 0$, $\sum M_{G_y} = 0$ and equating $\delta_{zB} = \delta_{zF}$ lead[7] to

$$\begin{aligned} \phi_F - \phi_G + \frac{M_Ph}{4EI} &= 0 \\ \phi_B + \phi_C - \phi_A - \frac{M_Ph}{12EI} &= 0 \\ \phi_G - \phi_A + \frac{M_Ph}{18EI} &= 0. \end{aligned} \tag{e}$$

Assuming that the last hinge is formed at D, $\phi_D = 0$ and (*d*) and (*e*) yield $\phi_C = \frac{5M_Ph}{6EI}$, $\phi_E = \frac{35M_Ph}{72EI}$, $\phi_F = \frac{11M_Ph}{18EI}$, $\phi_G = \frac{31M_Ph}{36EI}$, $\phi_A = \frac{11M_Ph}{12EI}$ and $\phi_B = \frac{M_Ph}{6EI}$. It should be noted that the solution of (*d*) and (*e*) involves very little numerical work due obviously to the fact that each equation involves only two or three unknowns.

To estimate the lateral deflection of each story, taking the summation of moment about point D in Fig. 9*e* yields

$$\delta_{zD} = -\frac{5M_Ph^2}{3EI}.$$

[6] For brevity, ΣM_{F_v} denotes the summation of moment about point F in the conjugate frame for δ_v.

[7] $\delta_{zB} = -\phi_A h - \frac{M_Ph^2}{6EI}$ and $\delta_{zF} = -\phi_G h - \frac{2M_Ph^2}{9EI}$, both assumed positive or toward the right.

Taking moment about point B yields

$$\delta_{xB} = -\frac{13M_P h^2}{12EI}.$$

The negative signs indicate that the deflections are toward the left.

Example 7

To illustrate the treatment of frames with inclined members, consider the two-bay gable frame (Fig. 10*a*) which is subjected to a hori-

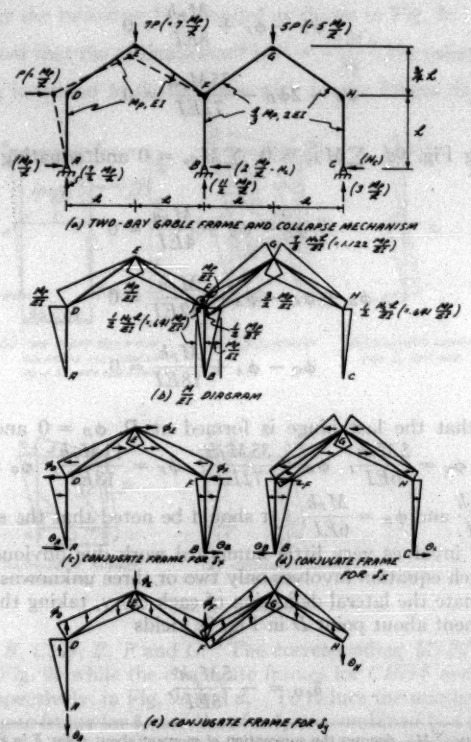
(a) TWO-BAY GABLE FRAME AND COLLAPSE MECHANISM
(b) $\frac{M}{EI}$ DIAGRAM
(c) CONJUGATE FRAME FOR δ_x
(d) CONJUGATE FRAME FOR δ_x
(e) CONJUGATE FRAME FOR δ_y

FIG. 10. Example 7.

zontal load P at joint D and two vertical loads $7P$ and $5P$ applied at joints E and G, respectively. The plastic moment and the flexural

rigidity of the members as well as the collapse mechanism are indicated in the figure. It can be shown that the ultimate load is $P = \frac{M_P}{h}$ with plastic hinges developed at joints D, E and F. Under ultimate loads the structure is statically indeterminate to the first degree and, taking H_C as the redundant reaction, the corresponding M/EI diagram is shown in Fig. 10*b*. In this case $s = 6$, $r = 1$ and $s + r - 1 = 6$ indicating that six independent equations can be derived relating the rotations of the plastic hinges ϕ_D, ϕ_E and ϕ_F, the rotations of the actual hinges θ_A, θ_B and θ_C and the redundant reaction H_C.

In the conjugate frames shown in Fig. 10*c*, *d* and *e*, the directions of ϕ_D, ϕ_E, ϕ_F and θ_A should be consistent with the collapse mechanism. After these four quantities and H_C are determined by means of four of the six equations, θ_B and θ_C may be calculated from the remaining two equations with arbitrarily assumed directions, the correct directions being indicated by the signs of the solution.

In Fig. 10*d*, $\sum M_C = 0$ yields

$$H_C = 1.283 \frac{M_P}{h}. \qquad (f)$$

Substituting (*f*) in Fig. 10*b* results in an M/EI diagram expressed in terms of $\frac{M_P}{EI}$. Considering Fig. 10*c*, $\sum M_B = 0$ yields

$$\phi_D - 1.75\,\phi_E + \phi_F + 0.140 \frac{M_P h}{EI} = 0. \qquad (g)$$

In Fig. 10*e*, $\sum M_F = 0$ and $\sum M_H = 0$ lead to, respectively,

$$\begin{aligned} 2\theta_A - 2\phi_D + \phi_E - \frac{M_P h}{EI} &= 0 \\ 2\theta_A - 2\phi_D + 1.5\phi_E - \phi_F - 0.904 \frac{M_P h}{EI} &= 0. \end{aligned} \qquad (h)$$

Assuming the last hinge to be formed at D, $\phi_D = 0$ for which the solution of (*g*) and (*h*) yields $\phi_E = 0.189 \frac{M_P h}{EI}$, $\phi_F = 0.191 \frac{M_P h}{EI}$ and $\theta_A = 0.406 \frac{M_P h}{EI}$.

With the values of θ_A, ϕ_D, ϕ_E and ϕ_F known, equating the summation of forces to zero in Fig. 10*c* yields $\theta_B = 0.275 \frac{M_P h}{EI}$, and the same equilibrium condition in Fig. 10*d* leads to $\theta_C = 0.436 \frac{M_P h}{EI}$. With all the hinge rotations known, the rotation and deflection of any point in the

frame can be computed simply by calculating the shear and moment at the corresponding point in the conjugate frames.

CONCLUSIONS

It is evident that the conjugate frame method, when applied to beam problems, degenerates into the conjugate beam method. As obvious is the fact that the procedure employed in the last three examples lends itself readily to the deformation analysis of beams under ultimate loads.

Although no examples are given for frames composed of members with varying moment of inertia, the analysis of such cases presents no new problem other than the determination of the area and the location of the centroid of more complicated M/EI diagrams. In cases where these diagrams are higher-degree curves, the integrations defined by (2) may be carried out or they may be approximated by summations with the curves replaced by step functions. The above comments apply equally well to frames with curved members.

In the plastic design of rigid-frame structures composed of structural steel members, the ductility of the materials ensures, in common cases, that the hinge rotations required to develop the plastic collapse load can be sustained by the plastic hinges. Even then a deformation analysis should prove to be both wise and necessary in order to judge whether the deflection of the structure or portion thereof due to accidental overloading is within acceptable limit. In the ultimate strength design of reinforced concrete structures (11), the small strain capacity of concrete turns the hinge rotations into the major design consideration. To this end, among others, the conjugate frame method may prove to be a useful tool in addition to the ones heretofore available.

V.2
195

REFERENCES

(1) H. F. B. MUELLER-BRESLAU, "Beitrag zur Theorie des Fachwerks," *Z. Architekt. u. Ing. Hannover*, Vol. 31, p. 418 (1885).
(2) H. M. WESTERGAARD, "Deflection of Beams by the Conjugate Beam Method," *J. Western Soc. Engrs.*, November, 1921.
(3) J. A. VAN DEN BROEK, "Theory of Limit Design," *Trans. ASCE*, Vol. 105, p. 638 (1940).
(4) J. F. BAKER, "The Design of Steel Frames," *Struct. Engr.*, Vol. 27, p. 397 (1949).
(5) M. R. HORNE, "Fundamental Propositions in the Plastic Theory of Structures," *J. Inst. Civil Engrs.*, Vol. 34, p. 174 (1950).
(6) H. J. GREENBERG AND W. PRAGER, "Limit Design of Beams and Frames," *Trans. ASCE*, Vol. 117, p. 447 (1952).
(7) P. S. SYMONDS AND B. G. NEAL, "Recent Progress in the Plastic Methods of Structural Analysis," JOUR. FRANKLIN INST., Vol. 252, pp. 383, 469 (1951).
(8) P. S. SYMONDS AND B. G. NEAL, "The Interpretation of Failure Loads in the Plastic Theory of Continuous Beams and Frames," *J. Aero. Sci.*, Vol. 19, p. 15 (1952).
(9) K. E. KNUDSEN, C. H. YANG, B. G. JOHNSTON, L. S. BEEDLE AND W. H. WEISKOPF, "Plastic Strength and Deflections of Continuous Beams," *Weld. J.*, Vol. 32, p. 240-S (1953).
(10) B. G. NEAL, "The Plastic Methods of Structural Analysis," New York, John Wiley & Sons, Inc., 1956, p. 192.
(11) A. L. L. BAKER, "Further Research in Reinforced Concrete, and Its Application to Ultimate Load Design," Paper No. 5894, Proc. Inst. Civil Engrs. (1953).

THE FRANKLIN INSTITUTE

LIBRARY

The Committee on Library desires to add to the collections any technical works that members may wish to contribute. Contributions will be gratefully acknowledged and placed in the Library. Duplicates received will be transferred to other libraries as gifts of the donor. 303 items have been added the past month.

Photostat service. Photostat prints of any material in the collections can be supplied on request.

The Library and reading room are open from 9 A.M. until 5 P.M. on Mondays, Tuesdays, Thursdays, Fridays and Saturdays; and 2 P.M. until 10 P.M. on Wednesdays.

RECENT ADDITIONS

AERONAUTICS

HOERNER, SIGHARD F. Fluid-Dynamic Drag. Ed. 2. 1958.
MORGAN, HOWARD E. Turbojet Fundamentals. Ed. 2. 1958.

AGRICULTURE

SOCIETY OF CHEMICAL INDUSTRY. The Comparison of High- and Low-Volume Spraying Techniques on Fruit and Ground Crops. 1958.

ARCHAEOLOGY

ALLEN, AGNES. The Story of Archaeology. 1958.

ASTRONOMY

PEEK, BERTRAND M. The Planet Jupiter. 1958.

ATOMIC ENERGY

VILLAR, G. E. Energia Atomica. 1956.

BIBLIOGRAPHY

FULLER, DUDLEY D. A Survey of Journal Bearing Literature. 1958.
ITALY. CONSIGLIO NAZIONALE DELLE RICERCHE. Bibliographia Marconiana. 1958.

BIOLOGY

SOCIETY OF AMERICAN BACTERIOLOGISTS. COMMITTEE ON BACTERIOLOGICAL TECHNIQUE. Manual of Microbiological Methods. 1957.

CHEMISTRY AND CHEMICAL TECHNOLOGY

BRITISH GELATINE AND GLUE RESEARCH ASSOCIATION. Recent Advances in Gelatin and Glue Research. 1958.
DONALDSON, NORMAN. The Chemistry and Technology of Naphthalene Compounds. 1958.
EUROPEAN FEDERATION OF CHEMICAL ENGINEERING. Chemical Reaction Engineering. 1957.
FAIRES, R. A. AND PARKS, B. H. Radioisotope Laboratory Techniques. 1958.
FEDERATION OF PAINT AND VARNISH PRODUCTION CLUBS. Film Formation, Film Properties, and Film Deterioration. 1958.
GILREATH, ESMARCH S. Fundamental Concepts of Inorganic Chemistry. 1958.
HAMANN, S. D. Physico-Chemical Effects of Pressure. 1957.
INTERNATIONAL CONGRESS OF SURFACE ACTIVITY. Proceedings. 2nd. 1957.
INTERNATIONAL SYMPOSIUM ON ISOTOPE SEPARATION. Proceedings. 1st. 1958.
INTERNATIONAL UNION OF PURE AND APPLIED CHEMISTRY. ANALYTICAL CHEMISTRY SECTION. Modern Electroanalytical Methods. 1958.
KATZ, JOSEPH J. AND SEABORG, GLENN T. The Chemistry of Actinide Elements. 1957.
MEGSON, N. J. L. Phenolic Resin Chemistry. 1958.

SMITH, IVOR, ED. Chromatographic Techniques. 1958.
THOMSON, R. H. Naturally Occurring Quinones. 1957.

DICTIONARIES

Dictionary of Physics. 1958.

ELECTRICITY AND ELECTRICAL ENGINEERING

BELL TELEPHONE LABORATORIES, INC. Transistor Technology. 1958.
BOAST, WARREN BENEFIELD. Principles of Electric and Magnetic Circuits. Ed. 2. 1957.
CALDWELL, SAMUEL HAWKS. Switching Circuits and Logical Design. 1958.
HAMMOND, P. H. Feedback Theory and its Applications. 1958.
HELLER, SOL. TV and Radio Tube Troubles. 1958.
LAGO, GLADWYN VALIE AND WAIDELICH, DONALD LONG. Transients in Electrical Circuits. 1958.
PULLEN, KEATS A. Conductance Curve Design Manual. 1958.
TURNER, RUFUS P. Electronic Hobbyists' Handbook. 1958.
U. S. ADVISORY GROUP ON ELECTRON TUBES. National Conference on Tube Techniques. Proceedings. 3rd. 1958.

ENGINEERING

BISHOP, ALAN WILFRED AND HENKEL, DAVID JOHN. The Measurement of Soil Properties in the Triaxial Test. 1957.
GATEWOOD, BUFORD ECHOLS. Thermal Stresses, with Applications to Airplanes, Missiles, Turbines and Nuclear Reactors. 1957.
ROCARD, YVES. Dynamic Instability; Automobiles, Aircraft, Suspension Bridges. 1957.

GENERAL

CRAIG, JOHN H. Newton at the Mint. 1946.

MANUFACTURE

BELANGER, EMIL J. Modern Manufacturing Formulary. 1958.
EARLY, DONALD F. AND REED, EDWARD A. Techniques of Pressworking Sheet Metal. 1958.

MATHEMATICS

BOOTH, KATHLEEN H. V. Programming for an Automatic Digital Calculator. 1958.
PECK, LESLIE G. AND HAZELWOOD, R. NICHOLS. Finite Queuing Tables. 1958.
RICHTMYER, ROBERT D. Difference Methods for Initial Value Problems. 1957.
RIORDAN, JOHN. An Introduction to Combinatorial Analysis. 1958.

METALLURGY

COWLES, ALFRED. The True Story of Aluminum. 1958.
HANSEN, MAX AND ANDERKO, KURT. Constitution of Binary Alloys. 1958.

NUCLEAR ENGINEERING

HALL, W. B. Reactor Heat Transfer. 1958.
INTERNATIONAL UNION OF PURE AND APPLIED PHYSICS. Proceedings of the Rehovoth Conference on Nuclear Structure. 1958.
SYRETT, J. J. Nuclear Reactor Theory. 1958.
U. S. ARGONNE NATIONAL LABORATORY, CHICAGO. Nuclear Reactor Experiments. 1958.

OPTICS

HOUSTOUN, ROBERT ALEXANDER. Physical Optics. 1957.

PATENTS

HIGGINS, FRANK VICTOR. One Hundred One Don'ts for Inventors. 1957.

PHYSICS

BETHE, HANS ALBRECHT AND SALPETER, EDWIN. Quantum Mechanics of One- and Two Electron Atoms. 1957.

BOHR, NIELS HENRIK DAVID. Atomic Physics and Human Knowledge. 1958.
CONWAY, H. G. Fluid Pressure Mechanisms. Ed. 2. 1958.
HOOPER, JOHN EDWARD AND SCHARFF, MORTEN. The Cosmic Radiation. 1958.
IOFFE, A. F. Semiconductor Thermoelements and Thermoelectric Cooling. 1957.
KAY, JOHN MENZIES. An Introduction to Fluid Mechanics and Heat Transfer. 1957.
MANSFIELD, W. K. Elementary Nuclear Physics. 1958.
PERRINE, JAMES OWEN. Physics and Mathematics in Electrical Communication. 1958.
SOO, S. L. Thermodynamics of Engineering Science. 1958.
WRIGHT, W. D. The Measurement of Colour. 1958.

PLASTICS

FISHER, EDWIN GEORGE. Extrusion of Plastics. 1958.
SIMONDS, HERBERT RUMSEY. A Concise Guide to Plastics. 1957.

SANITARY ENGINEERING

EHLERS, VICTOR MARCUS AND STEEL, ERNEST W. Municipal and Rural Sanitation. Ed. 5. 1958.

SPACE FLIGHT

BEARD, R. B. AND ROTHERHAM, A. C. Space Flight and Satellite Vehicles. 1958.
The Russian Literature of Satellites. Part 1. 1958.

STATISTICS

BROSS, IRWIN D. J. Design for Decision. 1957.

SUGAR

EDSON, HUBERT. Sugar, from Scarcity to Surplus. 1958.

WOOD

BROWN, NELSON COURTLAND AND BETHEL, JAMES SAMUEL. Lumber. Ed. 2. 1958.

DO YOU KNOW OF THE FRANKLIN INSTITUTE'S NEED FOR GIFTS?

Since 1824 The Franklin Institute, through wise and conservative management, has been partially self-supporting.

As an old institution, established in the public interest, The Franklin Institute has tried to earn most of its cost by diligent and productive work. Like many other institutions of a non-profit nature, The Institute has, in these years of an expanding economy and rising spiral of costs, found it increasingly difficult to perform the broad educational services of which the growing nation and territories are ever in need.

Despite an erroneous public impression gained, perhaps, by the excellence and wide range of services performed, that it is a wealthy, richly endowed organization, The Institute always needs funds.

There is a warm satisfaction in giving financial support to an organization that will use it constructively to help advance and improve our type of civilization.

Your gift or bequest, large or small, will be deeply appreciated. We shall be pleased to give any additional information regarding gifts or memorials.

Where property is transferred, title should be in the name of The Franklin Institute of the State of Pennsylvania for the Promotion of the Mechanic Arts.

Please write to: The Secretary, The Franklin Institute, Benjamin Franklin Parkway at Twentieth Street, Philadelphia 3, Pennsylvania.

BARTOL RESEARCH FOUNDATION
W. F. G. SWANN, DIRECTOR

E2 − M1 MIXING RATIOS IN $2^+ \rightarrow 2^+ \rightarrow 0^+$ TRANSITIONS *

BY

V. R. POTNIS [1] AND C. E. MANDEVILLE [2]

When a nuclear energy level decays by emission of electromagnetic radiation, depending upon the spin sequence, transitions of any one of several different multipole orders may be possible. In the case of a $2^+ \rightarrow 2^+ \rightarrow 0^+$ spin arrangement, the first transition, $2^+ \rightarrow 2^+$, will often be magnetic dipole or electric quadrupole in character. Such a transition is said to be mixed. The gamma ray emitted second in time always results from a pure $E2$ transition, the spin change ranges from $2 - 0$ to $2 + 0$, and so has only the value 2. In the case of the mixed transition, the relative intensities, $I(E2)$ and $I(M1)$, are respectively proportional to the squares of the matrix elements which describe the two types of transition. The quantity δ is defined as

$$\delta = \pm \sqrt{I(E2)/I(M1)}. \tag{1}$$

In a recent report (1),[3] Sakai has sought to associate certain values of δ with the $2^+ \rightarrow 2^+ \rightarrow 0^+$ de-excitation of even-even nuclei in certain regions of the atomic table. More specifically, he has attempted to develop a form of systematics involving the nuclear shell model which relates the sign and magnitude of δ to regions of neutron number which precede the closing of the $g_{9/2}$, $h_{11/2}$, and $i_{13/2}$ sub-shells. These "islands" of nuclei occur for $38 \leq N \leq 48$, $64 \leq N \leq 74$, and $110 \leq N \leq 124$. From his consideration of published data, Sakai has concluded that the sign of δ is negative in the first and third islands and positive in the second.

The value of δ is often determined from spatial correlation experiments involving the two emitted gamma rays of the $2^+ \rightarrow 2^+ \rightarrow 0^+$ transitions. Because of the systematic significance which has been attached (1) to the value of δ, previously reported measurements of this quantity for some even-even nuclei of the third island have been re-evaluated.

The angular correlation function for two gamma ray quanta emitted successively in cascade is

$$W(\theta) = 1 + A_2 P_2 (\cos \theta) + A_4 P_4 (\cos \theta) \tag{2}$$

* Assisted by the joint program of the Office of Naval Research and the U. S. Atomic Energy Commission.

[1] Permanent address: Gwalior (M.P.), India.

[2] Assistant Director.

[3] The boldface numbers in parentheses refer to the references appended to this article.

where $P_2(\cos\theta)$ and $P_4(\cos\theta)$ are the Legendre polynomials, and the coefficients A_2 and A_4 depend on the spins and the multipole orders of the emitted radiations. The mixing ratio, δ, is related to the coefficients A_2 and A_4 by the equations,

$$A_2 = \frac{1}{1+\delta^2}(0.250 + 0.732\delta - 0.077\delta^2)$$
$$A_4 = \frac{0.326\delta^2}{1+\delta^2}. \tag{3}$$

Equations 3 are plotted in Fig. 1. The quantity δ can also be obtained

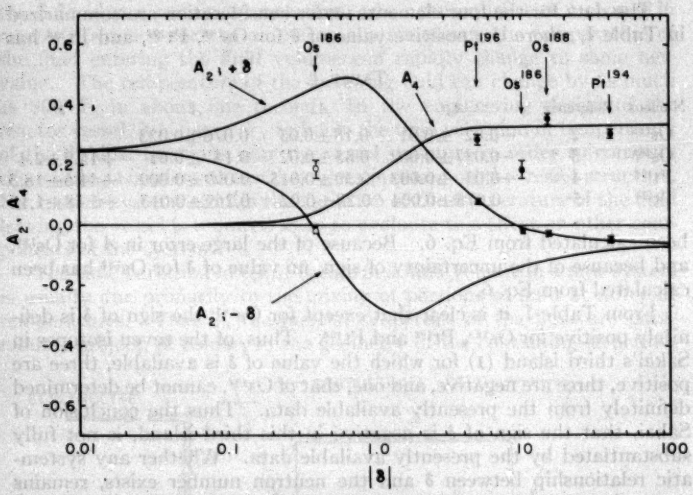

FIG. 1. Coefficients A_2 and A_4 plotted as a function of δ. Values of A_2 and A_4 corresponding to δ negative for Os^{186} are indicated by the open circles.

from the anisotropy A defined as

$$A = \frac{W(180°) - W(90°)}{W(90°)} \tag{4}$$

or in terms of A_2 and A_4,

$$A = \frac{1 + A_2 + A_4}{1 + A_2/2 + 3A_4/8} - 1. \tag{5}$$

Equation 5 is of course obtained from Eqs. 2 and 3. Equation 5 can

further be reduced to

$$A = \frac{3 + 8.782\delta + 0.715\delta^2}{7 - 2.927\delta + 9.286\delta^2} \qquad (6)$$

From experimentally determined correlation functions, values of A_2 and A_4, and of A, can be obtained.

The observed values of A_2 and A_4 are plotted in Fig. 1. For the cases of Os^{188}, Pt^{194}, and Pt^{196}, the observed values (3–5) of A_2 and A_4 lie upon or near curves calculated for a positive value of δ. The values (2) of A_2 and A_4 for Os^{186} could be interpreted as suggesting either a positive or negative value of δ.

The data for the four elements under consideration are summarized in Table I, where the positive value of δ for Os^{188}, Pt^{194}, and Pt^{196} has

TABLE I.

Nucleus	Reference	A_2	A_4	A	δ
Os^{186}	2	-0.02 ± 0.01	0.18 ± 0.03	0.076 ± 0.023	
Os^{188}	3	-0.037 ± 0.002	0.35 ± 0.02	0.14 ± 0.01	$+15.9 \pm 2.4$
Pt^{194}	4	-0.05 ± 0.003	0.30 ± 0.015	0.099 ± 0.009	$+44.6 \pm 18.3$
Pt^{196}	5	0.075 ± 0.004	0.28 ± 0.02	0.269 ± 0.013	$+5.48 \pm 1.10$

been calculated from Eq. 6. Because of the large error in A for Os^{186}, and because of the uncertainty of sign, no value of δ for Os^{186} has been calculated from Eq. 6.

From Table I, it is clear that except for Os^{186}, the sign of δ is definitely positive for Os^{188}, Pt^{194} and Pt^{196}. Thus, of the seven isotopes in Sakai's third island (1) for which the value of δ is available, three are positive, three are negative, and one, that of Os^{186}, cannot be determined definitely from the presently available data. Thus the conclusion of Sakai, that the sign of δ is negative in this third island, is not fully substantiated by the presently available data. Whether any systematic relationship between δ and the neutron number exists, remains uncertain.

REFERENCES

(1) MITSUO SAKAI, Report on Even-Even Nuclei, Institute for Nuclear Study, University of Tokyo, Japan. INSJ-6, February 24, 1958.
(2) T. LINDQVIST AND I. MARKLAND, *Nucl. Phys.*, Vol. 4, p. 189 (1957).
(3) V. R. POTNIS, V. S. DUBEY AND C. E. MANDEVILLE, *Phys. Rev.*, Vol. 102, p. 459 (1956).
(4) C. E. MANDEVILLE, J. VARMA AND B. L. SARAF, *Phys. Rev.*, Vol. 98, p. 94 (1955).
(5) V. R. POTNIS, *Indian Journal of Physics*, Vol. XXX, p. 375 (1956).

THE FRANKLIN INSTITUTE LABORATORIES
NICOL H. SMITH, DIRECTOR

AN ELECTROLYTIC METHOD FOR TRANSIENT MIXING MEASUREMENTS *

BY
MARVIN P. NORIN [1]

In certain fluid systems it is necessary to know the transient temperature behavior of a fluid volume in the system when the system is subjected to a change in operating conditions. A nuclear reactor vessel, for example, may contain large plenums or volumes of coolant wherein the fluid is at a certain temperature. As a consequence of a change in reactor operation such as an emergency shutdown, the temperature of the fluid entering the fluid volume can rapidly change to some new value. The temperature of the incoming fluid can change by as much as 300° F. in about one second. In the engineering design of the reactor vessel, it is necessary to know the time variation in temperature of the fluid at locations near the vessel structure in order to compute the ensuing transient thermal stresses imposed on the vessel structure. For reactor systems studies the variation of the temperature of the fluid leaving the vessel is required so as to evaluate this effect on other components of the system.

The time variation in temperature of a fluid volume in a flow system is usually due primarily to the mixing of portions of fluid at different temperatures. That is, the inertial properties of the fluid are paramount, subject, of course, to the geometry of the containing structure.

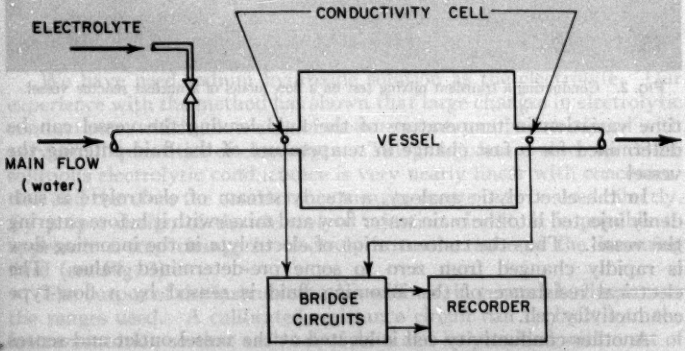

FIG. 1. Electrolytic method for transient mixing measurements.

* Work sponsored by Atomic Power Development Associates, Detroit, Mich.

[1] Senior Research Engineer, Heat Transfer & Fluid Mechanics Branch.

The thermal properties of the fluid may be neglected. For this case, the temperature changes in transient mixing may be simulated by an electrolytic method which has been developed at The Franklin Institute Laboratories.

To illustrate the method, consider the diagram of Fig. 1. What is required here is the mixing characteristics of the vessel such that the

FIG. 2. Conducting a transient mixing test on a flow model of a nuclear reactor vessel.

time variation in temperature of the fluid leaving the vessel can be determined for a fast change in temperature of the fluid entering the vessel.

In the electrolytic analogy, a steady stream of electrolyte is suddenly injected into the main water flow and mixes with it before entering the vessel. Thus the concentration of electrolyte in the incoming flow is rapidly changed from zero to some pre-determined value. The electrical resistance of the incoming fluid is sensed by a flow-type conductivity cell.

Another conductivity cell is located at the vessel outlet and senses the resistance of the fluid leaving the vessel. The conductivity cells are connected in the active arms of bridge circuits. The bridge circuits are connected to a multiple-channel recorder which gives a time record

of the electrical resistance or conductance at the cell locations. These data can then be converted to values of electrolyte concentration.

Now if the inertial properties of the fluid are paramount in the mixing process, then the diffusion properties of the electrolyte may be neglected in accounting for the changes in concentration. Thus, the changes in concentration are closely analogous to temperature changes. The mixing characteristics measured with the electrolytic method can then be used to predict transient behavior.

There is no inherent inertial-type time lag in a conductivity cell such as that found in a thermocouple. Any time lag is only that necessary for "washing away" of fluid at the electrodes. This can be minimized by good design of the cell so as to allow free passage of the fluid past the electrolyte.

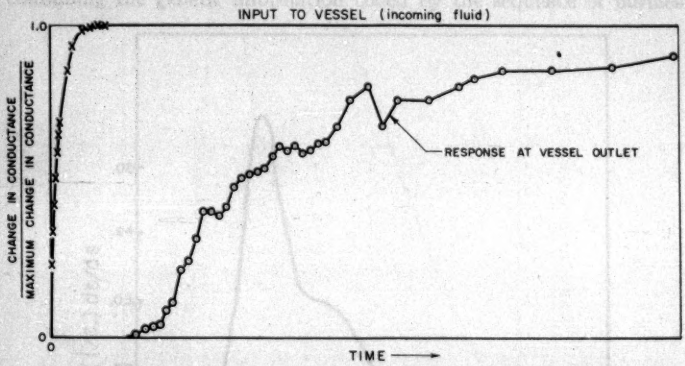

FIG. 3. Sample response curve—transient mixing in a nuclear reactor vessel.

We have used sodium hydroxide solution as the electrolyte. Our experience with the method has shown that large changes in electrolytic conductance, which allow ease of measurement, can be introduced with very small quantities of electrolyte. This is important since for dilute solutions electrolytic conductance is very nearly linear with concentration and therefore the conductance measurements may be used directly. By proper design of the electrolyte injection circuit, it is possible to approach a step change in electrolytic conductance of the incoming fluid (see Fig. 3).

The output of the instrumentation will not, in general, be linear over the ranges used. A calibrated resistance circuit can be built into the instrumentation so that each set of data can be provided with a set of calibrated values. It is necessary to use a-c. power for the conductivity cells so as to avoid polarization. We have used a 2500-cps. power supply.

An experimental setup for mixing measurements in a flow model of a nuclear reactor vessel is shown in Fig. 2. A sample response curve for a cell location in the vessel outlet is given in Fig. 3 for the input shown. In Fig. 3 the dimensionless ratio of the change in conductance to the maximum change in conductance is plotted against time. By converting to concentration ratios (not necessary in the linear range of the conductance *versus* concentration curve) one can use the curves of Fig. 3 to predict the time-temperature behavior at the vessel outlet in response to the change in temperature of the incoming fluid. This response can also be used to calculate the response to inputs other than step changes. Or, another approach would be to design an electrolyte injection system which would produce the desired input and measure the response directly.

Seminar on* A Physical Chemical Study of Calf Thymus Deoxyribonucleic Acid.—DR. VERNE NORMAN SCHUMAKER of the Department of Biochemistry, University of Pennsylvania, Philadelphia, Pennsylvania, addressed the Seminar of The Biochemical Research Foundation on Tuesday, April twenty-second.

Fresh problems, significant and challenging, are afforded the physical biochemist by the nucleic acids. Deoxyribonucleic acid (DNA), according to recent concepts, is the bearer of the genetic information of the living cell; it may be considered to be a macromolecular blueprint containing the genetic information coded by the sequence of purines

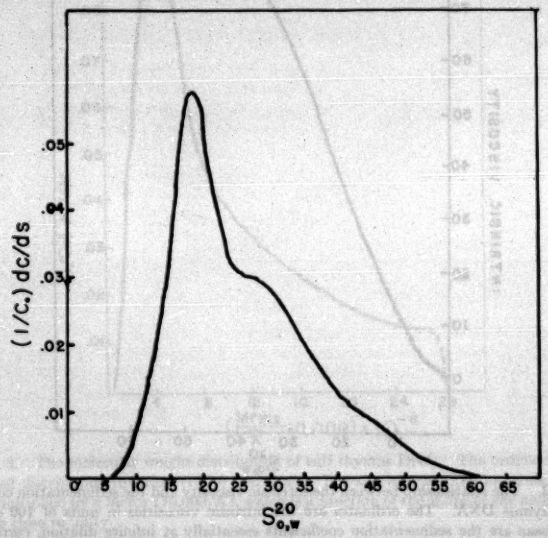

FIG. 1. The sedimentation coefficient distribution of calf thymus DNA. The abscissae are the sedimentation coefficients corrected to 20° C. in water. Since the concentration at which the ultracentrifuge run was made was 0.001%, correction for concentration dependence can be neglected. The ordinates are values of the normalized distribution function, $(1/Co)(dC/dS)$. Corrections for the radial shape of the centrifuge cell and for the inhomogeneous centrifugal field which would distort the distribution function have been applied.

* The work reported in this communication was performed at the Virus Laboratory, University of California, Berkeley, Calif. This work was supported in part by a grant from the National Science Foundation.

and pyrimidines along a doubly stranded helix. Hence, the study of the physical chemical properties of this molecule may be of importance as a first step toward "cracking" the genetic code.

The difficulties inherent in measuring the molecular weight as well as many other physical properties of DNA are intimately related to the tremendous asymmetry of this biological polymer. Hydrodynamic interactions between these extended molecules occur even in fairly dilute solutions and are pronounced at the concentrations employed when using schlieren optical techniques. Hydrodynamic interactions

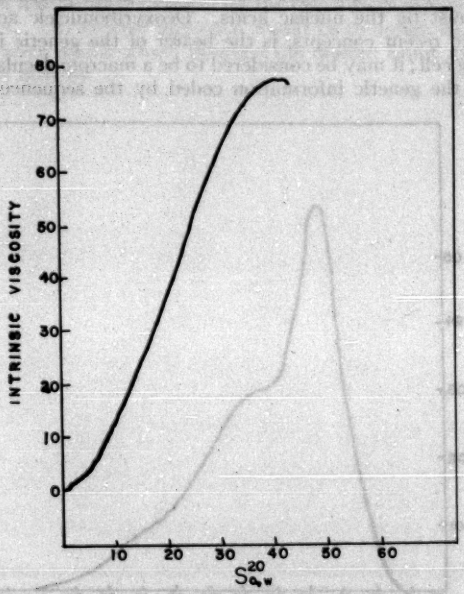

FIG. 2. The relationship between the intrinsic viscosity and the sedimentation coefficient for calf thymus DNA. The ordinates are the intrinsic viscosities in units of 100 cm./gm. The abscissae are the sedimentation coefficients essentially at infinite dilution, corrected to 20° in water.

are not significant if extremely dilute solutions are studied. For example, ten years ago ultracentrifuge measurements of calf thymus DNA had always been performed at concentrations sufficiently high to resolve the sedimenting boundary with the schlieren optical system (1). Recently, when concentrations were reduced 50 fold and the sedimenting boundary observed with an ultraviolet absorption optical system, the observed properties of the molecule changed markedly. With the

schlieren optical system, a sharp spike with a sedimentation coefficient of 10 svedbergs had been observed. At the lower concentration and employing UV optics, there was now seen to be a whole spectum of molecules with sedimentation coefficients ranging between 5 and 60 svedbergs (see Fig. 1) (2, 3).

This extreme polydispersity in sedimentation coefficient exhibited by calf thymus DNA could conceivably be caused by a corresponding polydispersity in either the molecular weight or the shape of these

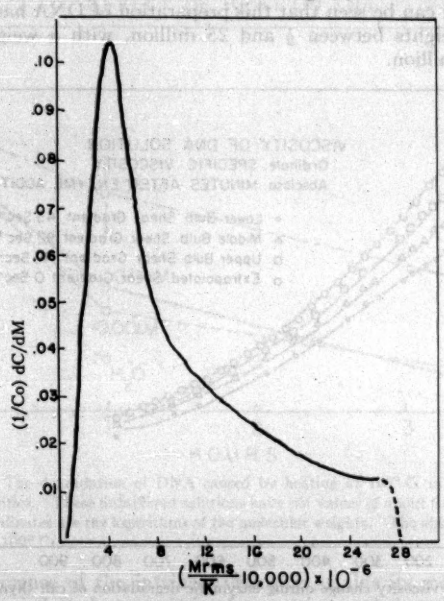

FIG. 3. The molecular weight distribution of calf thymus DNA. The ordinates are the normalized distribution function $(1/Co)\ (dC/dM)$. The abscissae are the molecular weights $\times 10^{-6}$ multiplied by a factor $(10{,}000/K)$, which is a function of the shape of the molecule and should be close to unity.

particles in solution. In order to decide between these two extreme possibilities, the DNA preparation was divided by preparatory centrifugation into 10 fractions, each fraction containing molecules of different sedimentation characteristics. The sedimentation coefficient distribution and the intrinsic viscosity of each fraction were then measured, and from this information the relation between the sedimentation coefficient and intrinsic viscosity was worked out for calf thymus nucleic acid. This relation is shown in Fig. 2; the intrinsic viscosity

increases as the sedimentation coefficient increases, which is just what would be expected if the polydispersity in sedimentation coefficient were *primarily* due to a polydispersity in molecular weight. A decrease in the intrinsic viscosity would be found if the polydispersity were due to shape factors alone.

The molecular weight distribution can be calculated from the data of Figs. 1 and 2, assuming that the polydispersity is *entirely* due to the variation in the molecular weight. This has been done and is presented in Fig. 3. It can be seen that this preparation of DNA has a range of molecular weights between ½ and 25 million, with a weight average value of 10 million.

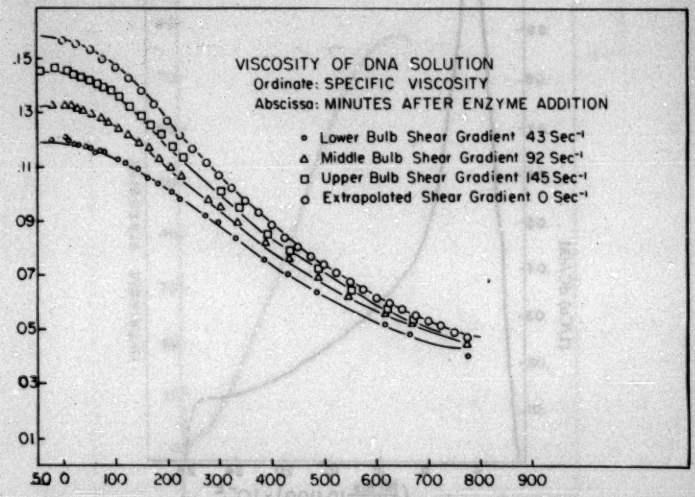

FIG. 4. The viscosity change during enzymatic degradation of calf thymus DNA as a function of time. The three lower curves represent the experimentally determined values of the reduced viscosity at three different shear gradients. The upper curve is the extrapolated reduced viscosity at zero shear gradient. The ordinate is the specific viscosity, and the abscissa is time in minutes.

Occasionally, knowledge of intimate structural detail may be gained by physical-chemical studies. Important architectural information about DNA has been obtained by a study of the kinetics of the enzymatic degradation of this molecule. In solution DNA is a rope-like structure. If this "rope" has but one strand, then at each attack by the degrading enzyme, it should break, and the result should be a large decrease in the molecular weight and, for highly asymmetric particles, the intrinsic viscosity. If the DNA "rope" is composed of two strands,

held together by weak crosslinkages, then the molecule will not break until the enzyme has cleaved both strands at adjacent positions along the rope. Hence, a study of the intrinsic viscosity of a solution of DNA undergoing enzymatic degradation should afford considerable structural information. This study has been made, and the results are are presented in Fig. 4. It is obvious from this figure that there is a protracted lag period after the introduction of the enzyme before the

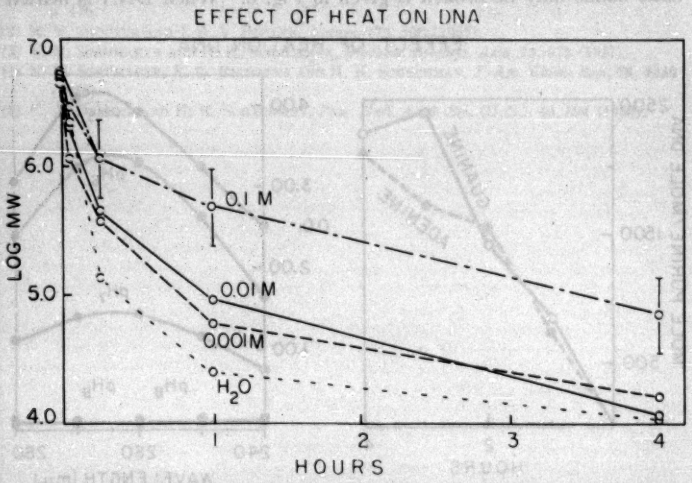

FIG. 5. The degradation of DNA caused by heating at 100° C. in NaCl solutions of various molarities. These unbuffered solutions have pH values of about 6.5 at room temperature. The ordinates are the logarithms of the molecular weights. The abscissae are the times of heating at 100° C.

rate of decrease of the intrinsic viscosity attains its maximum value. This lag period is characteristic of a multi-stranded structure, and the one strand rope model for DNA may be eliminated at once. Detailed mathematical analysis of the shape of the intrinsic viscosity *vs.* time curve of Fig. 4 shows that the data are best described by a two-strand rope model for DNA and that both of the strands are continuous along the length of the molecule, containing few if any preformed interruptions (4).

Additional evidence for a non-interrupted doubly-stranded structure for DNA comes from examination of the effects of heat degradation. Heating solutions of DNA at 100° C. at various ionic strengths causes slow but progressive breakdown of the macromolecule. (See Fig. 5.) However, the intrinsic viscosity decreases 50 fold during the first 2 or 3

minutes of heating (5). This suggests that the molecular rigidity, which gives a highly extended structure possessing a large intrinsic viscosity, is due to multiple hydrogen bonding between the two chains. Upon heating, the weak hydrogen bonds break at once, and the intrinsic viscosity falls markedly. Changes in the molecular weight, however, reflect cleavage of strong "backbone" bonding—probably the 3',5'-phosphate diester linkages. Some information as to how these backbone bonds may be broken is given in Fig. 6. When DNA is heated

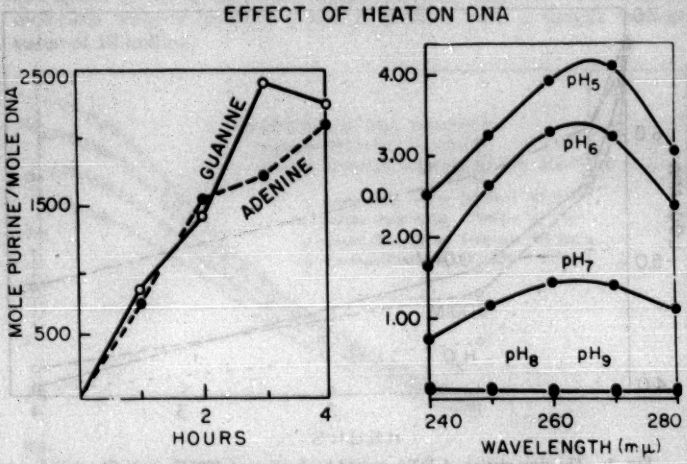

FIG. 6. The left-hand figure shows the release of the purines adenine and guanine from DNA as a function of the time of heating at 100° C. in a neutral but unbuffered solution. Paper chromatography was used for the identification and the estimation of the bases. The right-hand figure shows the relative optical density increments obtained after heating DNA at 100° C. at various pH values for one hour, then precipitating the DNA with acid and examining the supernatant liquid.

at 100° C. at acid or neutral pH values, a great amount of ultraviolet absorbing material is released into solution. By paper chromatography this material yields the purines adenine and guanine, an indication of the sensitivity of the N-glycosidic bond to heating, particularly at acid pH values. The splitting of the N-glycosidic bond frees the reducing end of the sugar which may then activate the cleavage of the diester phosphate bond.

In summary, application of physical chemical techniques has given a detailed picture of the molecular weight distribution of a sample of calf thymus nucleic acid, which extends from ½ to 25 million, and yields

a weight average value of 10 million. The structure of the DNA molecule has also been examined and the results obtained are best explained by a two-strand rope model. The integrity of the strands and the sensitivity of various chemical bonds within the molecules to heat treatment have been included in this study.

REFERENCES

(1) D. O. JORDAN, "The Nucleic Acids," New York, Academic Press, Inc., 1955, Vol. I, p. 470.
(2) K. V. SHOOTER AND J. A. V. BUTLER, *Nature*, **175**, 500 (1955).
(3) V. N. SCHUMAKER AND H. K. SCHACHMAN, *Biochim. Biophys. Acta*, **23**, 628 (1957).
(4) V. N. SCHUMAKER, E. G. RICHARDS AND H. K. SCHACHMAN, *J. Am. Chem. Soc.*, **78**, 4230 (1956).
(5) C. A. DEKKER AND H. K. SCHACHMAN, *Proc. Natl. Acad. Sci.* (U. S.), **40**, 894 (1954).

NUCLEAR RADIATION DETECTION, by William J. Price. 382 pages, diagrams, 6 × 9 in. New York, McGraw-Hill Book Co., Inc., 1958. Price, $9.00.

The era during which users of nuclear radiation detectors designed and constructed their own equipment has passed on. Generally speaking, commercial sources now supply most of the required instruments, and, indeed, one is likely to become confused by the large variety of detectors which are now available.

This book presents, in a most intelligible manner, basic scientific information which should enable even a novice to determine which type of instrument best fulfills his particular requirements. On the other hand, the experienced research physicist who is already thoroughly conversant with the principles of operation and properties of the various detection devices covered will welcome this extremely well-organized collection of basic material which has heretofore been difficult to extricate from the very extensive and widely-scattered literature on the many aspects of the subject. Furthermore, fundamental considerations which are important in the interpretation of the measurements obtained with the various types of detector are discussed; this is a matter of obvious importance to all who design or use radiation detection equipment, or who are dependent upon measurements made by others.

Chapter 1 deals with the properties of nuclear radiation, specifically with respect to interactions with matter. A brief survey of detection methods, followed by a discussion of the statistical nature of detecting systems, introduces chapters dealing with ionization chambers, Geiger-Muller counters, proportional counters, scintillation detectors, photographic emulsions and other detection methods (that is, cloud chambers, crystal counters, Cerenkov detectors, chemical dosimeters, calorimeters). A separate chapter is then devoted to neutron detection methods, and finally there is a detailed treatment of the principles of operation of some of the electronic circuits associated with nuclear radiation detectors.

The book is well-written and illustrated, contains an ample bibliography, and is logically organized. It will undoubtedly prove of great value in the training of students of nuclear science and technology, and would serve admirably as a text for a course in nucleonics instrumentation. There are numerous illustrative examples with solutions interspersed throughout the text, as well as a collection of problems at the conclusion of each chapter.

In the opinion of the reviewer (who is admittedly biased) the omission of a chapter on cosmic-ray detectors, which would have been most timely, is unfortunate. There are only occasional references to the application of some of the techniques to cosmic-ray experiments, but no consistent policy is evident. Nevertheless, *Nuclear Radiation Detection* is an excellent book which certainly serves the purposes for which it was written.

M. A. POMERANTZ
Bartol Research Foundation

THE GYROSCOPE—THEORY AND APPLICATIONS, by James B. Scarborough. 257 pages, diagrams, 6 × 9 in. New York and London, Interscience Publishers, 1958. Price, $6.50.

While the dynamics of the gyroscope are included in most books on mechanics, we also find special treatises, such as Klein and Sommerfeld's "Theorie des Kreisels," Gray's "Gyrostatics and Rotational Motion," Grammel's "Der Kreisel" and Greenhill's "Gyroscopic Theory," all of an advanced nature. At the other extreme, there are numerous elementary books of a popular nature. In the intermediate class we have Crabtree's "Spinning Tops and Gyroscopic Motion" and "Mechanics of the Gyroscope," by Deimel. Prof. Scarborough's book is a welcome text adding to this latter group, with a good analytical and vector treatment, with many practical applications on important engineering problems.

The theory of the gyroscope well illustrates the principle of the space rate of change in angular momentum; and the reactions set up are the moments or torques required to cause these changes. In the more complicated problems we have couplings between the

various coordinates defining the system. Such gyroscopic couplings are of importance in the understanding of the operation of technical applications. For these applications, as well as an elementary understanding of the basic theory, the analytical approach, as used by the author, is needed. Of special interest is the well chosen group of applied problems, such as the top, ship stabilizers, the gyroscopic compass, direction indicators, the monorail car, applications to machinery as well as some astronomical applications.

The author's analytical approach to the various problems could be considerably improved by introducing a more physical discussion of the interactions. Thus, in the discussion of the rolling hoop, it seems unnecessary to introduce a prescribed curvature with radius R and corresponding "centrifugal" force mv^2 to account for the lateral space-rate of change of linear momentum $mv\dot{\phi}$, due to a *precessing oscillation* ϕ about its vertical axis, in moving along its path. The lateral component of the ground reaction, which is not shown, is simply $F = m(r\ddot{\theta} + r\omega\dot{\phi})$, since $v = r\omega$, while the vertical component is approx. $N = mg$. On taking moments about a transverse axis through the center of gravity (that is, tangent to its mean path), we have $A\ddot{\theta} + C\omega\dot{\phi} = Nr\theta - Fr$, giving $(A + mr^2)\ddot{\theta} + mr^2\omega\dot{\phi} + C\omega\dot{\phi} = mgr\theta$. With $A\ddot{\phi} - C\omega\dot{\theta} = 0$, about the vertical, we have the oscillation equations for the hoop.

In the analysis of more complicated systems with several degrees of freedom, with the direct application of Euler's equations, it is necessary to include the interactions between parts of the system, unless a more generalized method of analysis, as with Lagrange's equations, is used. Such latter methods are not used in this book.

RUPEN EKSERGIAN
The Franklin Institute Laboratories

ALIPHATIC FLUORINE COMPOUNDS, by Alan M. Lovelace, William Postelnek and Douglas A. Rausch. 370 pages, 6 × 9 in. New York, Reinhold Publishing Corp., 1958. Price, $12.50.

This book on the preparation and properties of aliphatic compounds will be useful to any chemist who is interested in the synthesis of fluorine-containing organic compounds.

The various methods used to introduce fluorine into organic molecules are discussed concisely and generous reference to the literature is evident from the list of 224 references at the end of this section. Other chapters deal with the classical types of organic compounds such as alkanes, alkenes, alcohols, ethers, etc. Two chapters are devoted to nitrogen compounds and these contain sections on azomethines, triazines in addition to the more common types of compounds such as amines, nitriles, nitrocompounds, etc. A discussion of organometallic and -metalloid compounds is included.

Each chapter contains a brief description of the various methods used to prepare the derivative. A table of compounds, arranged according to empirical formula and indicating the preparative method by number, the yield, physical properties and reference to the original literature, is also given in each chapter. Altogether these tables contain information about 4500 compounds. The authors have carefully reviewed the literature through 1955 and have included important contributions made during the following two years.

Obviously the authors could not give a detailed discussion of the properties of all aliphatic fluorine compounds but they have done a very creditable job of selecting important topics for somewhat expanded coverage. They have adequately provided the reader with references to cover the classes of compounds of lesser interest to most chemists.

PAUL TARRANT
University of Florida

PROCEEDINGS OF THE SECOND INTERNATIONAL CONGRESS OF SURFACE ACTIVITY, VOL. I, GAS/LIQUID AND LIQUID/LIQUID INTERFACE. 521 pages, diagrams, 6 × 9¼ in. New York, Academic Press Inc., 1958. Price: $15.00; complete set of 4 vols., $50.00.

The Proceedings, Volume I, are subdivided into the following parts: 1. Insoluble Films; 2. Soluble Films; 3. Foams; 4. Evaporation Retardation; 5. Monolayers Liquid/Liquid Interface; 6. Solubilization and Micelles; 7. Emulsions; 8. General Phenomena.

Under these headings, a good review of the

modern research on surface activity at the International meeting is given, where most of the specialists presented their reviews and results. The papers that the reviewer considers most interesting are: H. E. Ries and W. A. Kimball on "Structure of Fatty-acid Monolayers and a Mechanism for Collapse," in Part 1; B. V. Derjaguin and A. S. Titijevskaya, "Static and Kinetic Stability of Free Films and Froths," in Part 3; Part 4 describing the newly developed conservation of water by spreading hexadecanol films on the surface water reservoirs; the article of M. B. Smith and A. E. Alexander on "Solubilization of Soap Micelles," in Part 6; and M. Linton and K. L. Sutherland on "Dynamic Surface Forces Drop Circulation, and Liquid/Liquid Mass Transfer," in Part 8.

These papers present new results not previously published that appear to have permanent intrinsic value to the reviewer. The whole presentation at the Congress presented a very high standard of scientific endeavor and all the articles are important in their particular field. The whole volume is probably the best representation of the research in the field of surface phenomena at the moment and is well recommended for this purpose.

WLADIMIR PHILIPPOFF
The Franklin Institute Laboratories

PROCEEDINGS OF THE SECOND INTERNATIONAL CONGRESS OF SURFACE ACTIVITY, VOL. II, SOLID/GAS INTERFACE, edited by J. H. Schulman. 348 pages, illustrations, 6 × 9¼ in. New York, Academic Press, Inc., 1958. Price: $12.60; complete set of 4 vols., $50.00.

This volume on solid-gas interface presents the papers of the Congress in two broad classifications, physical adsorption containing 23 papers and chemisorption with 12 papers. Although many nations were represented, fortunately for the English readers, the contributions with the exception of a few discussions are presented in this language. The utility of the collection would have been enhanced by having the individual discussions immediately following the pertinent papers. An index also would be helpful.

The introductory lecture of Professor G. M. Schwab to the section on chemisorption was a most fitting and welcome contribution. The proceedings of a Congress of this important nature should have such introductions giving a brief review of the state of the research and a critical summary of the work presented, to point out to the young as well as other workers in the fields the areas where effort might be intensified for greater progress. The contributions are given in a very readable style. In general, each paper and discussion contains an adequate up-to-date set of references. While this volume will serve as a reference collection of recent contributions to the field of research, its value for the advanced worker will increase as additions are made from future proceedings especially if indexes are included.

R. S. DALTER
The Franklin Institute Laboratories

PROCEEDINGS OF THE SECOND INTERNATIONAL CONGRESS OF SURFACE ACTIVITY, VOL. III, ELECTRICAL PHENOMENA AND SOLID-LIQUID INTERFACE, edited by J. H. Schulman. 621 pages, diagrams, 6 × 9¼ in. New York, Academic Press, Inc., 1958. Price: $16.80; complete set of 4 vols., $50.00.

Volume III of the Proceedings of the Second International Congress of Surface Activity deals with Electrical Phenomena and the Solid-Liquid Interface. There are fifteen papers devoted to the first topic and fifty-one which deal mainly with the second. The author has grouped these later papers under six sub-headings, namely: Contact Angles, spreading and wetting; Flotation; Adhesion; Adsorption; Lubrication; and Nucleation.

A large variety of phenomena are presented under the heading of electrical phenomena. These include studies on the "U-Effect" which describe the voltages which arise due to mechanical vibrations of the electrical double layer, corrosion effects and the kinetics of the adsorption of organic materials and metal surfaces to name a few. Many of these papers are necessarily brief and those readers not working directly in these fields will find it necessary to do a considerable amount of background reading in order to appreciate the full impact of many of the experiments on physical chemistry theories.

J. J. Bikerman and J. Gustalla in two separate papers point out some oft-times

overlooked considerations which surround the interpretations of surface tension data. These have to do with the apparent inapplicability (except in special cases) of the Young Equation which relates interfacial tension, contact angle and surface tensions at solid-liquid interfaces. These papers are important since the Young equations (or some derivative thereof) are used in interpreting a large amount of current experimental data.

The adsorption of low and high molecular weight material on metallic and nonmetallic surfaces is treated both from the experimental and theoretical viewpoints. Despite the briefness of many of the articles, they serve as informative reviews.

The effects of surface active media on such physical properties as creep, strain and rupture are treated in a paper by P. Rehbinder and V. Lichtman. This work was performed on single metal crystals and thus provides a method of correlating adsorption results with crystal structure.

One of the more interesting articles on nucleation deals with the formation of ice crystals from super-cooled vapors. This article presents recent data obtained on the physics of cloud formation and the role played by condensation nuclei.

This volume covers an enormous amount of material and the references and the discussion sections are most welcome since the phenomena in general cover both solid state physics and physical chemistry. In general the articles are well illustrated. This book brings together under one cover a group of studies of an important class of surface sensitive reactions.

JAMES B. DREW
The Franklin Institute Laboratories

PROCEEDINGS OF THE SECOND INTERNATIONAL CONGRESS OF SURFACE ACTIVITY, VOL. IV, SOLID/LIQUID INTERFACE (WASHINGS, ETC.) AND CELL/WATER INTERFACE, edited by J. H. Schulman. 352 pages, diagrams, 6 × 9¼ in. New York, Academic Press, Inc., 1958. Price: $12.60; complete set of 4 vols., $50.00.

As the title implies, the volumes are a collection of technical papers presented at the Second International Congress of Surface Activity. Vol. IV is subdivided into three main sections: Washing, with 17 papers followed by a discussion; Suspensions and Agglomerations, with 9 papers and a discussion; and Cell Water/Interface (Biological), with 13 papers and a discussion.

Because the volume consists of technical papers, the author assumes that the reader is working in the same field and there is essentially no introduction to the subject For example, the work on surface activity of biological cells appears to be addressed to biologists interested in surface activity rather than to the whole field of workers who are interested in surface activity The editor, as he indicated in the Editor's Note, has collected the original papers and presented them to the publisher As a result the papers are in three languages; English, French and German. Each paper is abstracted in the language in which it was written. It would have been helpful to present the abstract of each paper in the three languages. The quality of the papers is excellent with ample references to current literature and journal articles. The volume will serve as a reference to recent work in the respective fields.

WILLIAM SCHUELE
The Franklin Institute Laboratories

ELEMENTS OF WATER SUPPLY AND WASTE-WATER DISPOSAL, by Gordon Maskew Fair and John Charles Geyer. 615 pages, diagrams, 6 × 9 in. New York, John Wiley & Sons, Inc., 1958. Price, $8.95.

Since this book has been written with the undergraduate student of sanitary engineering in mind, the 175 problems at the end of the book illustrating the scientific principles presented are an outstanding feature.

While not as complete as the authors' larger volume on "Water Supply and Waste-Water Disposal," the present work is entirely adequate in presenting the fundamental laws involved in the treatment of raw water supplies and waste effluents. The two subjects are often discussed together and much duplication is thus avoided.

Typical of the contents are those chapters dealing with "Collection of Surface Water," "Transmission of Water," "Distribution of Water," "Screening, Sedimentation and Flotation," "Filtration," "Biological Treat-

ment," and "Sludge Treatment and Disposal." As in any textbook of this nature, the appendix contains many tables and lists of water treatment chemicals that can be extremely helpful. A feature of this section is a diagram which will be helpful in dealing with the Hazen-Williams formula for determining flow of water in pipes.

A. B. MIDDLETON
Philadelphia Quartz Co.

OBSERVATION AND INTERPRETATION, A SYMPOSIUM OF PHILOSOPHERS AND PHYSICISTS. A Report of the Proceedings of the Ninth Symposium of the Colstor Research Society, edited by S. Korner. 218 pages, plates, 7¼ × 9¼ in. New York, Academic Press, Inc., 1958. Price, $8.00.

The tape recorder is a boon to the book companies. People active in research are usually loathe to undertake the job of writing a book. However, there is usually no great difficulty in the transformation of the tape recorder of a conference to print. Unfortunately, it remains true that the cost in effort of a project is, in most cases, closely proportional to its final value.

The title, *Observation and Interpretation*, is only weakly descriptive of the symposium from which the content of the book under review has been taken. The conference concerned itself with various philosophical problems associated with the interpretation of quantum mechanics. The discussions dealt mainly with the foundations of the concept of probability, the problems of objectivity and subjectivity in quantum mechanics and the quantum theory of measurement. The conference was attended by some forty philosophers and physicists. Seventeen papers, ranging in length from about twenty minutes to about an hour were read; these papers constitute somewhat less than half of the conference report, the remainder being devoted to discussion.

Although several of the individual papers are interesting, the report of the conference does not, to my mind, constitute a significant book. There is no unifying thread binding the discussions of the conference together, no general conception provided which would allow us to understand why the often conflicting discussions of the conference should find themselves between the same covers. The papers were, for the most part, not particularly new. The function of the conference presumably was to permit discussion between physicists and philosophers on matters of mutual interest. In this, the conference was not as successful as one might have hoped it would be.

The book may be of interest to philosophers of science in that it reveals something of the range of reactions of physicists and philosophers to quantum mechanics. The book also shows that experts can often engage in arguments as pointlessly and as fruitlessly as amateurs.

LEONARD EISENBUD
Bartol Research Foundation

PROCEEDINGS OF THE COLLOQUIUM SPECTROSCOPICUM INTERNATIONALE VI, edited by W. van Tongeren and F. Freese. 663 pages, illustrations, 7¼ × 9¼ in. New York and London, Pergamon Press, Inc., 1957. Price, $25.00.

On the 14th through the 19th of May, 1956, the Sixth International Colloquium on Spectroscopy was held in Amsterdam, Netherlands. This book contains the papers presented to that meeting. An adequate review of a book of this type is nearly impossible to give as the papers are very heterogeneous. Experimental work in spectroscopy of the ultra-violet, the visible, and the infrared regions of the spectra and covering work on sources, instruments, and applications are presented. Perhaps the fields covered can best be shown by listing the titles of the sessions as given in the Table of Contents and the number of papers under each title: (1) Plain Spectroscopy (10 papers); (2) Emission Spectroscopy (8 papers); (3) Arc Emission (17 papers); (4) Spark Emission (15 papers); (5) Emission (General) (9 papers); (6) Instrumentation (Emission) (19 papers); (7) Instrumentation of Absorption Methods (8 papers); (8) Ultra-Violet Absorptiometry (7 papers); and (9) Infrared Spectroscopy (15 papers).

These papers are presented in French, German and English by scientists from twenty countries including Western Europe, Russia and the satellites, China, South Africa, and the U. S. A.

Following each paper, questions and comments from the floor are recorded. Many of the papers are abstracted in English and some in English, French and German. There are about a dozen papers in which only the summaries are presented, as the papers were not received by the editors.

This volume contains such a variety of papers presenting new techniques for all the fields of spectroscopy that a study of this work should be a necessity to all spectrographers and designers of spectrographs.

LUTHER C. CONANT, JR.
The Franklin Institute Laboratories

NOTES ON ANALOG-DIGITAL CONVERSION TECHNIQUES, edited by J. W. Brean, M. S. Osman, D. T. Ross, J. E. Ward, and A. K. Susskind. 410 pages, diagrams, 5¼ × 9 in. New York, John Wiley & Sons, Inc., 1958. Price, $10.00.

Five members of M.I.T.'s Servomechanisms Laboratory have combined efforts to treat this specialized subject. Perhaps "specialized" is not the correct word because the techniques of analog-to-digital conversion now cut across many technical fields. These include such widely separated practices as radar, computation, and numerical control of machinery. The analog quantities treated may be voltage signals as well as physical motions, and in the two cases the means of conversion to digital form are divergent indeed.

Casual use of the term "digital" is also an oversimplification. What is implied is the sampling and quantizing of the information with the eventual application of some form of code. It can be seen that the theoretical background of sampling and the principles of code development are absorbing subjects in themselves. These are taken up by the authors before turning to the detailed considerations of analog-to-digital conversion mechanisms.

The engineering considerations confronting the designer in the instance of a numerically-controlled machine tool are intricate but interesting. Questions of electronic circuits, optics, magnetics, and mechanics of extraordinary accuracy may be involved. The book attempts to give a state-of-the-art picture of each specific technique involved. Decoding of the digitally stored information or instructions is discussed following the means of coding. Finally the over-all design of digital instrumentation systems is taken up to show how the components may affect each other.

The book appears as an informal publication employing offset printing and showing some lack of good editing. Parts are wordy, as though ideas and information were hard to find, while some portions are brief and unclear. These comments do not, however, reflect upon the authors' technical competence, of which there is ample evidence through the points raised in the text. Rather, there is the suggestion that the whole publication project was hurried and had to depend upon the spare time busy men could snatch from their other work. One serious shortcoming, particularly in a book like this, where terms and definitions are so important, is the absence of any kind of index. However, the reviewer has already found the text and illustrations useful in his work, and it is certainly to be expected that others will. It might be pointed out also in closing that this is the group that did the first serious work on the numerical control of large milling machines. The very extensive projects carried out in the Servomechanisms Laboratory undoubtedly provide much of the experience that is assembled in this impressively comprehensive book.

C. W. HARGENS
The Franklin Institute Laboratories

BOOK NOTES

SCIENTIFIC PROGRAMMING IN BUSINESS AND INDUSTRY, by Andrew Vazsonyi. 474 pages, diagrams, 6 × 9 in. New York, John Wiley & Sons, Inc., 1958. Price, $13.50.

Written for the businessmen who want to use scientific techniques in solving managerial problems, this book sets forth in understandable language, the ways in which mathematics can aid management—linear programming, statistical decision theory and operations research. The author carefully presents fundamentals and then goes into detail about their use in practical business problems such as transportation allocation, production, inventory, warehousing, stable employment, assembly line scheduling, accounting, etc. In these days, no business executive can afford to ignore the techniques of mathematics now being applied so successfully in all lines of business; if he knows nothing about them, he should get this book and study it carefully.

VECTOR SPACES AND MATRICES, by Robert M. Thrall and Leonard Tornheim. 318 pages, 6 × 9 in. New York, John Wiley & Sons, Inc., 1957. Price, $6.75.

In an attempt to bridge the gap between beginning and higher levels of the theory of vector spaces and matrices, the authors have used a dual approach on two levels—one concrete (via matrices) and the other axiomatic (via linear transformation). Eleven chapters cover the field thoroughly, including vector spaces, linear transformations, determinants, orthogonal and unitary equivalence, polynomial rings, linear inequalities, etc. The theory of games is briefly touched on in the final chapter.

CIRCUIT ANALYSIS OF TRANSMISSION LINES, by John Stewart. 186 pages, diagrams, 6 × 9 in. New York, John Wiley & Sons, Inc., 1958. Price, $5.50.

This new addition to the literature provides a compact but comprehensive treatment of the ordinary transmission line, by the usual approximation to a "lossless" line. The Maxwell equations are not gone into, hence the test is suitable for instruction at the undergraduate level. It is well arranged for this purpose, taking up in turn the derivation of the basic equations for "lossless" and "lossy" lines, wave propagation, resonant lines, and cavities, equivalent lumped circuits, standing-wave ratio and impedance measurements, and the use of the Smith chart for graphical solutions. Basic data for transmission line calculations are included in a five page appendix. While the emphasis is on radio-frequency lines, the audio and power engineer will also find the book of interest and assistance.

HIGH-SPEED DATA PROCESSING, by C. C. Gotlieb and J. N. P. Hume. 338 pages, diagrams, 6 × 9 in. New York, McGraw-Hill Book Co., Inc., 1958. Price, $9.50.

The authors have thoroughly outlined the general techniques of processing data at high speeds, particularly for business purposes. This text covers a wide range of subjects, from the method of representing information in a processor to advances in automatic programming. Not limiting itself to any particular machine, the book covers data processing of all types and from all manufacturers, using a hypothetical machine as a working model.

MORPHOGENESIS: THE ANALYSIS OF MOLLUSCAN DEVELOPMENT, by Chr. P. Raven. 311 pages, diagrams, 5¾ × 8¼ in. New York, London, Paris, Pergamon Press, Inc., 1958. Price, $10.00.

This volume is a survey, both descriptive and experimental, of the present state of knowledge on development in the molluscs. The chapters deal mainly with the causal analysis of morphogenesis. Cytochemical and experimental embryological investigations on molluscs have been completely covered, and cytological aspects of develop-

ment are especially emphasized. Researches from the author's own laboratory claim an important place in this book.

HIGH QUALITY SOUND REPRODUCTION, by James Moir. 591 pages, plates, diagrams, 5½ × 8½ in. New York, The Macmillan Company, 1958. Price, $14.00.

In this profusely illustrated volume on sound reproduction, the author discusses the different characteristics of acoustic conditions of auditoria. Considerable space is devoted to the design of amplifiers and to a discussion of loudspeaker mountings and enclosures. An appendix is included at the end of each chapter for easy reference. The professional engineer, as well as the amateur interested in the problem of reproducing sound with a high degree of fidelity, will find this book provides a wealth of material.

PHYSICS FOR ENGINEERS AND SCIENTISTS, by Richard G. Fowler and Donald I. Meyer. 546 pages, illustrations, 6 × 9 in. Boston, Allyn and Bacon, Inc., 1958. Price, $8.00.

A "new look" physics text which discards the classical division of subject matter for a unified approach and emphasizes modern insights and developments. Calculus is used, but may be omitted for more elementary courses. Instructors should appreciate the convenient division into 30 topical chapters averaging 17 pages and suitable for a week's work each. Students will appreciate the wealth of excellent illustrations.

TABLE FOR THE SOLUTION OF CUBIC EQUATIONS, by Herbert E. Salzer, Charles H. Richards and Isabelle Arsham. 161 pages, 5½ × 8 in. New York, McGraw-Hill Book Co., Inc., 1958. Price, $7.50.

This useful table makes it possible to find the three roots for any cubic equation having real coefficients, in a few minutes with a desk calculator. More accurate and easier to use than other existing tables, this table will be a valuable aid for engineers, physicists and applied mathematicians. Adequate instructions for using the table are given in the introduction, including interpolation. The table covers every possible set of real coefficients.

AGRICOLA ON METALS, edited by Bern Dibner. 128 pages, illustrations, 8½ × 10¾ in. Conn., Burndy Library, 1958. Price, $2.50.

The mining and metallurgical industries of 16th century Germany is the subject of Georgius Agricola's book. This historic work, originally titled "De Re Metallica" and written in Latin, was translated by Herbert Hoover and his wife in 1912 after five years of research. Reproducing over 70 selected illustrations from the original edition, the Editor of the present offering, Bern Dibner, presents a distillation for the reader interested primarily in the historical significance of the origin of metals. This text is a record of a highly developed industrial culture that flourished some 200 years ahead of what we call "the industrial revolution."

PRINCIPLES OF GEOCHEMISTRY, by Brian Mason. Second edition, 310 pages, diagrams, 6 × 9 in. New York, John Wiley & Sons, Inc., 1958. Price, $8.50.

A pleasantly written systematic account of the chief facts and ideas of the chemistry of the earth and of its chemical and physical evolution, adapted from notes for a one-semester course taught by the author, who is Curator of Physical Geology and Mineralogy at the American Museum of Natural History and a Professor at Columbia. It should be useful to students of geology, astronomy, and chemistry. There is a substantial bibliography, with annotations.

FUNDAMENTALS OF CHEMICAL ENGINEERING, by Maurice G. Larian. 644 pages, diagrams, 6 × 9 in. Englewood Cliffs (N. J.). Prentice-Hall, Inc., 1958. Price, $10.50.

A new text for undergraduates, this book emphasizes the analytical rather than the empirical approach. Three main sections cover General Principles (flow of fluids, heat and mass transfer, evaporation), Separation of Mixtures by Interphase Mass Transfer Operations (drying of solids, distillation techniques, extraction and gas absorption), and Mechanical Separation of Heterogeneous Mixtures (gravitational and centrifugal methods and filtration). The author, Professor of Chemical Engineering at Michigan State University, has been guided by his

own classroom experiences in the preparation of the text.

ATOMIC ENERGY LEVELS, AS DERIVED FROM THE ANALYSIS OF OPTICAL SPECTRA, VOL. III, by Charlotte E. Moore. 245 pages, 9 × 11½ in. Washington, U. S. Government Printing Office, 1958. Price, $2.50; to foreign countries, $3.13 (in U. S. exchange).

Volume III in this series covers the atomic energy levels of the elements Molybdenum through Lanthanum ($Z = 42$ through 57) and Hafnium through Actinium ($Z = 72$ through 89). It includes 124 spectra, with the data presented as in Vols. I and II. With the publication of the present volume, the tabulation of the Periodic Table is complete except for two groups of rare-earth elements which will be published as Vol. IV. Until this last volume is available, a current list of references to analyses of rare-earth spectra is included in Vol. III. The series is published by the National Bureau of Standards.

SERIAL PUBLICATIONS OF THE SOVIET UNION 1939–1957, compiled by Rudolf Smits, 459 pages, 9 × 11½ in. Washington, U. S. Government Printing Office, 1958. Price, $2.75.

This bibliographic checklist of Soviet serial publications includes government and non-official publications appearing either regularly or irregularly in the Soviet Union in 1939 or later—except those in oriental languages. The checklist, published by The Library of Congress, includes the title, place of publication, issuing body and year the publication began, as well as the names of U. S. libraries holding the publication. A subject guide referring to specific publications will help the English reader immeasurably. With the increasing emphasis on Soviet work, this checklist will be a valuable aid to scientists in this country.

PUBLICATIONS RECEIVED

MATHEMATICAL TABLES AND FORMULAE, by F. J. Camm. 144 pages, 4¼ × 7¼ in. New York, Philosophical Library, 1958. Price, $2.75.

OPERATIONAL MATHEMATICS, by Ruel V. Churchill. Second edition, 337 pages, diagrams, 6 × 9 in. New York, McGraw-Hill Book Co., Inc., 1958. Price, $7.00.

DIFFERENTIAL EQUATIONS, by Forest Ray Moulton. Unabridged and unaltered republication of the first edition, 395 pages, 5½ × 8 in. New York, Dover Publications, 1958. Price, $2.00 (paper).

MATHEMATICAL TABLES, by Herbert Bristol Dwight. Second edition, 220 pages, 5½ × 8 in. New York, Dover Publications, 1958. Price, $1.75 (paper).

MICROWAVE TRANSMISSION DESIGN DATA, by Theodore Moreno. Unabridged and unaltered republication of the first edition, 248 pages, 5½ × 8 in. New York, Dover Publications, 1958. Price, $1.50 (paper).

HISTORY OF MATHEMATICS, by D. E. Smith. Unaltered and unabridged republication of the last edition. New York, Dover Publications, 1958. Vol. I, 596 pages, 5½ × 8 in. Vol. II, 725 pages. Price, $2.75 each or $5.00 for both.

CONCISE INTERNATIONAL DICTIONARY OF MECHANICS AND GEOLOGY (English-French-German-Spanish), by S. A. Cooper. 400 pages, 4¼ × 7¼ in. New York, Philosophical Library, 1958. Price, $6.00.

AUDIO DESIGN HANDBOOK, by H. A. Hartley. 224 pages, diagrams, 5½ × 8½ in. New York, Gernsback Library, Inc., 1958. Price: $2.90 (paper); $5.00 (hard cover).

ELECTRONIC MEASURING INSTRUMENTS, by E. H. W. Banner. Second edition, revised, 496 pages, diagrams, 5½ × 8¼ in. New York, The Macmillan Company, 1958. Price, $7.95.

INTRODUCTION TO NUCLEAR ENGINEERING, by Richard Stephenson. Second edition, 491 pages, illustrations, 6 × 9 in. New York, McGraw-Hill Book Co., Inc., 1958. Price, $9.50.

CHEMISTRY, by James V. Quagliano. 877 pages, diagrams, 6 × 9 in. Englewood Cliffs (N. J.), Prentice-Hall, Inc., 1958. Price, $6.95.

A COMPREHENSIVE BIBLIOGRAPHY ON OPERATIONS RESEARCH. 188 pages, 8½ × 11 in. New York, John Wiley & Sons, Inc., 1958. Price, $6.50.

A SELECTED BIBLIOGRAPHY OF RESEARCH AND DEVELOPMENT AND ITS IMPACT ON THE ECONOMY. 21 pages, 7¾ × 10½ in. Washington, D. C., National Science Foundation, 1958. Price, not given.

TABLES OF TEMPERATURE, RELATIVE HUMIDITY AND PRECIPITATION FOR THE WORLD. 6 × 9¾ in. London, Her Majesty's Stationery Office, 1958. One volume (composite), or six parts, covering North America, South America, Europe, Africa, Asia and Australasia. Various paging, various prices, paper.

CURRENT TOPICS

Space Technology Tools.—New space technology tools, developed to help produce vehicles for flight into outer space, have been disclosed by the General Electric Company. Included in the family of new G-E space technology tools is America's biggest plasma jet generator for testing space models under the high-temperature and the chemical conditions of atmospheric re-entry from outer space, a unique, 120-ft. long shock tunnel, largest in the country, used to study space vehicle design requirements at velocities up to 25 times greater than the speed of sound, a solar furnace that automatically tracks the sun to provide clean, radiant heat energy for making non-contaminating tests, and electronic mass-accelerators—which will hurl a mass at velocities over twice as great as those produced by a 16-in. cannon —for free-flight tests.

According to George F. Metcalf, top General Electric space flight executive and general manager of the Company's Missile and Ordnance Systems Department, "these electronic, atomic, high-temperature, and high-speed probing devices support the modern space pioneer in the same way the axe and flintlock served the early American frontiersman."

Located at the Company's Missile Ordnance Systems Department, in Philadelphia, some of the equipment is being used to help solve the nose cone re-entry problem on the Air Force's ATLAS and THOR ballistic missile programs. The equipment is operated by engineers and scientists in G-E's Aerosciences Laboratory.

Newest of the space technology tools is the giant plasma generator, just now completing its development stage. Installed at G-E's Switchgear Department, one of the few facilities in the free world capable of generating the electric current it needs, the plasma jet yields temperatures more than twice the surface temperature of the sun.

The large, air-stabilized electric arc, enclosed by a chamber 18 in. through and 3 ft. high, as contrasted to forerunners of 4 by 10 in., is a three-phase a-c. model and has been run at the rate of 15,000 kw. At this rate of usage, based upon the average daily home use, the power needed to operate the plasma generator at its peak is equivalent to that flowing into 5,400,000 homes.

"Advantages of an arc of this size are that more nearly full-scale models of re-entry vehicles can be tested in its plasma flow and that the simulated Mach 12–25 speed of the plasma jet more nearly approximates actual space-flight conditions," Metcalf said.

Much smaller stabilized arcs, announced by G-E over a year ago, have been used for testing materials in small-scale models and have assisted engineers to study ionic propulsion methods and upper atmospheric conditions. G-E, a pioneer in stabilized arc development, has designed and built both liquid and gas stabilized arcs.

Stabilized arcs, whether liquid or gas, differ from normal electric arcs in that the arc column is controlled, or stabilized, by a squeezing blanket of liquid or gas. This blanket, forced

into the arc container tangentially, develops a hollow center, or vortex, through which the arc is struck. The arc column is restricted by the size of the vortex, and increased current can be fed into the arc, raising the temperature correspondingly. A plasma jet is then forced out to test materials at high speeds and high temperatures. In conventional arcs, increased current causes the arc column to broaden, spreading the heat over a wider area; hence the value of stabilization for high heat concentration.

Perhaps the most impressive of G-E's space technology tools is this country's largest shock tunnel, 6 in. by 120 ft., which permits high-temperature and high speed studies—aerothermodynamics. Unlike other, conventional shock tubes, this space technology tunnel is equipped with an expansion nozzle and a large reservoir, which contains the specimen. Studied by means of Schlieren photography, specimens are subjected to Mach 15–25 blasts of air that are compressed and driven, by exploding gases, down the tube. The 18,000° F. and 5000 psi. air then flows through the expansion nozzle in front of the reservoir over the specimen. Flow patterns set up by these fast-moving gases yield data that will largely determine spacecraft design.

Three smaller, companion tubes, of varying lengths, diameters, and inside configurations, support G-E's large, space-age shock tunnel by eliminating smaller testing problems and by providing basic information on high-temperature, gaseous physics.

For studies requiring relatively low temperatures, aeroscientists at G-E use a solar furnace. This radiant energy source has the advantage of providing clean heat cheaply. It takes heat directly from the sun, or, on cloudy days, from a large arc light. When using the sun as a source of heat, the heliostat-equipped solar furnace is fed by the sun's rays automatically; for the heliostat, using mirrors, directs the sun into the furnace's concave reflector, where its 3000° C. heat is focused onto a specimen. A hollow quartz hemisphere, capable of being evacuated or of allowing gas mixtures that simulate space vehicle environments, further enhances the value of this otherwise simple mechanism.

Other members of the family of space technology tools have been conceived. An example is the arc discharge hypersonic gun, operated by striking arcs between evenly spaced electrodes along a tube to heat a gas—helium, for example—whose expansion will force a projectile at increasing speeds down the tube. The uniformly increasing pressure behind the mass should propel it, by the time it reaches the end of the tube, at a muzzle velocity vastly greater than that produced by a 16-in. cannon.

Chemical means of propulsion, for example, yield less than 25,000 fps., while electrical means theoretically may push a mass to 60,000 fps. The purpose for such high velocities is to provide free flight tests after the mass leaves the tube at speeds equivalent to those in space. The mass so propelled, possibly a model space vehicle, can subsequently be studied, by spectroscopic or telemetric means, to provide information on actual space conditions.

Device Measures Transistor Switching Time.—A device for testing transistor switching times incorporating a new precision technique for measuring durations in the millimicrosecond region has been announced by

Atronic Products, Inc., Bala-Cynwyd, Pa.

Designed specifically for analyzing the time characteristics of high speed transistors, the API 300 will measure the switching time of the leading or trailing edge of the output pulse with an error of 3.0 millimicroseconds in the 3 to 100 millimicrosecond range. Direct meter reading featuring a presettable go-no-go level makes the unit highly adaptable to production testing as well as to laboratory application.

In operation, the transistor under test is inserted into the input connector of the API 300. Self contained transistor bias voltages are provided, and an extremely precise driving pulse is applied to the transistor. By sampling that portion of the output pulse to be measured with a pulse whose characteristics are known, time is essentially converted to a voltage whose amplitude is proportional to duration. This voltage is amplified and displayed on a meter in terms of millimicroseconds. Functionally, the API 300 consists of:

1. *Input Section* which holds the transistor and makes the proper input and output connections.

2. *Power Supply* which provides all voltages including the transistor bias voltages. The unit operates from a 60 cycle, 110 volt source.

3. *Pulse Generator.* This section generates a precision pulse with a rise time of 1.0 millimicrosecond. This pulse is used to drive the transistor. It is also fed into the Delay Section.

4. *Delay Section* consists of an extremely accurate delay line which delays the precision pulse a fixed amount before being fed into the Gate Section.

5. *Gate Section* is triggered by the pulse from the Delay Section. It samples the transistor output; integrates it and produces a d-c. level proportional to the switching time. This signal is amplified and fed to the output section.

6. *Output Section.* The output of the Gate Section is a voltage level whose amplitude is proportional to time. This is fed into a voltmeter whose dial is calibrated in millimicroseconds for the direct reading of the durations to be measured. By this technique, extremely precise measurements can be made in the 3 to 100 millimicrosecond region.

The model API 300 is available either as a bench top unit or in a rack mounting version. Other models are available which will separate carrier storage time from fall time and provide measurements in different ranges of switching speeds.

New Dust Control Equipment and Chem-Jet Systems.—New equipment especially developed for the control of fine dust will be exhibited by The Johnson-March Corp., Philadelphia dust control engineers, at the American Mining Congress Show to be held in San Francisco from September 22 through 25.

Featured at the dust control exhibit will be new equipment for the control of dust at discharge of dry collectors and for fly ash conditioning, sintering discharge, bin unloading, rail car unloading, and similar applications.

A working model of a Johnson-March unit known as a Type A Hydro-Precipitator Scrubber will be shown. This equipment is used for the scrubbing of gases containing dusts ranging below five microns in particle size and for fume control. It is specifically designed for use with roasters, dryers, pulverizers, and in smelting and sintering plant operations.

The scrubber is said to perform at

99.8 per cent efficiency with dust loadings at five grains per cubic foot and with 70 per cent of the material below the five-micron-size.

The company's Chem-Jet System for controlling dust in metallic and non-metallic mining operations also will be on display. This unit suppresses dust at its source before it can become airborne instead of collecting the dust as older mechanical or dry systems do. Multiple jets apply very small quantities of a surface-active solution containing Compound M-R, a compound specially formulated to reduce surface tension. An average of 1½ gallons of solution per ton of material is added. This ½ of 1 per cent added moisture does not actually wet or adversely affect the raw material treated.

Also on exhibit will be Compound SP, a solution for outdoor storage protection. Samples taken from piles of various raw materials which were treated by the compound will be shown. These samples will show the binding effect of the compound on the material, shallow depth of penetration of the compound, and unweathered condition of the protected material. Compound SP does not affect later use of the stored material.

Reactor Safety Fuse.—A reactor safety "fuse," which automatically shuts down high power nuclear research reactors if operating control is lost, has been designed, built, and successfully tested for the Atomic Energy Commission by Atomics International, a division of North American Aviation, Inc.

The fuse is a safety device designed to provide absolute protection by shutting down "pool" type research reactors without the use of external controls should an abnormal operating condition occur. The development is part of the Commission's reactor safety program.

The fuse was tested recently at the Commission's experimental facility, known as Special Power Excursion Reactor Test (SPERT), at the National Reactor Testing Station in Idaho. It was subjected to severe power surges or "transients." SPERT, operated by Phillips Petroleum Company, was designed to study the characteristics of power surges in nuclear reactors.

The fuse prevented the reactor power from rising excessively during a severe transient in which the rate of power increase was tripling each one-hundredth of a second. The fuse terminated the power surge at a level 25 times lower than the reactor would have reached without the device.

In the test, the total energy generated by the reactor was less than one-tenth that which would have been produced without the fuse. Energy release is an indication of the potential hazard resulting from an abnormal reactor operating condition.

The fuse is completely self-contained and requires no operator or external connections. It includes a cylinder, part of which is in the reactor core. The part of the cylinder outside the core contains boron trifluoride gas. In the event of a reactor transient, or an excessively high level of operation, the gas is automatically released into the other part of the cylinder. The gas acts as a reactor "poison" by absorbing neutrons needed to maintain the nuclear chain reaction. The gas transfer brings the reactor under control almost instantaneously and without damage to the reactor.

Medical Photography.—A process which provides better medical pho-

tography in capillary structure sequence pictures—through use of an instrument adapted from another scientific field—has been developed at the University of Wisconsin Hospitals.

Greater clarity and illumination in capillary photos were achieved by using a metallurgic microscope as source of light. The new process replaces the old method of a quartz rod as light supply in the capillaroscope. The combination was developed by Dr. Enrique Valdivia, instructor in pathology at the UW Medical School, with the technical assistance of Homer Montague, department of photography director at the hospitals.

The new process provides a full diffusion of light without heat while the old method of focused light through a quartz rod tip limited the lighted area and produced intensive heat in the tip which required continuous liquid cooling. The need for cooling is eliminated in the new procedure.

The innovation provides sharp detail in the pulmonary structure and permits greater enlargement without loss of clarity.

The process was developed for use in recording the capillary structure change in the lung of a guinea pig under simulated high altitude conditions, part of a continuing study of high altitude acclimatization at the UW Medical School.

Combination Immunization Shot.—A four-in-one shot designed to immunize children against poliomyelitis, whooping cough, diphtheria and tetanus has been tested successfully in approximately 300 Detroit children, according to an article in the June 28 issue of the *Journal of the American Medical Association*.

Children who participated in the study ranged in age from 2½ months to 5 years. Seventy-five per cent, or 224 of them, completed the series of three monthly inoculations, and comparisons of bloods obtained before and after the inoculations showed favorable response, the article says.

The product, known by the trademark Quadrigen, is not yet available for commercial distribution. Developed by Parke, Davis & Company, it is the result of two years' research on combining polio vaccine with a three-in-one shot, diphtheria and tetanus toxoids and whooping cough vaccine (DPT), now in general use by pediatricians.

The purpose of the research program was to develop a vaccine which would protect children against polio, as well as the other 3 diseases, without increasing the volume of vaccine or number of injections the children now receive for diphtheria, tetanus and whooping cough.

By a special series of manufacturing processes, the four components are concentrated and provide effectiveness with three doses of ½ cc. (just over 8 drops) of Quadrigen for each inoculation. The Detroit trial was conducted to test the response of children to the combined vaccine.

A significant finding in the lengthy study was the low incidence of naturally acquired resistance to polio in 7–9 month old children, indicating a need for vaccine inoculation prior to this age. Injections of Quadrigen produced good antibody response to the polio component, as well as to the other 3 antigens of the four-way vaccine in children from 2½ months to five years of age. A fourth dose was found to be desirable for children younger than four months.

Three Detroit Health Department physicians—Dr. Joseph G. Molner,

V.2
195

Health Commissioner; Dr. C. D. Barrett, Jr., Director of Maternal and Child Health; and Dr. C. P. Anderson, Deputy Commissioner of Health, Medical Service—conducted the trial in conjunction with Dr. E. A. Timm, Dr. B. I. Wilner, Dr. H. E. Carnes and Dr. I. W. McLean, Jr., members of the Parke-Davis research staff. The seven doctors collaborated in writing this first report on Quadrigen for the *Journal* of the American Medical Association.

Children who participated in the study are currently receiving a routine "booster" dose of Quadrigen 15 to 16 months following their primary series of inoculations. Antibody evaluation studies of this booster will be a part of a more complete report at a later date, according to the authors.

High-Vacuum Thermionic Converter.—A working model of a thermionic converter—a device that produces electricity directly from heat—has been described by scientists of the General Electric Research Laboratory, Schenectady, N. Y. The development was revealed at a meeting of the American Physical Society at Cornell University.

The new device, a combination of metal and ceramic disks surrounding a high vacuum, is the size of a quarter, and produces electricity when the flame of a blowtorch is played upon it. Last year the GE Research Laboratory announced the results of Dr. Volney C. Wilson's original work on the thermionic converter. The new converter, with its high vacuum, is in contrast to the original, which was filled with gas.

"In the relatively short time that has elapsed since the announcement of the original converter, we have made great progress in exploring the capacities and limitations of such devices," declared Dr. Virgil L. Stout, manager of the Physical Electronics Section of the Research Laboratory. "In the process we have gone from an experimental laboratory device to a working model, and there is no doubt that further research and development will lead us not only to more complete scientific understanding, but also to practical applications."

Possible applications, he added, could be found wherever a high temperature source of heat is available and a supply of electricity is needed. Any source of heat, nuclear or conventional, could be used. The converter, as a result, should prove valuable in a wide variety of applications, including aircraft, missiles, and satellites. It is estimated that converters of this size will be made capable of operating in the one- to ten-watt range.

The new converter is constructed by means of techniques similar to those used for high temperature electronic tubes, according to a paper co-authored by Dr. Harold F. Webster and James E. Beggs. Beggs, the inventor of the device, worked closely with Webster, who performed theoretical analyses. This type of design, Webster pointed out in presenting the paper, has the advantage of operating at a lower temperature than the gas-filled converter (1500° F. *vs* 3000° F.), which makes material requirements easier to meet.

In the thermionic converter, two electrodes are held at high, but different, temperatures. Electrons are "boiled out" of the hotter cathode and are collected by the relatively cool anode. They can then flow through an external circuit and do work.

The original announcement of Wilson's converter referred to "new approaches" to the gas environment

within the foot-long glass tube. Dr. Wilson revealed at the Cornell meeting that the gas involved is cesium vapor, and that the vapor partially ionizes, thus neutralizing the space-charge effect that would otherwise block the flow of electrons from cathode to anode.

Equally important, he added, is the fact that the cesium coats the electrodes, thus affecting their work functions (the amount of energy that must be used in order to free an electron from the electrode and release it into the surrounding space). The difference between the work functions of the cathode and the anode is the key to the successful operation of the thermionic converter, Wilson revealed since this difference provides the voltage that drives the electrons through the circuit.

The problem of reducing the internal resistance of the converter can be approached in several ways, he pointed out. One is by using a partly ionized gas, as he did in his original model. A second is by placing the electrodes extremely close together, which is the method used in the new high vacuum converter.

Standard Case Improves Pulse Transformer Packages.—A new standard plastic case specifically designed to eliminate the mounting and encapsulating problems of a wide range of Pulse Transformers has been announced by the Milton Ross Metals Company, of Southampton, Pa. The case, a complete pulse transformer package rather than just the encapsulation shell of former types, has four special features: Custom fit for all sizes of transformers; unobstructed access for assembling and wiring the components; a leak resistant press-fit seal; and a special keyway for identifying connectors and inserting the package.

Available in a variety of military approved materials which permit operations at temperatures up to 500° F., the new case is composed of two matched parts: A circular shell for holding the potting compound and a flat plastic header with connecting pins molded-in for mounting and wiring the component.

The header, or PMS (Plastic to Metal Seal), is flanged to fit a recessed ring in the shell. This provides a three-surface, press-fit seal which minimizes leakage of the encapsulating material. For certain types of transformers the PMS contains a threaded metal insert for the cup-core mounting screw.

To provide custom fit for a wide range of transformers the cases are available in 25 different diameters ranging from $\frac{3}{16}$ in. to $2\frac{1}{2}$ in. There is also a choice of 25 different heights from $\frac{3}{16}$ in. to $2\frac{1}{2}$ in. Cases may be specified with 4-5-6-7-8-9 or 10 pins in various pitch-circle diameters up to $1\frac{1}{2}$ in.